EXPERIMENTAL RESERVOIR ENGINEERING

LABORATORY WORKBOOK

O. Torsæter

M. Abtahi

DEPARTMENT OF PETROLEUM ENGINEERING AND APPLIED GEOPHYSICS

NORWEGIAN UNIVERSITY OF SCIENCE AND TECHNOLOGY

EXPERIMENTAL RESERVOIR ENGINEERING LABORATORY WORK BOOK

O. Torsæter

M. Abtahi

**Department of Petroleum engineering
and Applied Geophysics**

Norwegian University of Science and Technology

January, 2003

PREFACE

This book is intended primarily as a text in the course SIG4015 Reservoir Property Determination by Core Analysis and Well Testing at the Norwegian University of Science and Technology. Part of this course introduces the basic laboratory equipment and procedures used in core analysis and the theoretical aspects of the parameters. The book also includes detailed description of laboratory exercises suitable for student work.

Appreciation is expressed to the Dr.ing. students Medad Tweheyo Twimukye and Hoang Minh Hai for their contributions to this work.

<div style="text-align: right">

Ole Torsæter
Manoochehr Abtahi

</div>

CONTENTS

1. INTRODUCTION

Knowledge of petrophysical and hydrodynamic properties of reservoir rocks are of fundamental importance to the petroleum engineer. These data are obtained from two major sources: core analysis and well logging. In this book we present some details about the analysis of cores and review the nature and quality of the information that can be deduced from cores.

Cores are obtained during the drilling of a well by replacing the drill bit with a diamond core bit and a core barrel. The core barrel is basically a hollow pipe receiving the continuous rock cylinder, and the rock is inside the core barrel when brought to surface. Continuous mechanical coring is a costly procedure due to:

- The drill string must be pulled out of the hole to replace the normal bit by core bit and core barrel.
- The coring operation itself is slow.
- The recovery of rocks drilled is not complete.
- A single core is usually not more than 9 m long, so extra trips out of hole are required.

Coring should therefore be detailed programmed, specially in production wells. In an exploration well the coring can not always be accurately planned due to lack of knowledge about the rock. Now and then there is a need for sample in an already drilled interval, and then sidewall coring can be applied. In sidewall coring a wireline-conveyed core gun is used, where a hollow cylindrical "bullet" is fired in to the wall of the hole. These plugs are small and usually not very valuable for reservoir engineers.

During drilling, the core becomes contaminated with drilling mud filtrate and the reduction of pressure and temperature while bringing the core to surface results in gas dissolution and further expansion of fluids. The fluid content of the core observed on the surface can not be used as a quantitative measure of saturation of oil, gas and water in the reservoir. However, if water based mud is used the presence of oil in the core indicates that the rock information is oil bearing.

When the core arrives in the laboratory plugs are usually drilled 20-30 cm apart throughout the reservoir interval. All these plugs are analyzed with respect to porosity, permeability, saturation and lithology. This analysis is usually called routine core analysis. The results from routine core analysis are used in interpretation and evaluation of the reservoir. Examples are prediction of gas, oil and water production, definition of fluid contacts and volume in place, definition of completion intervals etc. Data from routine core analysis and from supplementary tests and the application of these data area summarized in Table 1.1.

Table 1.1: Routine core analysis and supplementary measurements.

Data	Application
Routine core analysis	
Porosity	Storage capacity
Permeability	Flow capacity
Saturations	Define the mobile hydrocarbons (productive zones and contacts), type of hydrocarbons
Lithology	Rock type and characteristics (fractures, layering etc.)
Supplementary measurement	
Vertical permeability	Effect of coning, gravity drainage etc.
Core-gamma surface log	Identify lost core sections, correlate cores and logs
Matrix density	Calibrate the density log
Oil and water analysis	Densities, viscosities, interfacial tension, composition etc.

Special core analysis includes several measurements with the objective of obtaining detailed information about multiphase flow behavior. Special core analysis gives information about the distribution of oil, gas, and water in the reservoir (capillary pressure data), residual oil saturation and multiphase flow characteristics (relative permeabilities). Measurements of electrical and acoustic properties are occasionally included in special core analysis. This information is mainly used in the interpretation of well logs.

The effect of pressure and temperature on rock and fluid properties is in some reservoir formations significant, and laboratory measurements should therefore be made at, or corrected to, reservoir conditions wherever possible. Included in special core analysis is in some cases detailed petrographical analysis of rocks (grain size distribution, clay identification, diagenesis etc.). Wettability analysis and special tests for enhanced oil recovery (EOR) are also often part of special core analysis. Table 1.2 is a list of the various special core analysis tests.

Table 1.2: Special core analysis.

Tests/Studies	Data/Properties
Static tests	
Compressibility studies	Permeability and porosity vs. pressure
Petrographical studies	Mineral identification, diagenesis, clay identification, grain size distribution, pore geometry etc.
Wettability	Contact angle and wettability index
Capillarity	Capillary pressure vs. saturation
Acoustic tests	
Electric tests	
Dynamic tests	
Flow studies	Relative permeability and end point saturations
EOR-Flow tests	Injectivity and residual saturation

2. CLEANING AND SATURATION DETERMINATION

2.1 Definitions

Before measuring porosity and permeability, the core samples must be cleaned of residual fluids and thoroughly dried. The cleaning process may also be apart of fluid saturation determination.

Fluid saturation is defined as the ratio of the volume of fluid in a given core sample to the pore volume of the sample

$$S_w = \frac{V_w}{V_p} \qquad S_o = \frac{V_o}{V_p} \qquad S_g = \frac{V_g}{V_p} \tag{2.1}$$

$$S_w + S_o + S_g = 1 \tag{2.2}$$

where V_w, V_o, V_g and V_p are water, oil, gas and pore volumes respectively and S_w, S_o and S_g are water, oil and gas saturations. Note that fluid saturation may be reported either as a fraction of total porosity or as a fraction of effective porosity. Since fluid in pore spaces that are not interconnected can not be produced from a well, the saturations are more meaningful if expressed on the basis of effective porosity. The weight of water collected from the sample is calculated from the volume of water by the relationship

$$W_w = \rho_w V_w \tag{2.3}$$

where ρ_w is water density in g/cm^3. The weight of oil removed from the core may be computed as the weight of liquid less weight of water

$$W_o = W_L - W_w \tag{2.4}$$

where W_L is the weight of liquids removed from the core sample in gram. Oil volume may then be calculated as W_o/ρ_o. Pore volume V_p is determined by a porosity measurement, and oil and water saturation may be calculated by Eq. (2.1). Gas saturation can be determined using Eq. (2.2)

2.2 Measurement Methods

2.2.1 Direct Injection of Solvent

The solvent is injected into the sample in a continuous process. The sample is held in a rubber sleeve thus forcing the flow to be uniaxial.

2.2.2 Centrifuge Flushing

A centrifuge which has been fitted with a special head sprays warm solvent onto the sample. The centrifugal force then moves the solvent through the sample. The used solvent can be collected and recycled.

2.2.3 Gas Driven Solvent Extraction

The sample is placed in a pressurized atmosphere of solvent containing dissolved gas. The solvent fills the pores of sample. When the pressure is decreased, the gas comes out of solution, expands, and drives fluids out of the rock pore space. This process can be repeated as many times as necessary.

2.2.4 Soxhlet Extraction

A Soxhlet extraction apparatus is the most common method for cleaning sample, and is routinely used by most laboratories. As shown in Figure 2.1a, toluene is brought to a slow boil in a Pyrex flask; its vapors move upwards and the core becomes engulfed in the toluene vapors (at approximately 110^0C). Eventual water within the core sample in the thimble will be vaporized. The toluene and water vapors enter the inner chamber of the condenser, the cold water circulating about the inner chamber condenses both vapors to immiscible liquids. Recondensed toluene together with liquid water falls from the base of the condenser onto the core sample in the thimble; the toluene soaks the core sample and dissolves any oil with which it come into contact. When the liquid level within the Soxhlet tube reaches the top of the siphon tube arrangement, the liquids within the Soxhlet tube are automatically emptied by a siphon effect and flow into the boiling flask. The toluene is then ready to start another cycle.

A complete extraction may take several days to several weeks in the case of low API gravity crude or presence of heavy residual hydrocarbon deposit within the core. Low permeability rock may also require a long extraction time.

2.2.5 Dean-Stark Distillation-Extraction

The Dean-Stark distillation provides a direct determination of water content. The oil and water area extracted by dripping a solvent, usually toluene or a mixture of acetone and chloroform, over the plug samples. In this method, the water and solvent are vaporized, recondensed in a cooled tube in the top of the apparatus and the water is collected in a calibrated chamber (Figure 2.1b). The solvent overflows and drips back over the samples. The oil removed from the samples remains in solution in the solvent. Oil content is calculated by the difference between the weight of water recovered and the total weight loss after extraction and drying.
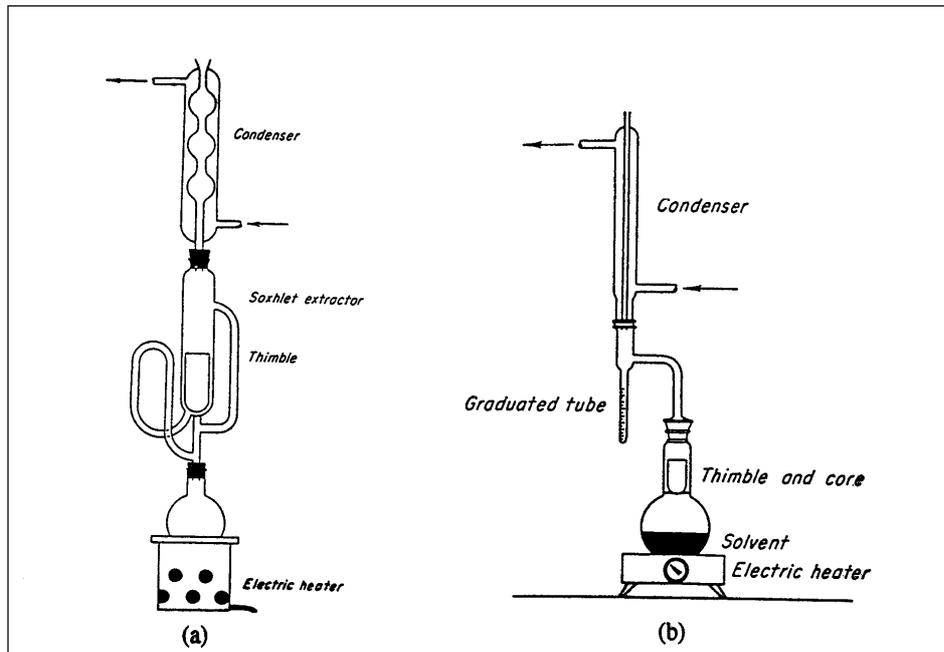
Fig. 2.1: Schematic diagram of Soxhlet (a) and Dean- Stark (b) apparatus.

2.2.6 Vacuum Distillation

The oil and water content of cores may be determined by this method. As shown in Figure 2.2, a sample is placed within a leakproof vacuum system and heated to a maximum temperature of 230^0C. Liquids within the sample are vaporized and passed through a condensing column that is cooled by liquid nitrogen.
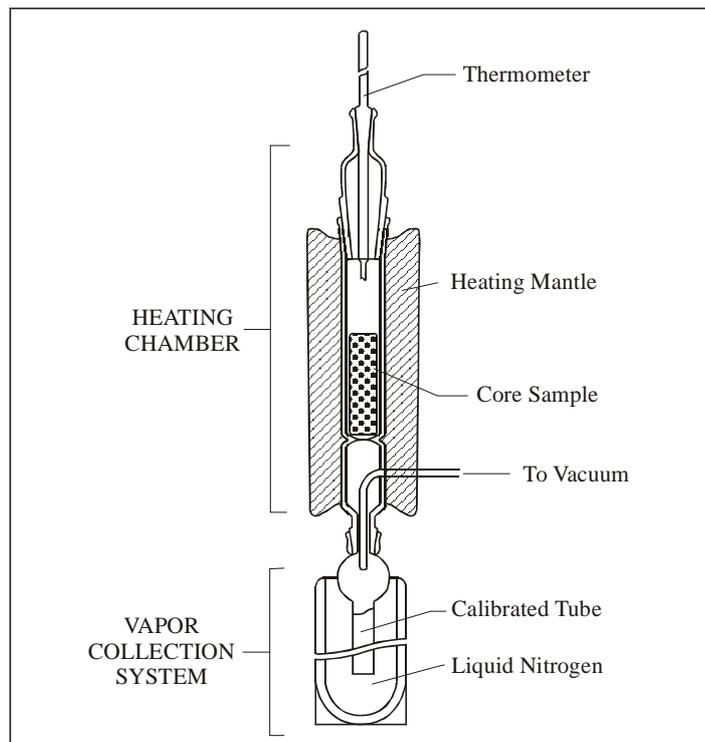
Fig. 2.2: Vacuum distillation Apparatus.

5

2.2.7   Summary

The direct-injection method is effective, but slow. The method of flushing by using centrifuge is limited to plug-sized samples. The samples also must have sufficient mechanical strength to withstand the stress imposed by centrifuging. However, the procedure is fast. The gas driven-extraction method is slow. The disadvantage here is that it is not suitable for poorly consolidated samples or chalky limestones. The distillation in a Soxhlet apparatus is slow, but is gentle on the samples. The procedure is simple and very accurate water content determination can be made. Vacuum distillation is often used for full diameter cores because the process is relatively rapid. Vacuum distillation is also frequently used for poorly consolidated cores since the process does not damage the sample. The oil and water values are measured directly and dependently of each other.

In each of these methods, the number of cycles or amount of solvent which must be used depends on the nature of the hydrocarbons being removed and the solvent used. Often, more than one solvent must be used to clean a sample. The solvents selected must not react with the minerals in the core. The commonly used solvents are:

- Acetone
- Benzene
- Benzen-methol Alcohol
- Carbon-tetrachloride
- Chloroform
- Methylene Dichloride
- Mexane
- Naphtha
- Tetra Chloroethylene
- Toluene
- Trichloro Ethylene
- Xylene

Toluene and benzene are most frequently used to remove oil and methanol and water is used to remove salt from interstitial or filtrate water. The cleaning procedures used are specifically important in special core analysis tests, as the cleaning itself may change wettabilities.

The core sample is dried for the purpose of removing connate water from the pores, or to remove solvents used in cleaning the cores. When hydratable minerals are present, the drying procedure is critical since interstitial water must be removed without mineral alteration. Drying is commonly performed in a regular oven or a vacuum oven at temperatures between 50^0C to 105^0C. If problems with clay are expected, drying the samples at 60^0C and 40 % relative humidity will not damage the samples.

2.3   Experiments

2.3.1   Saturation Determination, Dean-Stark Distillation Method (Experiment 1)

Description:

The objective of the experiment is to determine the oil, water and gas saturation of a core sample.

Procedure:

1. Weigh a clean, dry thimble. Use tongs to handle the thimble.

2. Place the cylindrical core plug inside the thimble, then quickly weigh the thimble and sample.

3. Fill the extraction flask two-thirds full with toluene. Place the thimble with sample into the long neck flask.

4. Tighten the ground joint fittings, but do not apply any lubricant for creating tighter joints. Start circulating cold water in the condenser.

5. Turn on the heating jacket or plate and adjust the rate of boiling so that the reflux from the condenser is a few drops of solvent per second. The water circulation rate should be adjusted so that excessive cooling does not prevent the condenser solvent from reaching the core sample.

6. Continue the extraction until the solvent is clear. Change solvent if necessary.

7. Read the volume of collected water in the graduated tube. Turn off the heater and cooling water and place the sample into the oven (from 105^0C to 120^0C), until the sample weight does not change. The dried sample should be stored in a desiccater.

8. Obtain the weight of the thimble and the dry core.

9. Calculate the loss in weight W_L, of the core sample due to the removal of oil and water.

10. Measure the density of a separate sample of the oil.

11. Calculate the oil, water and gas saturations after the pore volume V_p of the sample is determined.

Data and calculations:

Sample No: Porosity, ϕ:

W_{org} g	W_{dry} g	ρ_w g/ cm^3	ρ_o g/ cm^3	V_w cm^3	W_o g	V_o cm^3	V_p cm^3	S_o	S_w	S_g

Where

   W_{org}: Weight of original saturated sample
   W_{dry}: Weight of desaturated and dry sample

Equations:

$$W_L = W_{org} - W_{dry}$$

$$W_o = W_L - W_w$$

$$V_b = \pi (D/2)^2 L$$

$$V_p = \phi V_b$$

where D and L are diameter and length of the core sample, respectively.

3. LIQUID DENSITY

3.1   Definitions

Density (ρ) is defined as the mass of the fluid per unit volume. In general, it varies with pressure and temperature. The dimension of density is *kg/m³* in *SI* or *lb/ft³* in the English system.

Specific gravity (γ) is defined as the ratio of the weight of a volume of liquid to the weight of an equal volume of water at the same temperature. The specific gravity of liquid in the oil industry is often measured by some form of hydrometer that has its special scale. The American Petroleum Institute (API) has adopted a hydrometer for oil lighter than water for which the scale, referred to as the API scale, is

$$^0API = \frac{141.5}{\gamma} - 131.5 \tag{3.1}$$

Note: When reporting the density the units of mass and volume used at the measured temperature must be explicitly stated, e.g. grams per milliliter (cm³) at T(^{0}C). The standard reference temperature for international trade in petroleum and its products is 15^0C (60^0F), but other reference temperatures may be used for other special purposes.

3.2   Measurement of Density

The most commonly used methods for determining density or specific gravity of a liquid are:

1. Westphal balance
2. Specific gravity balance (chain-o-matic)
3. API hydrometer
4. Pycnometer
5. Bicapillary pycnometer.

The first two methods are based on the principle of Archimedes: A body immersed in a liquid is buoyed up by a force equal to the weight of the liquid it displaces. A known volume of the liquid to be tested is weighted by these methods. The balances are so constructed that they should exactly balance in air.

The API hydrometer is usually used for determining oil gravity in the oil field. When a hydrometer is placed in oil, it will float with its axis vertical after it has displaced a mass of oil equal to the mass of hydrometer (Fig. 3.1a). The hydrometer can be used at atmospheric pressure or at any other pressure in a pressure cylinder.

The pycnometer (Fig. 3.1b) is an accurately made flask, which can be filled with a known volume of liquid. The specific gravity of liquid is defined as the ratio of the weight of a volume of the liquid to the weight of an equal volume of water at the same temperature.

Both weights should be corrected for buoyancy (due to air) if a high degree of accuracy is required. The ratio of the differences between the weights of the flask filled with liquid and empty weight, to the weight of the flask filled with distilled water and empty weight, is the specific gravity of the unknown fluid. The water and the liquid must both be at the same temperature.

The bicapillary pycnometer (Fig. 3.1c) is another tool for accurate determination of density. The density of the liquid sample drawn into the pycnometer is determined from its volume and weight.
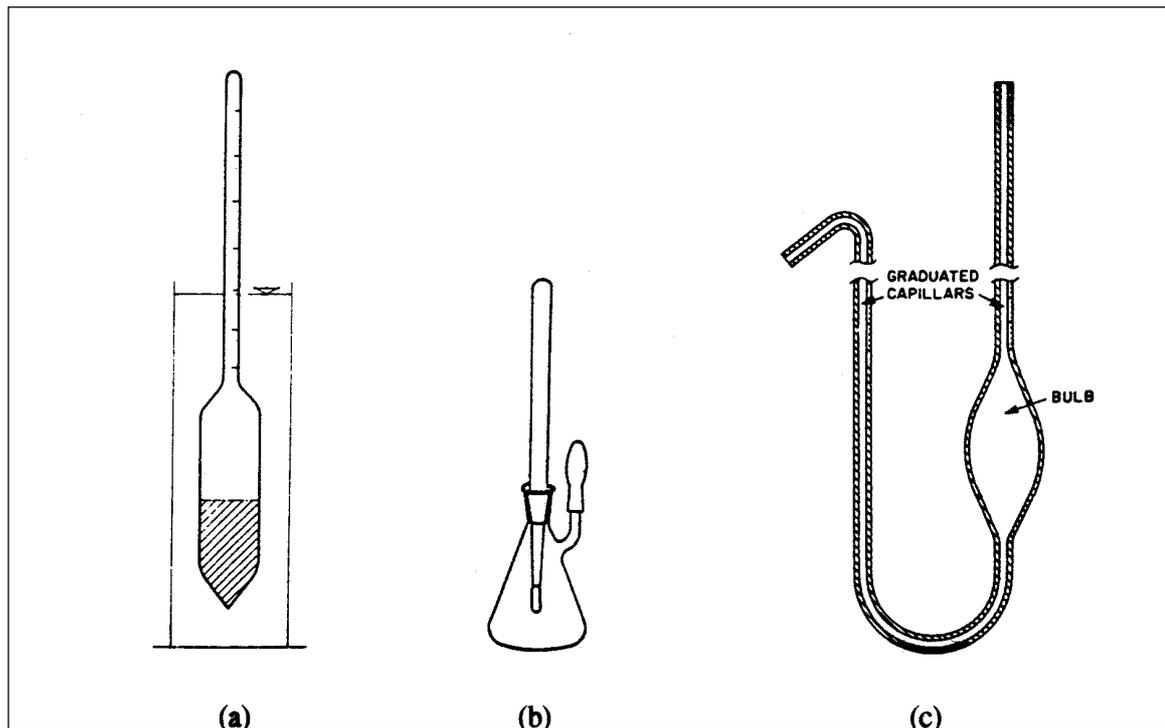
Fig. 3.1: Schematic diagram of hydrometer (a), pycnometer (b),
and bicapillary pycnometer (c)

3.3   Experiments

3.3.1   Fluid density using the Pycnometer method (Experiment 2)

Description:

This method covers the determination of the density or relative density (specific gravity) of crude petroleum and of petroleum products handled as liquids with vapor pressure 1.8 bar or less, e.g. stabilized crude oil, stabilized gasoline, naphthane, kerosines, gas oils, lubricating oils, and non-waxy fuel oils.

Procedure:

1. Thoroughly clean the pycnometer and stopper with a surfactant cleaning fluid, rinse well with distilled water. Finally rinse with acetone and dry.

2. Weigh the clean, dry pycnometer with stopper and thermometer at room temperature.

3. Fill the pycnometer with the liquid (oil, brine) at the same room temperature.

4. Put on the stopper and thermometer and be sure there is no gas bubble inside, and then dry the exterior surface of the pycnometer by wiping with a lint-free cloth or paper.

5. Weigh the filled pycnometer.

Calculation and report:

1. Calculate the liquid density and the average density based on your data.
2. Calculate the *absolute* error for each measurement.
3. Calculate the specific gravity.
4. Error source analysis of the pycnometer method.

Table: Density of water, kg/m^3 at different temperatures

18.0^0C----998.5934	18.5^0C----998.4995	19.0^0C----998.4030
19.5^0C----998.3070	20.0^0C----998.2019	20.5^0C----998.0973
21.0^0C----997.9902	21.5^0C----997.8805	22.0^0C----997.7683
22.5^0C----997.6536	23.0^0C----997.5363	24.0^0C----997.2944

Temperature: ^{0}C

Fluid	Pycnometer mass (g)	Pycnometer + liquid (g)	Pycnometer volume (cm^3)	Density, ρ (g/cm^3)	Specific gravity, γ	Absolute error, *Ea* (g/cm^3)
$\rho_{avr}=$						

Equations: Average Density $(\rho_{avr}) = \dfrac{1}{n}\sum_{i=1}^{n}\rho_i$

Ea = | (*Average Density*) – (*Measured Density*) |

11

4. VISCOSITY

4.1 Definitions

Viscosity is defined as the internal resistance of fluid to flow. The basic equation of deformation is given by

$$\tau = \mu \dot{\gamma} \qquad (4.1)$$

where τ is shear stress, $\dot{\gamma}$ is the shear rate defined as $\partial v_x / \partial_y$ and μ is the viscosity. The term τ can be defined as *F/A* where *F* is force required to keep the upper plate moving at constant velocity v in the x-direction and *A* is area of the plate in contact with the fluid (Fig. 4.1). By fluid viscosity, the force is transmitted through the fluid to the lower plate in such a way that the x-component of the fluid velocity linearly depends on the distance from the lower plate.
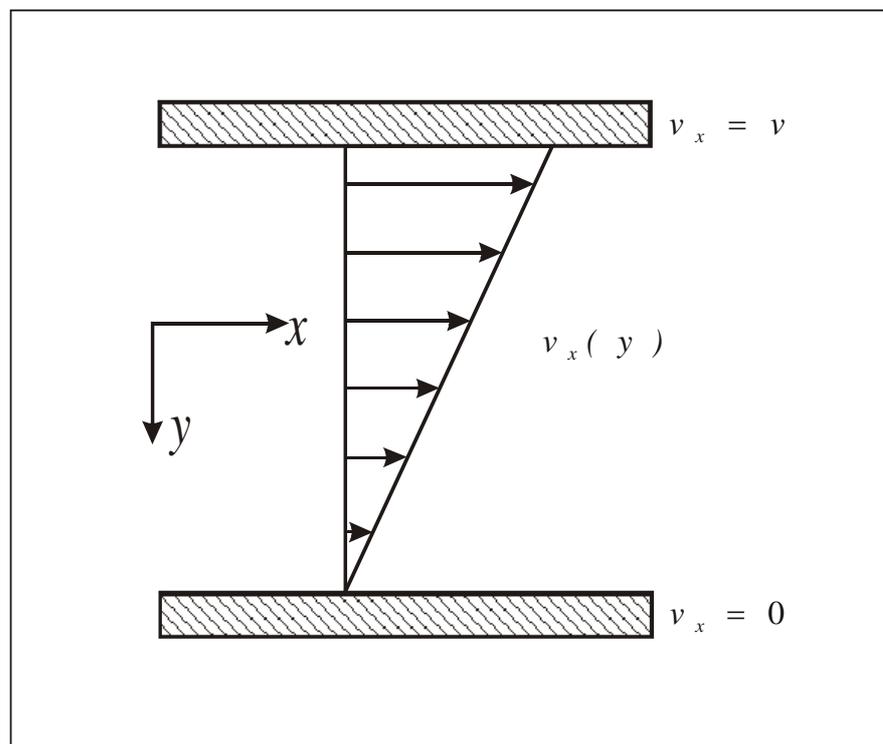
Fig. 4.1: Steady-state velocity profile of a fluid entrained between two flat surfaces.

It is assumed that the fluid does not slip at the plate surface. Newtonian fluids, such as water and gases, have shear-independent viscosity and the shear stress is proportional to the shear rate (Fig. 4.2).
In the oil industry viscosity generally is expressed in centipoise, cp (1 *cp* $= 10^{-3}$ *Pa.s*).
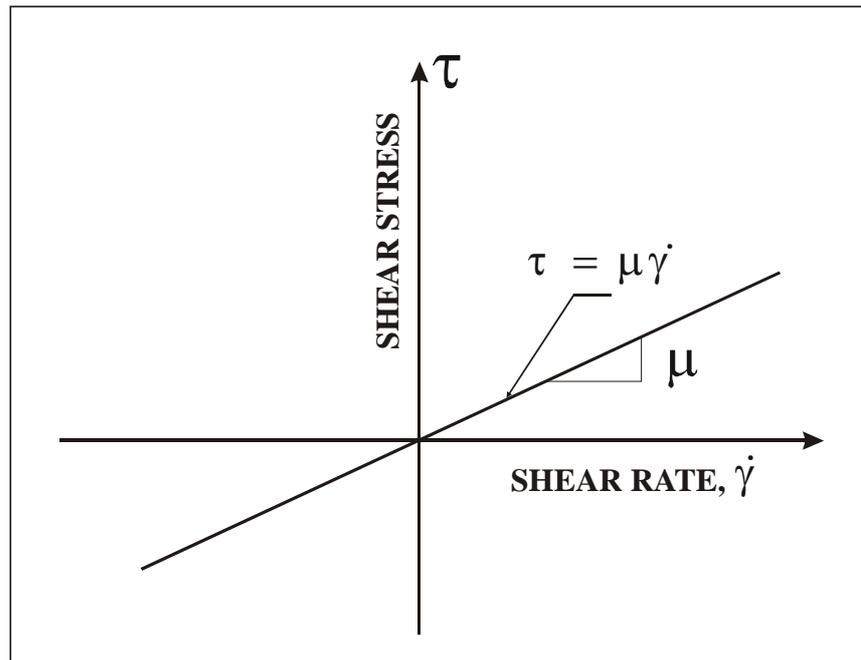
Fig. 4.2: Shear stress vs. shear rate for a Newtonian fluid.

4.2   Effect of Pressure and Temperature on Viscosity

Viscosity of fluids varies with pressure and temperature. For most fluids the viscosity is rather sensitive to changes in temperature, but relatively insensitive to pressure until rather high pressures have been attained. The viscosity of liquids usually rises with pressure at constant temperature. Water is an exception to this rule; its viscosity decreases with increasing pressure at constant temperature. For most cases of practical interest, however, the effect of pressure on the viscosity of liquids can be ignored.

Temperature has different effects on viscosity of liquids and gases. A decrease in temperature causes the viscosity of a liquid to rise. Effect of molecular weight on the viscosity of liquids is as follows; the liquid viscosity increases with increasing molecular weight.

4.3   Methods for Measuring Viscosity

4.3.1   Capillary Type Viscometer

Viscosity of liquids is determined by instruments called viscosimeter or viscometer. One type of viscometer for liquids is the *Ostwald viscometer* (Fig. 4.3). In this viscometer, the viscosity is deduced from the comparison of the times required for a given volume of the tested liquids and of a reference liquid to flow through a given capillary tube under specified initial head conditions. During the measurement the temperature of the liquid should be kept constant by immersing the instrument in a temperature-controlled water bath.
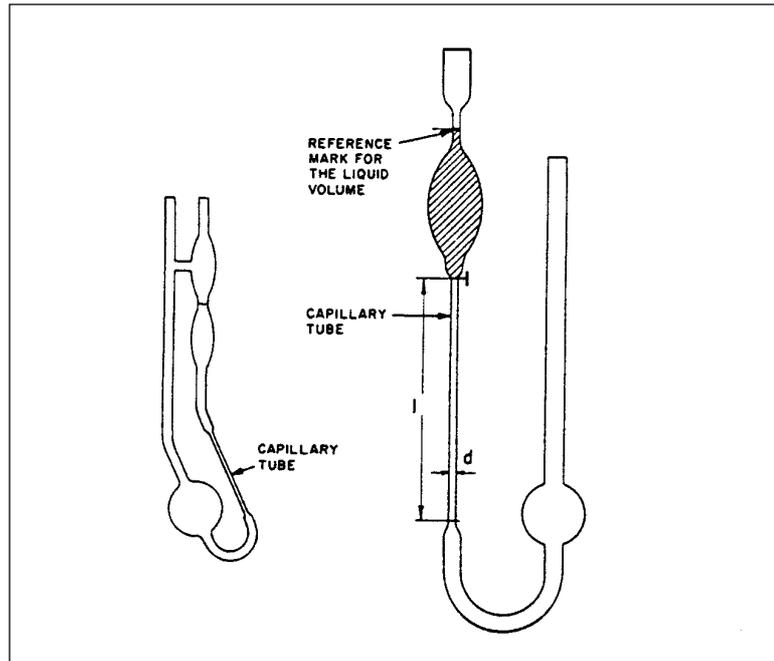
Fig. 4.3: Two types of Ostwald viscometers.

In this method the Poiseuille's law for a capillary tube with a laminar flow regime is used

$$Q = \frac{V}{t} = \frac{\Delta P \pi r^4}{8 \mu l}$$

(4.2)

where t is time required for a given volume of liquid V with density of ρ and viscosity of μ to flow through the capillary tube of length l and radius r by means of pressure gradient ΔP. The driving force ΔP at this instrument is $\rho g l$. Then

$$\frac{V}{t} = \frac{\pi r^4 \rho g l}{8 \mu l}$$

(4.3)

or

$$\mu = \frac{\pi r^4 \rho g t}{8V} = \text{Const.} \rho t$$

(4.4)

The capillary constant is determined from a liquid with known viscosity.

4.3.2 Falling Ball Viscometer

Another instrument commonly used for determining viscosity of a liquid is the *falling (or rolling) ball viscometer* (Fig. 4.4), which is based on Stoke's law for a sphere falling in a fluid under effect of gravity. A polished steel ball is dropped into a glass tube of a

somewhat larger diameter containing the liquid, and the time required for the ball to fall at constant velocity through a specified distance between reference marks is recorded. The following equation is used

$$\mu = t\left(\rho_b - \rho_f\right)K \qquad (4.5)$$

where μ = absolute viscosity, *cp*
      t = falling time, *s*
      ρ_b = density of the ball, *g/cm³*
      ρ_f = density of fluid at measuring temperature, *g/cm³*
      K = ball constant.

The ball constant K is not dimensionless, but involves the mechanical equivalent of heat.
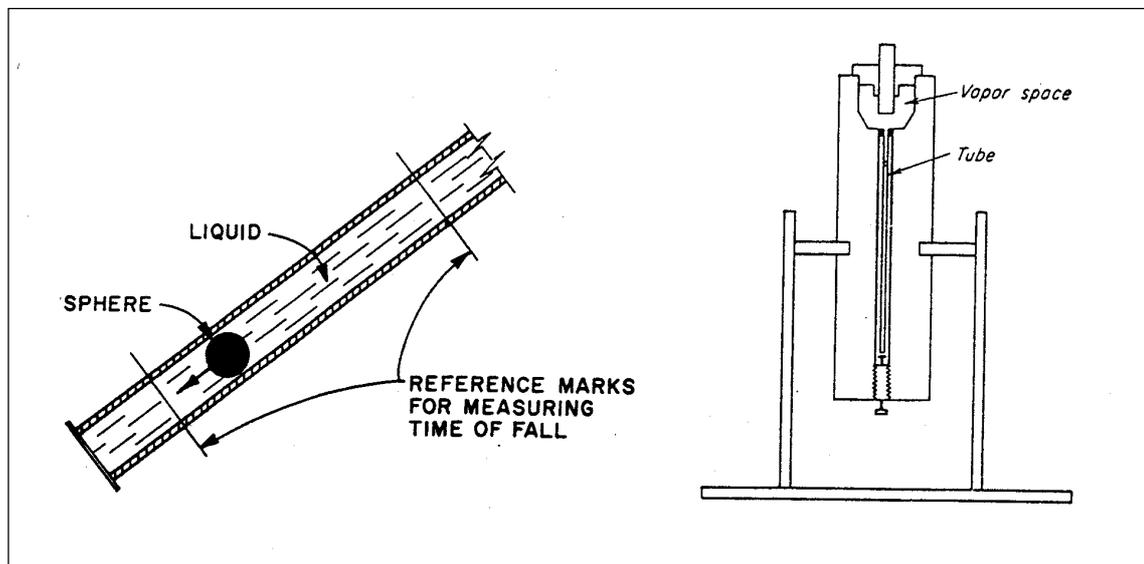
Fig. 4.4: Schematic diagram of the falling ball viscometer.

The rolling ball viscometer will give good results as long as the fluid flow in the tube remains in the laminar range. In some instruments of this type both pressure and temperature may be controlled.

4.3.3   Rotational Viscometer

Other often used viscometers especially for non-Newtonian fluids are the rotational type consisting of two concentric cylinders, with the annulus containing the liquid whose viscosity is to be measured (Figure 4.5). Either the outer cylinder or the inner one is rotated at a constant speed, and the rotational deflection of the cylinder becomes a measure of the liquid's viscosity.
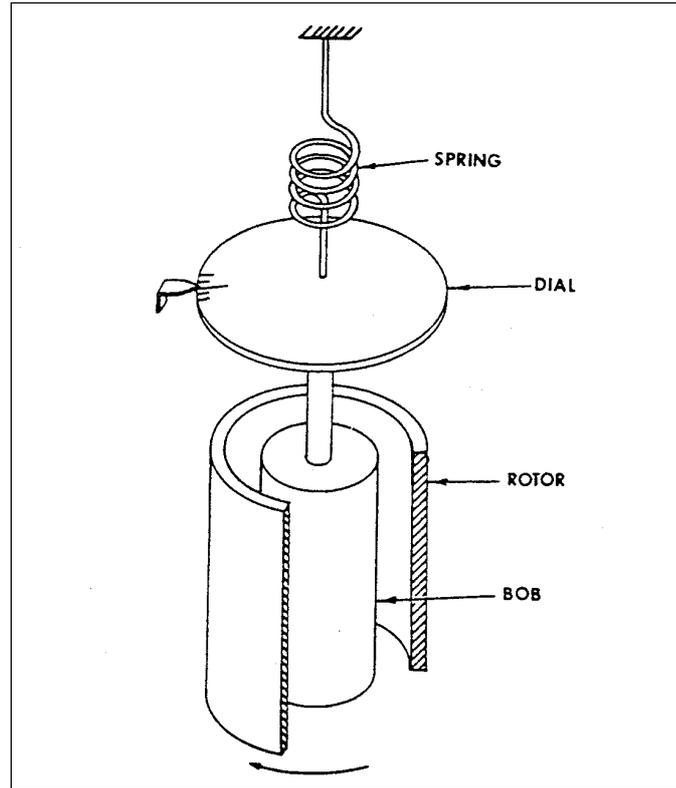
Fig. 4.5: Schematic diagram of the rotational viscometer.

When the distance between the cylinders d, is small, we can define the viscosity gradient for laminar flow regime as

$$\frac{dv}{dr} = \frac{\omega R}{d} \tag{4.6}$$

where R is radius of the inner cylinder (*bob*) and ω is angular velocity of the outer cylinder (rotor) defined by $\omega = 2\pi n$. When the rotor is rotating at a constant angular velocity ω and the *bob* is held motionless, the torque from the torsion spring on the *bob* must be equal but opposite in direction to the torque on the rotor from the motor. The effective area of the applied torque is $2\pi.R.h$ where h is length of the cylinder. The viscous drag on the *bob* is $k.\theta.R$, where k is the torsion constant of the spring and θ is angular displacement of the instrument in degrees. Then

$$\frac{F}{A} = \frac{k\theta R}{2\pi Rh} = \mu\frac{dv}{dr} = \mu\frac{\omega R}{d} \tag{4.7}$$

which gives

$$\mu = \frac{k\theta d}{2\pi h\omega R} = \frac{K\theta}{\omega h} \tag{4.8}$$

where K is the instrument's constant which is determined by calibration.

16

4.4   Experiments

4.4.1   Liquid Viscosity Measurement using Capillary Type Viscometer (Exp. 3)

Description:

The main objective of the measurement is to determine the kinematic viscosity of Newtonian liquid petroleum products.

For capillary viscometers the time is measured in seconds for a fixed volume of liquid to flow under gravity through the capillary at a closely controlled temperature. The kinematic viscosity is the product of the measured flow time and the calibration constant of the viscometer. The dynamic viscosity can be obtained by multiplying the measured kinematic viscosity by the density of the liquid.

Definitions:

Dynamic viscosity (μ) is the ratio between the applied shear stress and the rate of shear and is called coefficient of dynamic viscosity μ. This coefficient is thus a measure of the resistance to flow of the liquid; it is commonly called the viscosity of the liquid.

Kinematic viscosity (υ) is the ratio μ/ρ where ρ is fluid density.

Unit and dimensions:

	Symbol	**cgs unit**	**SI unit**	**Dimension**
Kinematic viscosity, υ	$1\ mm^2/s = 1\ cSt$ $1\ m^2/s = 10^6\ cSt$	cm^2/s	m^2/s	L^2/T
Dynamic viscosity, μ	$1\ Dyn.s/cm^2 = 100\ cp$ $1\ Newton.s/m^2 = 10^3\ cp$	$Dyn.s/cm^2$	$Newton.s/m^2$ $(= Pa.s)$	M/LT (FT/L^2)

Where cSt = centistokes, cp = centipoise
$1cp = 10^{-3}\ Pa.s,$ $1cSt = 10^{-6}\ [m^2/s]$

Procedure:

1. Select a clean, dry calibrated viscometer (Fig. 4.6) having a range covering the estimated viscosity (i.e. a wide capillary for a very viscous liquid and a narrower capillary for a less viscous liquid). The flow time should not be less than 200 seconds.

2. Charge the viscometer: To fill, turn viscometer upside down. Dip tube (2) into the liquid to be measured while applying suction to tube (1) until liquid reaches mark (8). After inverting to normal measuring position, close tube (1) before liquid reach mark (3).

3. Allow the charged viscometer to remain long enough to reach the room temperature. Read the calibration constants-directly from the viscometer.

4. Measuring operation: Open tube (1) and measure the time it takes the liquid to rise from mark (3) to mark (5). Measuring the time for rising from mark (5) to mark (7) allows viscosity measurement to be repeated to check the first measurement.

5. If two measurements agree within required error (generally 0.2-0.35%), use the average for calculating the reported kinematic viscosity.
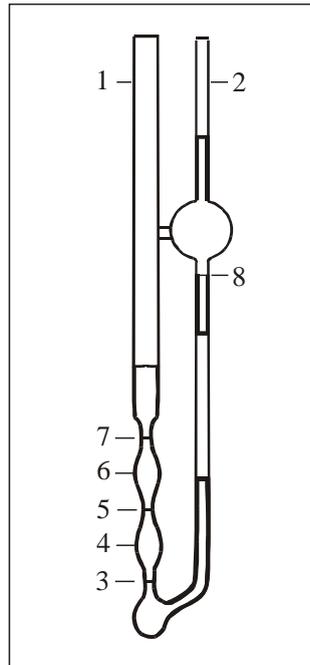
Fig. 4.6: **Viscometer apparatus.**

Calculation and report:

1. Calculate the kinematic viscosity υ from the measured flow time t and the instrument constant by means of the following equation:

$$\upsilon = C(t - \vartheta)$$

where:
   υ = kinematic viscosity, *cSt*
   C = calibration constant, *cSt/s*
   t = flow time, *s*
   ϑ = Hagenbach correction factor, when $t < 400$ seconds, it should be corrected according to the manual. When $t > 400$ seconds, $\vartheta = 0$.

2. Calculate the viscosity μ from the calculated kinematic viscosity υ and the density ρ by means of the following equation:

$$\mu = \rho_{avr}\upsilon$$

where:

μ = dynamic viscosity, *cp*

ρ_{avr} = average density in *g/cm³* at the same temperature used for measuring the flow time *t*.

υ = kinematic, *cSt*.

3. Report test results for both the kinematic and dynamic viscosity. Calculate the average dynamic viscosity.

Temperature: ___ ^{0}C

Sample	Constant C, (*cSt/s*)	Time (*s*)	Hagenbach factor, ϑ	Kinematic viscosity, υ (*cSt*)	Density, ρ_{avr} (*g/cm³*)	dynamic viscosity, μ (*cp*)
μ_{avr} =						

5. POROSITY

5.1 Definitions

From the viewpoint of petroleum engineers, the two most important properties of a reservoir rock are porosity and permeability. Porosity is a measure of storage capacity of a reservoir. It is defined as the ratio of the pore volume to bulk volume, and is may be expressed as either a percent or a fraction. In equation form

$$\phi = \frac{pore\ volume}{bulk\ volume} = \frac{bulk\ volume - grain\ volume}{bulk\ volume}$$

Two types of porosity may be measured: total or absolute porosity and effective porosity. *Total porosity* is the ratio of all the pore spaces in a rock to the bulk volume of the rock. *Effective porosity* ϕ_e is the ratio of interconnected void spaces to the bulk volume. Thus, only the effective porosity contains fluids that can be produced from wells. For granular materials such as sandstone, the effective porosity may approach the total porosity, however, for shales and for highly cemented or vugular rocks such as some limestones, large variations may exist between effective and total porosity.

Porosity may be classified according to its origin as either primary or secondary. *Primary or original porosity* is developed during deposition of the sediment. Secondary porosity is caused by some geologic process subsequent to formation of the deposit. These changes in the original pore spaces may be created by ground stresses, water movement, or various types of geological activities after the original sediments were deposited. Fracturing or formation of solution cavities often will increase the original porosity of the rock.
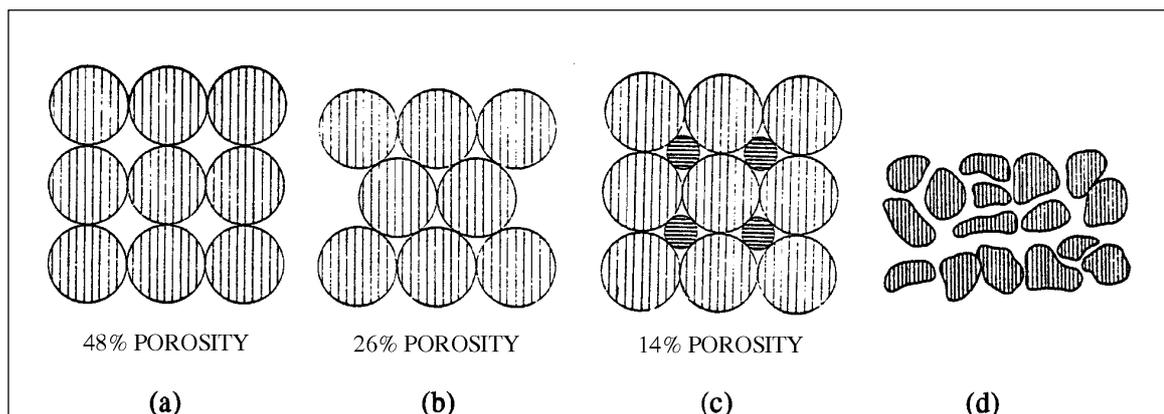
Fig. 5.1: Cubic packing (a), rhombohedral (b), cubic packing with two grain sizes (c), and typical sand with irregular grain shape (d).

For a uniform rock grain size, porosity is independent of the size of the grains. A maximum theoretical porosity of 48% is achieved with cubic packing of spherical grains, as shown in Fig. 5.1a. Rhombohedral packing, which is more representative of reservoir conditions, is shown in Fig. 5.1b; the porosity for this packing is 26%. If a second,

smaller size of spherical grains is introduced into cubic packing (Fig. 5.1c), the porosity decreases from 48% to 14%. Thus, porosity is dependent on the grain size distribution and the arrangement of the grains, as well as the amount of cementing materials. Not all grains are spherical, and grain shape also influences porosity. A typical reservoir sand is illustrated in Fig. 5.1d.

5.2   *Effect of Compaction on Porosity*

Compaction is the process of volume reduction due to an externally applied pressure. For extreme compaction pressures, all materials show some irreversible change in porosity. This is due to distortion and crushing of the grain or matrix elements of the materials, and in some cases, recrystallization. The variation of porosity with change in pressure can be represented by

$$\phi_2 = \phi_1 e^{c_f(P_2 - P_1)} \tag{5.1}$$

where ϕ_2 and ϕ_1 are porosities at pressure P_2 and P_1 respectively, and c_f is formation compressibility. Formation compressibility is defined as summation of both grain and pore compressibility. For most petroleum reservoirs, grain compressibility is considered to be negligible. Formation compressibility can be expressed as

$$c_f = \frac{1}{V}\frac{dV}{dP} \tag{5.2}$$

where dP is change in reservoir pressure. For porous rocks, the compressibility depends explicitly on porosity.

5.3   *Porosity Measurements on core plugs*

From the definition of porosity, it is evident that the porosity of a sample of porous material can be determined by measuring any two of the three quantities: Bulk volume, pore volume or grain volume. The porosity of reservoir rock may be determined by

- Core analysis
- Well logging technique
- Well testing

The question of which source of porosity data is most reliable can not be answered without reference to a specific interpretation problem. These techniques can all give correct porosity values under favourable conditions. The core analysis porosity determination has the advantage that no assumption need to be made as to mineral composition, borehole effects, etc. However, since the volume of the core is less than the rock volume which is investigated by a logging device, porosity values derived from logs are frequently more accurate in heterogeneous reservoirs.

In the following sections we will discuss how to estimate pore-, grain-, and bulk-volumes from core plugs.

5.3.1 Bulk Volume Measurement

Although the bulk volume may be computed from measurements of the dimensions of a uniformly shaped sample, the usual procedure utilises the observation of the volume of fluid displaced by the sample. The fluid displaced by a sample can be observed either *volumetrically* or *gravimetrically*. In either procedure it is necessary to prevent the fluid penetration into the pore space of the rock. This can be accomplished (1) by coating the sample with paraffin or a similar substance, (2) by saturating the core with the fluid into which it is to be immersed, or (3) by using mercury.

Gravimetric determinations of bulk volume can be accomplished by observing the loss in weight of the sample when immersed in a fluid or by change in weight of a pycnometer with and without the core sample.

5.3.2 Pore Volume Measurement

All the methods measuring pore volume yield effective porosity. The methods are based on either the extraction of a fluid from the rock or the introduction of a fluid into the pore spaces of the rock.

One of the most used methods is the helium technique, which employs Boyle's law. The helium gas in the reference cell isothermally expands into a sample cell. After expansion, the resultant equilibrium pressure is measured. The Helium porosimeter apparatus is shown schematically in Fig. 5.2.
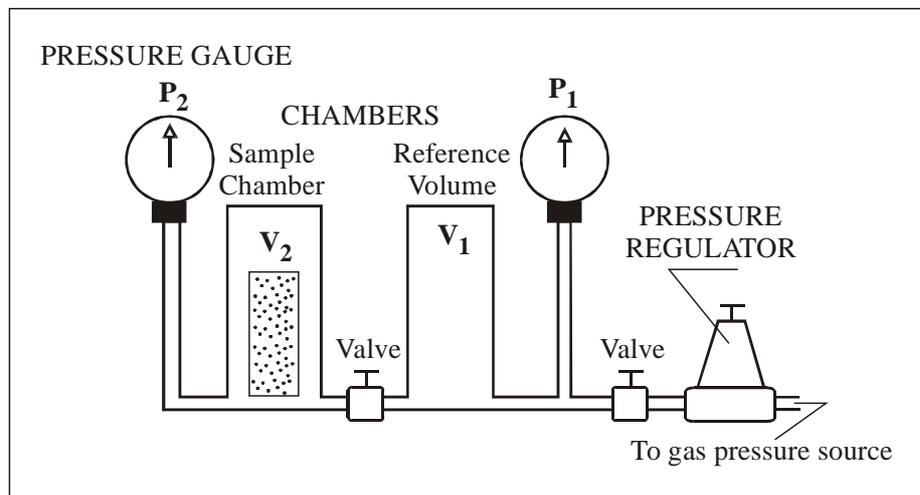
Fig. 5.2: Schematic diagram of helium porosimeter apparatus.

Helium has advantages over other gases because: (1) its small molecules rapidly penetrated small pores, (2) it is inert and does not adsorb on rock surfaces as air may do, (3) helium can be considered as an ideal gas (i.e., $z = 1.0$) for pressures and temperatures usually employed in the test, and (4) helium has a high diffusivity and therefore affords a useful means for determining porosity of low permeability rocks.

The schematic diagram of the helium porosimeter shown in Fig. 5.2 has a reference volume V_1, at pressure p_1, and a matrix cup with unknown volume V_2, and initial pressure p_2. The reference cell and the matrix cup are connected by tubing; the system can be brought to equilibrium when the core holder valve is opened, allowing determination of the unknown volume V_2 by measuring the resultant equilibrium pressure p. (Pressure p_1 and p_2 are controlled by the operator; usually $p_1 = 100$ and $p_2 = 0$ psig). When the core holder valve is opened, the volume of the system will be the equilibrium volume V, which is the sum of the volumes V_1 and V_2. Boyle's law is applicable if the expansion takes place isothermally. Thus the pressure-volume products are equal before and after opening the core holder valve:

$$p_1V_1 + p_2V_2 = p(V_1 + V_2)$$ (5.3)

Solving the equation for the unknown volume, V_2:

$$V_2 = \frac{(p - p_1)V_1}{p_2 - p}$$ (5.4)

Since all pressures in equation (5.4) must be absolute and it is customary to set $p_1 = 100$ *psig* and $p_2 = 0$ *psig*, Eq. (5.4) may be simplified as follows:

$$V_2 = \frac{V_1(100 - p)}{p}$$ (5.5)

where V_2 in *cm³* is the unknown volume in the matrix cup, and V_1 in *cm³* is the known volume of the reference cell. p in *psig* is pressure read directly from the gauge.

 Small volume changes occur in the system, including the changes in tubing and fittings caused by pressure changes during equalization. A correction factor, G, may be introduced to correct for the composite system expansion. The correction factor G is determined for porosimeters before they leave the manufacturer, and this correction is built into the gauge calibration in such a way that it is possible to read the volumes directly from the gauge.

Another method of pore volume determination is to saturate the sample with a liquid of known density, and noting the weight increase (gravimetric method).

When a rock has a small fraction of void space, it is difficult to measure porosity by the mentioned methods. At this case, mercury injection is used. The principle consists of forcing mercury under relatively high pressure in the rock pores. A pressure gauge is attached to the cylinder for reading pressure under which measuring fluid is forced into the pores. Fig. 5.3b shows a typical curve from the mercury injection method. The volume of mercury entering the core sample is obtained from the device with accuracy up to 0.01 cm³.
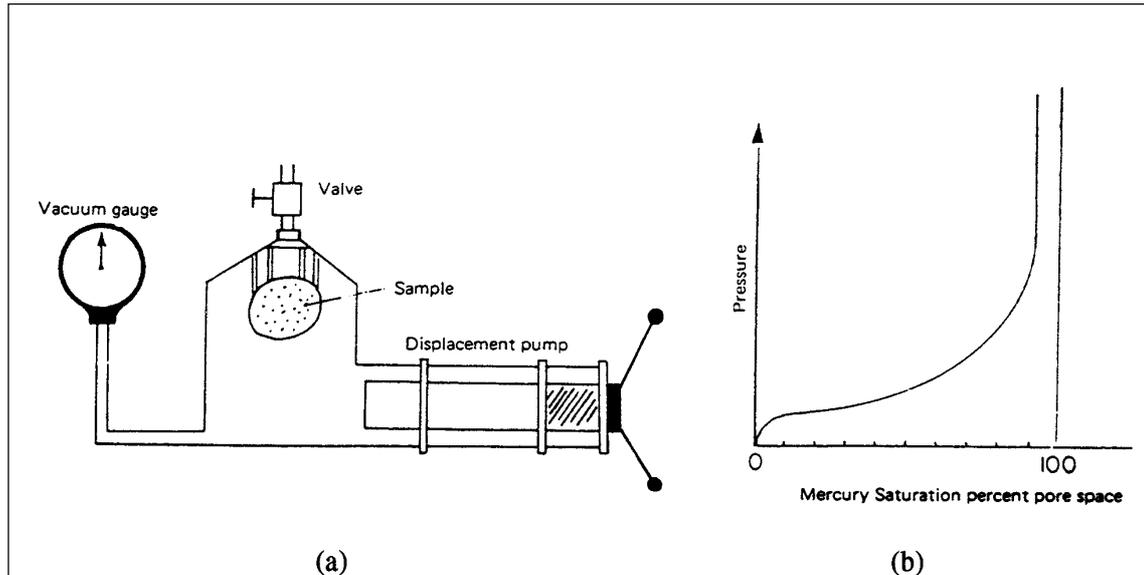
Fig. 5.3: Mercury injection pump (a) and porosity through mercury injection (b).

5.3.3　Grain Volume Measurement

The grain volume of pore samples is some times calculated from sample weight and knowledge of average density. Formations of varying lithology and, hence, grain density limit applicability of this method. Boyle's law is often employed with helium as the gas to determine grain volume. The technique is fairly rapid, and is valid on clean and dry sample.

The measurement of the grain volume of a core sample may also be based on the loss in weight of a saturated sample plunged in a liquid.

Grain volume may be measured by crushing a dry and clean core sample. The volume of crushed sample is then determined by (either pycnometer or) immersing in a suitable liquid.

5.4　Experiments

5.4.1　Effective Porosity Determination by Helium Porosimeter Method (Exp. 4)

Descriptions

The helium porosimeter uses the principle of gas expansion, as described by Boyle's law. A known volume (reference cell volume) of helium gas, at a predetermined pressure, is isothermally expanded into a sample chamber. After expansion, the resultant equilibrium pressure is measured. This pressure depends on the volume of the sample chamber minus the rock grain volume, and then the porosity can be calculated.

Procedure:

1. Measure the diameter and length of the core using calliper.

2. Give the porosimeter a helium supply, 10 bar.

3. Determine the volume of the matrix cup with core, V_2:

   3.1 Put the cleaned, dried core inside the matrix cup, and mount the cup in the cup holder.
   3.2 Open "source" and then "supply".
   3.3 Regulate the needle at 100.
   3.4 Close "source" and then "supply".
   3.5 Open "core holder".
   3.6 Take the reading on TOP SCALE, $V_2 =$ cm^3.

4. Determine the volume of the matrix cup without core, V_1:

   4.1 Take out the core from the matrix cup, and mount the cup in the cup holder.
   4.2 Open "source" and then "supply".
   4.3 Open "cell 1".
   4.4 Regulate the needle at 100.
   4.5 Close "source and then "supply".
   4.6 Open core "holder".
   4.7 Take the reading on MIDDLE SCALE, $V_1 =$ cm^3.

Calculations and report

1. Calculate and fill the data form.

Core No.:   D: cm,   L: cm.

V_1 (cm^3)	V_2 (cm^3)	V_g (cm^3)	V_b (cm^3)	ϕ_e

where
     V_1 = the volume of the matrix cup without core, cm^3.
     V_2 = the volume of the matrix cup with core, cm^3.
     $V_g = V_1 - V_2$, the volume of grain and non-connected pores, cm^3.
     V_b = the bulk volume of core, cm^3.
     $\phi_e = (V_b - V_g)/V_b$ effective (interconnected) porosity of the core, *fraction*.

5.4.2 Porosity Determination by Liquid Saturating Method (Experiment 5)

Description:

The determination of the effective liquid porosity of a porous plug is the initial part of the measurement of capillary pressure using porous plate method in core laboratories. Before

the capillary pressure is determined the volume of the saturating liquid (brine or oil) in the core must be known. Thus, the effective liquid porosity of the core can be calculated in the beginning of capillary pressure measurement.

Procedure:

1. Weigh dry Berea plug W_{dry}, measure its diameter D, and length L, with calliper (1 core for each group).

2. Put the cores in the beaker inside a vacuum container, run vacuum pump about 1 hour.

3. Saturate the cores with 36 g/l NaCl brine, $\rho_{brine} = 1.02 \text{g/cm}^3$.

4. Weigh the saturated cores, W_{sat}.

Calculations and report:

1. Calculate the saturated brine weight, $W_{brine} = W_{sat} - W_{dry}$.

2. Calculate the pore volume (saturated brine volume), $V_p = W_{sat}/\rho_{brine}$.

3. Calculate effective porosity, $\phi_e = V_p/V_b$.

Core No.:   *D*:   *cm*,   *L*:   *cm*.

W_{dry} (g)	W_{sat} (g)	W_{brine} (g)	V_p (cm^3)	ϕ_e

6. RESISTIVITY

6.1 Definitions

Porous rocks are comprised of solid grains and void space. The solids, with the exception of certain clay minerals, are nonconductors. The electrical properties of a rock depend on the geometry of the voids and the fluid with which those voids are filled. The fluids of interest in petroleum reservoirs are oil, gas, and water. Oil and gas are nonconductors. Water is a conductor when it contains dissolved salts, such as $NaCl$, $MgCl_2$, KCl normally found in formation reservoir water. Current is conducted in water by movement of ions and can therefore be termed *electrolytic conduction*.

The *resistivity* of a porous material is defined by

$$R = \frac{rA}{L} \tag{6.1}$$

where r = resistance, Ω
   A = cross-sectional area, m^2
   L = length, m

and resistivity is expressed in Ohm-meter ($\Omega.m$). However, for a complex material like rock containing water and oil, the resistivity of the rock depends on

- salinity of water
- temperature
- porosity
- pore geometry
- formation stress
- composition of rock.

The resistivity of an electric current in porous rock is due primarily to the movement of dissolved ions in the brine that fills the pore of the rock. The resistivity varies with temperature due to the increased activity of the ions in solution as temperature increases.

Due to the conductivity properties of reservoir formation water, the electrical well-log technique is an important tool in the determination of water saturation versus depth and thereby a reliable resource for in situ hydrocarbon evaluation.

The theory of the electrical resistivity log technique generally applied in petroleum engineering was developed by Archie in 1942, the so called Archie's equation. This empirical equation was derived for clean water-wet sandstones over a reasonable range of water saturation and porosities. In practice, Archie's equation should be modified according to the rock properties: clay contents, wettability, pore distribution, etc. The following is a brief presentation of the main electrical properties of reservoir rocks and related parameters.

Formation Factor: The most fundamental concept considering electrical properties of rocks is the formation factor F, as defined by Archie:

$$F = \frac{R_o}{R_w} \qquad (6.2)$$

where

R_o = the resistivity of the rock when saturated 100% with water, $\Omega.m$
R_w = the water resistivity, $\Omega.m$.

The formation factor shows a relationship between water saturated rock conductivity and bulk water conductivity. Obviously, the factor depends on the pore structure of the rock.

Resistivity Index: The second fundamental notion of electrical properties of porous rocks containing both water and hydrocarbons is the resistivity index I.

$$I = \frac{R_t}{R_o} \qquad (6.3)$$

where

R_t = the resistivity of the rock when saturated partially with water, $\Omega.m$
R_o = the resistivity of the same rock when saturated with 100% water, $\Omega.m$.

Tortuosity: Wyllie (52) developed the relation between the formation factor and other properties of rocks, like porosity ϕ and tortuosity τ. Tortuosity can be defined as $(L_a/L)^2$, where L is the length of the core and L_a represents the effective path length through the pores. Based on simple pore models the following relationship can be derived:

$$F = \frac{\tau}{\phi} \qquad (6.4)$$

where

F = formation factor
τ = tortuosity of the rock
ϕ = porosity of the rock.

Cementation factor: Archie suggested a slightly different relation between the formation factor and porosity by introducing the cementation factor:

$$F = \phi^{-m} \qquad (6.5)$$ where

ϕ = porosity of the rock
m = Archie's cementation factor.

Archie reported that the cementation factor probably ranged from 1.8 to 2.0 for consolidated sandstones and for clean unconsolidated sands was about 1.3.

Saturation Exponent: The famous Archie's equation gives the relationship of resistivity index with water saturation of rocks

$$I = \frac{R_t}{R_o} = S_w^{-n} \qquad\qquad (6.6) \text{where}$$

S_w = water saturation

n = saturation exponent, ranging from 1.4 to 2.2 ($n = 2.0$ if no data are given).

In this equation, R_t and R_o can be obtained from well logging data, saturation exponent n is experimentally determined in laboratory. Therefore, the in situ water saturation can be calculated with Archie's equation. Based on the material balance equation for the formation, $S_w + S_o + S_g = 1.0$, the hydrocarbon reserve in place may be calculated.

6.2 Effect of Conductive Solids

The clay minerals present in a natural rock act as a separate conductor and are sometimes referred to as "conductive solids". Actually, the water in the clay and the ions in the water act as the conducting materials. Fig. 6.1 shows variation of formation factor versus water resistivity for clean and clayey sands. The effect of the clay on the resistivity of the rock is dependent upon the amount, type and manner of distribution of the clay in the rock.
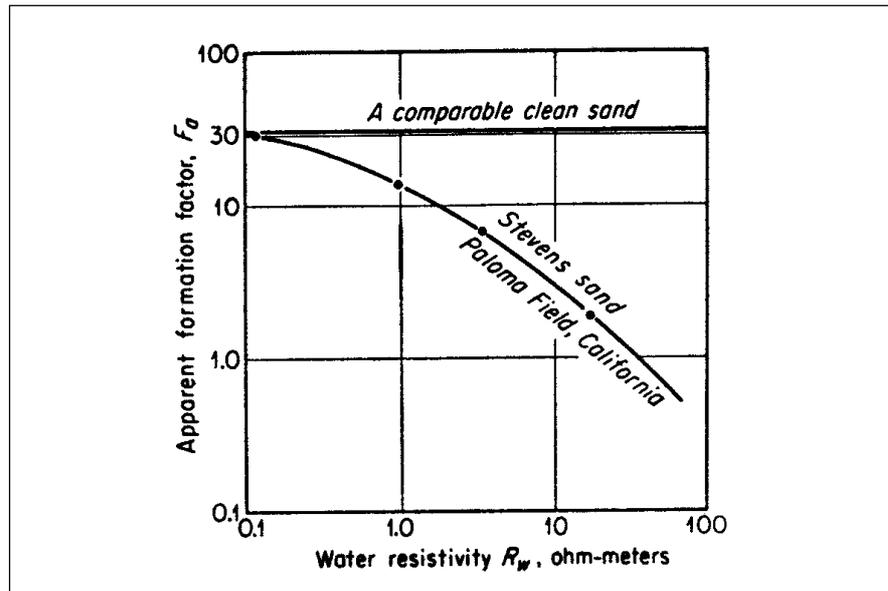
Fig. 6.1: Apparent formation factor versus water resistivity
for clayey and clean sands.

The formation factor for a clay-free sand is constant. The formation factor for clayey sand increases with decreasing water resistivity and approaches a constant value at a water resistivity of a bout 0.1 Ω.m. The apparent formation factor F_a was calculated from the definition of the formation factor and observed values of R_{oa} and R_w ($F_a = R_{oa}/R_w$). Wyllie proposed that the observed effect of clay minerals was similar to having two electrical circuits in parallel: the conducting clay minerals and the water-filled pores. Thus

$$\frac{1}{R_{oa}} = \frac{1}{R_c} + \frac{1}{FR_w} \qquad\qquad (6.7)$$

where R_{oa} is the resistivity of a shaly sand when 100% saturated with water of resistivity R_w. R_c is the resistivity due to the clay minerals. FR_w is the resistivity due to the distributed water, and F is the true formation factor of the rock (the constant value when the rock contains low-resistivity water).
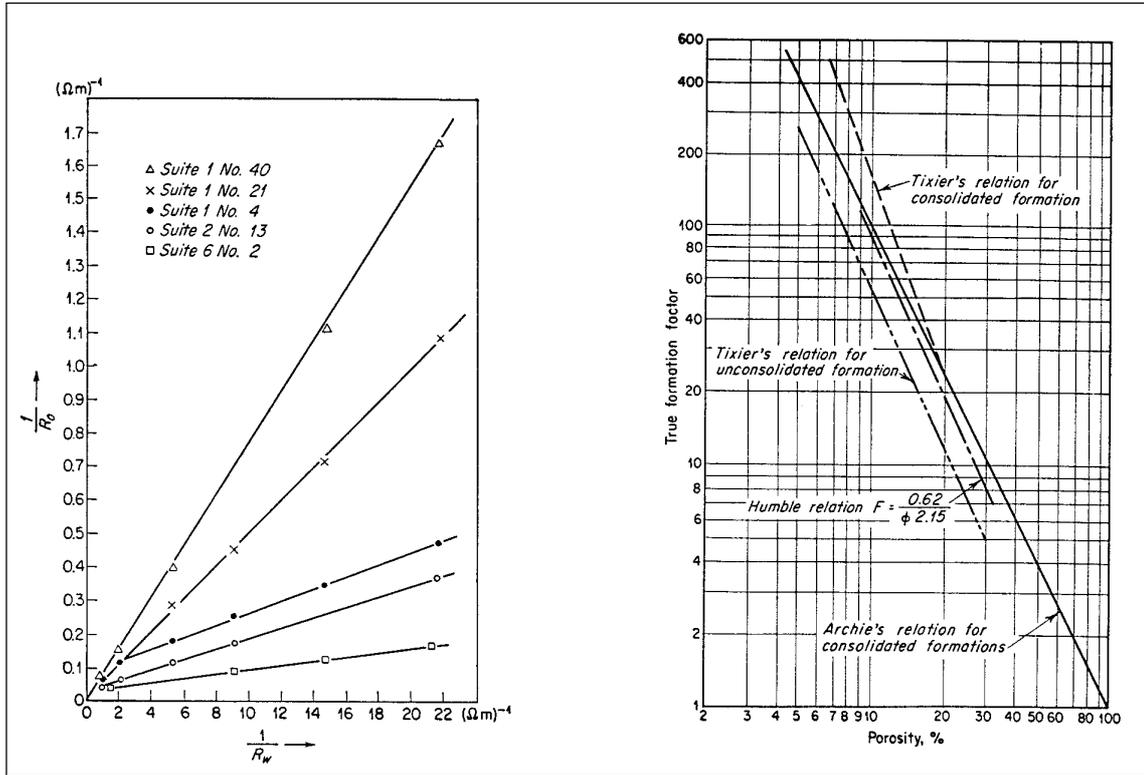
Fig. 6.2: Water-saturated rock conductivity as a function of water conductivity.

Fig.6.3: Formation factor as a function of porosity.

The data presented at the Fig. 6.2 represent graphically the confirmation of the relationship expressed in Eq. (6.7). The plots are linear and are of the general form

$$\frac{1}{R_{oa}} = C\frac{1}{R_w} + b \qquad\qquad (6.8)$$

where C is the slope of the line and b is the intercept. Comparing Eq. (6.7) with Eq. (6.8), it may be noted that $C = 1/F$ and $b = 1/R_c$. The line in which $b = 0$ indicates a clean sand, then

$$\frac{1}{R_{oa}} = C\frac{1}{R_w} = \frac{1}{FR_w} \qquad \text{or} \qquad R_o = FR_w \qquad\qquad (6.9)$$

Eq. (6.7) can be rearranged to express the apparent formation factor in term of R_c and FR_w

$$R_{oa} = \frac{R_c R_w}{R_w + \dfrac{R_c}{F}} \quad \text{and} \quad F_a = \frac{R_c}{R_w + \dfrac{R_c}{F}} \tag{6.10}$$

As $R_w \to 0$, $\displaystyle\lim_{R_w \to 0} F_a = \frac{R_c}{\dfrac{R_c}{F}} = F$. Therefore F_a approachs F as a limit as R_w become small.

This was observed in Fig. 6.1.

6.3   Effect of Overburden Pressure on Resistivity

Confinement or overburden pressure may cause a significant increase in resistivity. This usually occurs in rocks that are not well cemented and in lower porosity rocks. Archie, as mentioned before, reported results of correlating laboratory measurements of formation factor with porosity in the form

$$F = \phi^{-m} \tag{6.11}$$

Wyllie investigated the influence of particle size and cementation factor on the formation factor of a variety of materials. He concluded that the cemented aggregates exhibit a greater change in formation factor with a change in porosity than the unconsolidated aggregates. Then, the general form of the relation between formation factor and porosity should be

$$F = a\phi^{-m} \tag{6.12}$$

where m is a constant depending on cementation and a a constant controlled by the porosity of the unconsolidated matrix prior to cementation. A comparison of some suggested relationships between porosity and formation factor is shown in Fig. 6.3.

6.4   Resistivity of Partially Water-Saturated Rocks

When oil and gas are present within a porous rock together with a certain amount of formation water, its resistivity is larger than R_o since there is less available volume for the flow of electric current. This volume is a function of the water saturation S_w. Eq. (6.6) indicates that the resistivity index is a function of water saturation and the path depth. From the theoretical development, the following generalization can be drawn:

$$I = C'S_w^{-n} \tag{6.13}$$

where $I = R_t/R_o$ is the resistivity index, C' is some function of tortuosity and n is the saturation exponent. In Archie's equation n is 2.0 and in Williams relation 2.7 (Fig. 6.4). All the equations fitted to the experimental data have assumed that both C' and n of Eq. (6.13) were constants and furthermore that $C' = 1$.
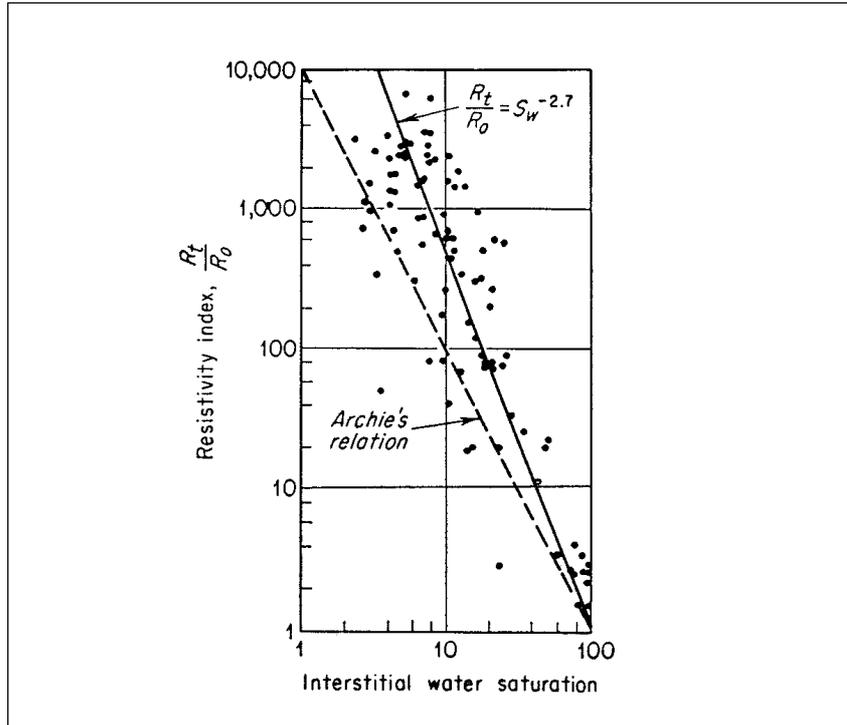
Fig. 6.4: Resistivity index versus water saturation.

The generally accepted formation which relates water saturations and true resistivity R_t is that of Archie, which may be written in the following different form:

$$S_w = \sqrt[n]{\frac{R_o}{R_t}} = \sqrt[n]{\frac{FR_w}{R_t}} = \sqrt[n]{\frac{R_w}{R_t}\frac{a}{\phi^m}} \qquad (6.14)$$

where a is unique property of the rock and n is the saturation exponent, which in most cases is assumed to be 2.0.

6.5   Experiments

6.5.1   Resistivity Measurements of Fluid-Saturated Rocks (Experiment 6)

Description:

The objective of this experiment is to measure the main electrical properties of porous rock like water resistivity, formation factor, tortuosity, cementation factor, resistivity index and saturation exponent.

Procedure:

Resistance measurements in our laboratory are a *ratio of voltage decrease method*, that is the ratio of voltage decrease between a reference resistor and a sample (to be measured) in series (Fig. 6.5). Then, the resistance of the sample is calculated and the resistivity of the sample can be developed when the size of the sample is known.
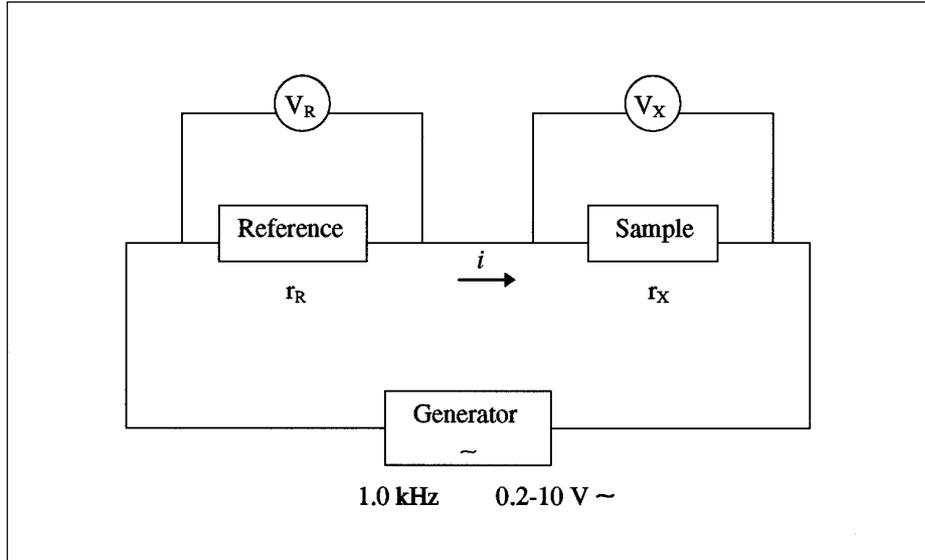
Fig. 6.5: The electrical circuit of resistance measurements.

Calculations and report:

1. Calculate water resistivity, R_w

Equation:

$$R_w = \frac{r_x A}{L} = \frac{r_x \pi D^2}{4L}$$

Reference resistance (r_R): Ω, V_X/V_R:

Water	Cell diameter D (m)	Cell length L (m)	Cell resistance, r_x (Ω)	Water resistivity R_w ($\Omega.m$)
36 g NaCl/l				

2. Calculate formation factor, F, tortuosity, τ, and cementation factor, m

Reference resistance (r_R): Ω, V_X/V_R:

Core No.	Core D (m)	Core L (m)	r_x (Ω)	R_o ($\Omega.m$)	Porosity ϕ	Cementation factor, m	Formation Factor, F	Tortu-osity, τ

R_w is equal to the value of R_w in (1).

3. Calculate resistivity index, I, saturation exponent, n

Reference resistance (r_R): Ω, V_X/V_R:

Core No.	Core D (m)	Core L (m)	r_x (Ω)	R_t ($\Omega.m$)	R_o ($\Omega.m$)	S_w	Resistivity Index, I	Saturation exponent, n

R_o is equal to the value of R_o in (2).

7. SURFACE AND INTERFACIAL TENSION

7.1 *Definitions*

Surface and interfacial tension of fluids result from molecular properties occurring at the surface or interface. Surface tension is the tendency of a liquid to expose a minimum free surface. Surface tension may be defined as the contractile tendency of a liquid surface exposed to gases. The interfacial tension is a similar tendency which exists when two immiscible liquids are in contact. In the following, interfacial tension will be denoted for both surface and interfacial tension.

Fig. 7.1 shows a spherical cap which is subjected to interfacial tension σ around the base of the cap and two normal pressures p_1 and p_2 at each point on the surface. The effect of the interfacial tension σ is to reduce the size of the sphere unless it is opposed by a sufficiently great difference between pressures p_1 and p_2.
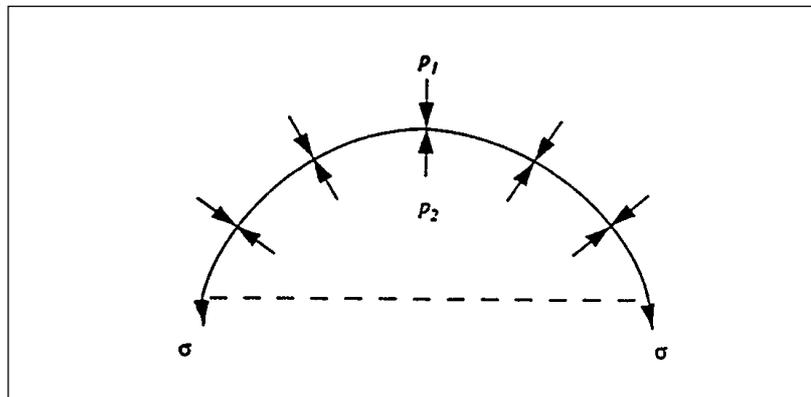
Fig. 7.1: Capillary equilibrium of a spherical cap.

The Young-Laplace equation for the mechanical equilibrium of an arbitrary surface is

$$p_2 - p_1 = \sigma \left(\frac{1}{r_1} + \frac{1}{r_2} \right) \tag{7.1}$$

where r_1 and r_2 are the principal radii of curvature. Introducing the mean radius of curvature r_m defined by

$$\frac{1}{r_m} = \frac{1}{2} \left(\frac{1}{r_1} + \frac{1}{r_2} \right) \tag{7.2}$$

The Young-Laplace equation becomes

$$p_1 - p_2 = \frac{2\sigma}{r_m} \qquad\qquad (7.3)$$

Note that the phase on the concave side of the surface must have pressure p_2 which is greater than the pressure p_1, on the convex side.

The surface tension of a liquid surface in contact with its own vapour or with air is found to depend only on the nature of the liquid, and on the temperature. Usually, surface tensions decrease as temperature increases.

7.2 Methods of Interfacial Tension Measurements

7.2.1 Capillary Rise Method

This method is based on rising of a liquid in a capillary tube and the fact that the height of the liquid, depends on interfacial tension. Let us consider a circular tube of radius r, wetted by the liquid to be tested. The liquid with density ρ immediately rises to a height h above the free liquid level in the vessel (Fig. 7.2). The column of liquid in the capillary must be held up against the gravity pull by a force, the so-called capillary suction. We may write

$$2\pi r \sigma \cos\theta (capillary\ suction) = g\rho h \pi r^2 (gravity\ pull)$$

where θ is contact angle between liquid and glass tube and g is acceleration of gravity.
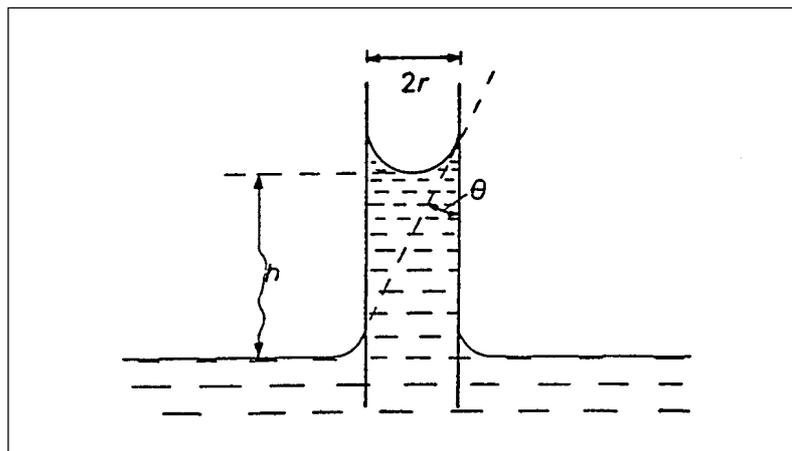
Fig. 7.2: Capillary-rise method.

Hence the value of σ is calculated by

$$\sigma = \frac{g\rho h r}{2\cos\theta} = \frac{r\Delta p}{2\cos\theta} \qquad (7.4)$$

where Δp is the hydrostatic pressure of the column of liquid in the capillary.

7.2.2   Wilhelmy Plate Method

A thin plate of glass or platinum will "carry" or hold up part of liquid which is in contact with the plate. The dynamic measurement of interfacial tension is shown in Fig. 7.3a. In this method, the necessary force to break the liquid film at this position will be determined

$$F = W_p + 2(x + y)\sigma \qquad (7.5)$$

where $2(x + y)$ is the contact area between the liquid and the plate, and W_p is the weight of the plate.
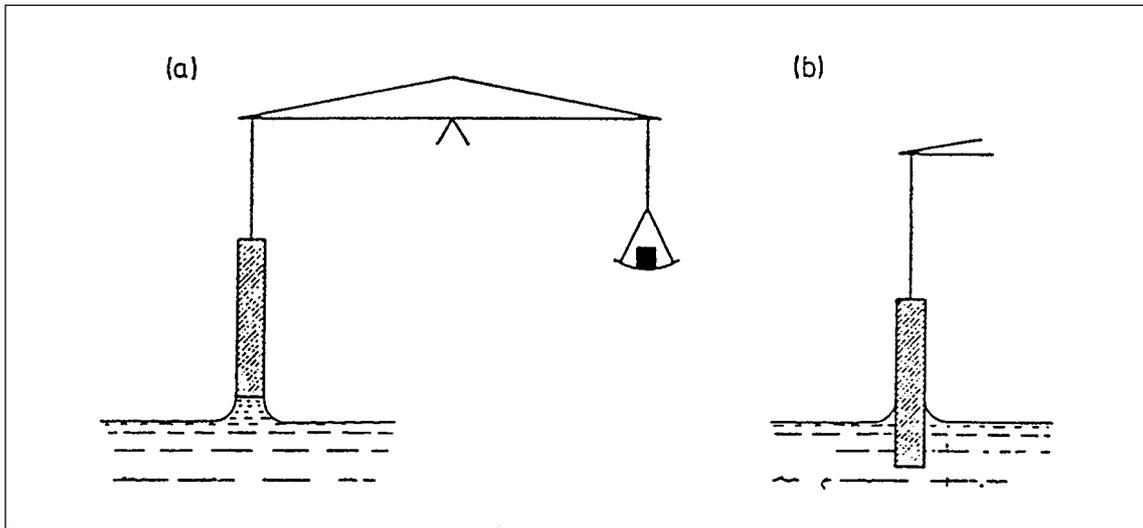
Fig. 7.3: Wilhelmy plate methods; Dynamic (a), and static method (b)

In the static method the plate is held at the position show in Fig. 7.3b, and the equation will be

$$F = W_p - b + 2(x + y)\sigma\cos\theta \qquad (7.6)$$

where b is buoyancy force of immersed part of the plate in the liquid and θ is contact angle.

This instrument can be calibrated such that the interfacial tension reads directly.

7.2.3 Ring Method

The ring or du Noüy method of measuring surface and interfacial tension is commonly used and the apparatus is called a ring tensiometer.

To measure interfacial tension, a platinum ring is placed in the test liquid. The force necessary to withdraw it from the liquid is determined (Fig. 7.4). When the ring is completely wetted by the liquid ($\theta = 0$), this equation is obtained

$$F = W_r - b + 2(2\pi r\sigma) \tag{7.7}$$

where F is measured force, r is radius of the ring at centre (the radius of the platinum thread is negligible compared to r), W_r is weight of the ring in air and b is buoyancy force of the ring immersed in the liquid. For interfacial measurements, the ring is placed in the interface and the force necessary to break the interfacial film with the ring is determined.
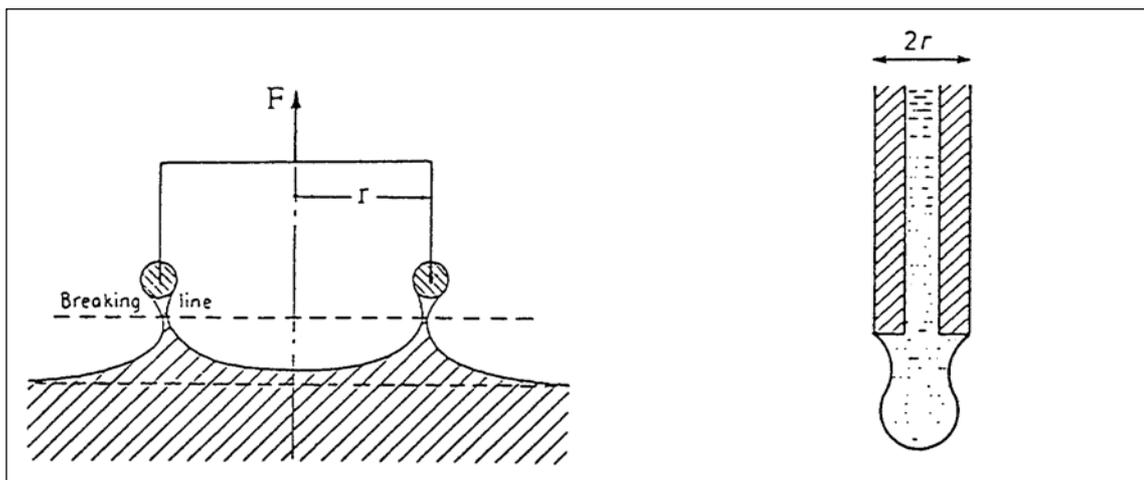
Fig. 7.4: Ring method.   **Fig. 7.5:** Hanging drop from a capillary tube.

The instrument can be regulated in such a way that the ring weight and buoyancy effect are taken care of with a correction factor C:

$$\sigma = C\frac{F}{2(2\pi r)} \tag{7.8}$$

7.2.4 Drop Weight Method

The drop weight method of measuring the interfacial tension of liquid with respect to air consists in determining the number of drops falling from a capillary. The drops are allowed to fall into a container until enough have been collected so that the weight per

drop can be determined accurately. The principle of the method is that the size of the drop falling from a capillary tube depends on the surface tension of the liquid (Fig. 7.5).

The maximum amount of liquid W, which can hang from a capillary tube with radius r without falling depends on the surface tension as

$$W = mg = 2\pi r \sigma \tag{7.9}$$

where m is the mass per drop. Observations of falling drops show that a considerable portion of the drop (up to 40%) may remain attached to the capillary end. This effect will be compensated with a correction factor f

$$\sigma = f \frac{mg}{2\pi r} \tag{7.10}$$

The correction factor f varies in the region of 0.5 to 1.0. The drop method can be used for the determination of both gas-liquid and liquid-liquid interfacial tensions.

7.2.5 Pendant Drop Method

Small drops will tend to be spherical because surface forces depend on area. In principle, one can determine the interface tension from measurements of the shape of the drop. In the case of the pendant drop, the most convenient and measurable shape dependent quantity is $S = d_s/d_e$. As indicated in Fig. 7.6, d_e is the equatorial diameter and d_s is the diameter measured distance d_e from the bottom of the drop. The interfacial tension can be calculated by the following equation

$$\sigma = \frac{\Delta \rho g d_e^2}{H} \tag{7.11}$$

where H is a shape determining variable. The relationship between the shape dependent quantity H and the experimentally measured shape dependent quantity S is determined empirically. A set of $1/H$ versus S values is obtained in form of tables (Tab. 7.1). The quantity of S is calculated after measuring d_e and d_s from shape of the pendant drop, and then $1/H$ can be determined from Tab. 7.1.
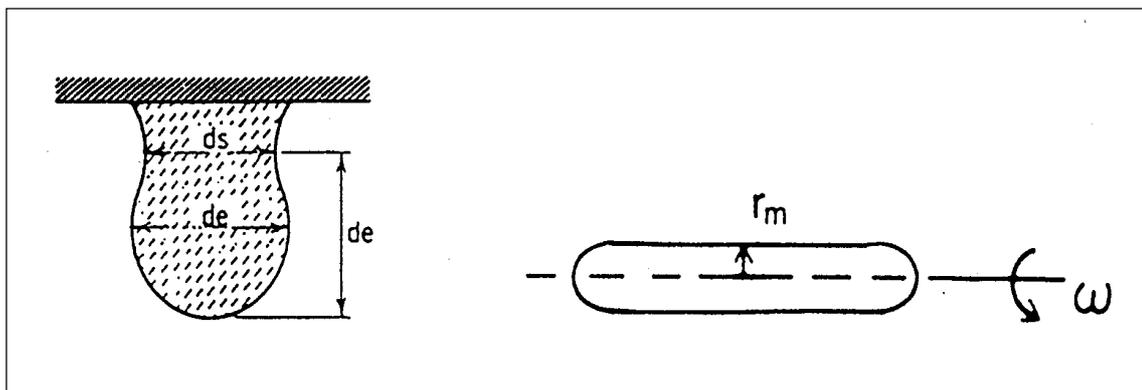
Fig. 7.6: Relationship between dimensions of a pendant drop.

Fig. 7.7: Schematic diagram of spinning drop.

The pendant drop method is widely used and has good accuracy.

Table 7.1: Values of 1/H versus S for pendant drop method.

s	0	1	2	3	4	5	6	7	8	9
0.30	7.09837	7.03966	6.98161	6.92421	6.86746	6.81135	6.75586	6.70099	6.64672	6.59306
0.31	6.53998	6.48748	6.43556	6.38421	6.33341	6.28317	6.23347	6.18431	6.13567	6.08756
0.32	6.03997	5.99288	5.94629	5.90019	5.85459	5.80946	5.76481	5.72063	5.67690	5.63364
0.33	5.59082	5.54845	5.50651	5.46501	5.42393	5.38327	5.34303	5.30320	5.26377	5.22474
0.34	5.18611	5.14786	5.11000	5.07252	5.03542	4.99868	4.96231	4.92629	4.89061	4.85527
0.35	4.82029	4.78564	4.75134	4.71737	4.68374	4.65043	4.61745	4.58479	4.55245	4.52042
0.36	4.48870	4.45729	4.42617	4.39536	4.36484	4.33461	4.30467	4.27501	4.24564	4.21654
0.37	4.18771	4.15916	4.13087	4.10285	4.07509	4.04759	4.02034	3.99334	3.96660	3.94010
0.38	3.91384	3.88786	3.86212	3.83661	3.81133	3.78627	3.76143	3.73682	3.71242	3.68824
0.39	3.66427	3.64051	3.61696	3.59362	3.57047	3.54752	3.52478	3.50223	3.47987	3.45770
0.40	3.43572	3.41393	3.39232	3.37089	3.34965	3.32858	3.30769	3.28698	3.26643	3.24606
0.41	3.22582	3.20576	3.18587	3.16614	3.14657	3.12717	3.10794	3.08886	3.06994	3.05118
0.42	3.03258	3.01413	2.99583	2.97769	2.95969	2.94184	2.92415	2.90659	2.88918	2.87192
0.43	2.85479	2.83781	2.82097	2.80426	2.78769	2.77125	2.75496	2.73880	2.72277	2.70687
0.44	2.69110	2.67545	2.65992	2.64452	2.62924	2.61408	2.59904	2.58412	2.56932	2.55463
0.45	2.54005	2.52559	2.51124	2.49700	2.48287	2.46885	2.45494	2.44114	2.42743	2.41384
0.46	2.40034	2.38695	2.37366	2.36047	2.34738	2.33439	2.32150	2.30870	2.29600	2.28339
0.47	2.27088	2.25846	2.24613	2.23390	2.22176	2.20970	2.19773	2.18586	2.17407	2.16236
0.48	2.15074	2.13921	2.12776	2.11640	2.10511	2.09391	2.08279	2.07175	2.06079	2.04991
0.49	2.03910	2.02838	2.01773	2.00715	1.99666	1.98623	1.97588	1.96561	1.95540	1.94527
0.50	1.93521	1.92522	1.91530	1.90545	1.89567	1.88596	1.87632	1.86674	1.85723	1.84778
0.51	1.83840	1.82909	1.81984	1.81065	1.80153	1.79247	1.78347	1.77453	1.76565	1.75683
0.52	1.74808	1.73938	1.73074	1.72216	1.71364	1.70517	1.69676	1.68841	1.68012	1.67188
0.53	1.66369	1.65556	1.64748	1.63946	1.63149	1.62357	1.61571	1.60790	1.60014	1.59242
0.54	1.58477	1.57716	1.56960	1.56209	1.55462	1.54721	1.53985	1.53253	1.52526	1.51804
0.55	1.51086	1.50373	1.49665	1.48961	1.48262	1.47567	1.46876	1.46190	1.45509	1.44831
0.56	1.44158	1.43489	1.42825	1.42164	1.41508	1.40856	1.40208	1.39564	1.38924	1.38288
0.57	1.37656	1.37028	1.36404	1.35784	1.35168	1.34555	1.33946	1.33341	1.32740	1.32142
0.58	1.31549	1.30958	1.30372	1.29788	1.29209	1.28633	1.28060	1.27491	1.26926	1.26364
0.59	1.25805	1.25250	1.24698	1.24149	1.23603	1.23061	1.22522	1.21987	1.21454	1.20925
0.60	1.20399	1.19875	1.19356	1.18839	1.18325	1.17814	1.17306	1.16801	1.16300	1.15801
0.61	1.15305	1.14812	1.14322	1.13834	1.13350	1.12868	1.13389	1.11913	1.11440	1.10969
0.62	1.10501	1.10036	1.09574	1.09114	1.08656	1.08202	1.07750	1.07300	1.06853	1.06409
0.63	1.05967	1.05528	1.05091	1.04657	1.04225	1.03796	1.03368	1.02944	1.20522	1.02102
0.64	1.01684	1.01269	1.00856	1.00446	1.00037	0.99631	0.99227	0.98826	0.98427	0.98029
0.65	0.97635	0.97242	0.96851	0.96463	0.96077	0.95692	0.95310	0.94930	0.94552	0.94176
0.66	0.93803	0.93431	0.93061	0.92693	0.92327	0.91964	0.91602	0.91242	0.90884	0.90528
0.67	0.90174	89822	89471	89122	88775	88430	88087	87746	87407	87069
0.68	86733	86399	86067	85736	85407	85080	84755	84431	84110	83790
0.69	83471	83154	82839	82525	82213	81903	81594	81287	80981	80677
0.70	80375	80074	79774	79477	79180	78886	78593	78301	78011	77722
0.71	77434	77148	76864	76581	76299	76019	75740	75463	75187	74912
0.72	74639	74367	74097	73828	73560	73293	73028	72764	72502	72241
0.73	71981	71722	71465	71208	70954	70700	70448	70196	69946	69698
0.74	69450	69204	68959	68715	68472	68230	67990	67751	67513	67276
0.75	67040	66805	66571	66338	66107	65876	65647	65419	65192	64966
0.76	64741	64518	64295	64073	63852	63632	63414	63196	62980	62764
0.77	62550	62336	62123	61912	61701	61491	61282	61075	60868	60662
0.78	60458	60254	60051	59849	59648	59447	59248	59050	58852	58656
0.79	58460	58265	58071	57878	57686	57494	57304	57114	56926	56738
0.80	56551	56364	56179	55994	55811	55628	55446	55264	55084	54904
0.81	54725	54547	54370	54193	54017	53842	53668	53494	53322	53150
0.82	52978	52800	52638	52469	52300	52133	51966	51800	51634	51470
0.83	51306	51142	50980	50818	50656	50496	50336	50176	50018	49860
0.84	49702	49546	49390	49234	49080	48926	48772	48620	48468	48316

0.85	48165	48015	47865	47716	45760	47420	47272	47126	46984	46834
0.86	46690	46545	46401	46258	46116	45974	45832	45691	45551	45411
0.87	45272	45134	44996	44858	44721	44585	44449	44313	44178	44044
0.88	43910	43777	43644	43512	43380	43249	43118	42988	42858	42729
0.89	42600	42472	42344	42216	42089	41963	41837	41711	41586	41462
0.90	41338	41214	41091	40968	40846	40724	40602	40481	40361	40241
0.91	40121	40001	39882	39764	39646	39528	39411	39294	39178	39062
0.92	38946	38831	38716	38602	38488	38374	38260	38147	38035	37922
0.93	37810	37699	37588	37477	37367	37256	37147	37037	36928	36819
0.94	36711	36603	36495	36387	36280	36173	36067	35960	35854	35749
0.95	35643	35538	35433	35328	35224	35120	35016	34913	34809	34706
0.96	34604	34501	34398	34296	34195	34093	33991	33890	33789	33688
0.97	33587	33487	33386	33286	33186	33086	32986	32887	32787	32688
0.98	32588	32489	32390	32290	32191	32092	31992	31893	31793	31694
0.99	31594	31494	31394	31294	31194	31093	30992	30891	30790	30688
1.00	30586	30483	30379							

7.2.6   Spinning Drop

In this method, a drop of a less dense fluid is injected into a container of the denser fluid, and the whole system is rotated as shown in Fig. 7.7. In the resulting centrifugal field, the drop elongates along the axis of rotation. The interfacial tension opposes the elongation because of the increase in area and a configuration which minimises system free energy is reached. The method is similar to that for the pendant drop with the gravitational acceleration g replaced by the appropriate acceleration term for a centrifugal field.

If the fluid densities are ρ_A and ρ_B, and the angular velocity ω of rotation are known, then interfacial tension can be calculated from the measured drop profile. When drop length is much greater than the radius r_m, the following approximate expression holds

$$\sigma = \frac{(\rho_A - \rho_B)\omega^2 r_m^3}{4}$$

(7.12)

The spinning drop device has been widely used in recent years to measure very low interfacial tensions. Unlike the other methods, no contact between the fluid interface and a solid surface is required.

7.3   Experiments

7.3.1   Interfacial Tension (IFT) Measurement, Pendant Drop Method (Experiment 7)

Pendant drop method is applied to determine the interfacial tension between two liquids. The method is intended for application to liquid pairs with normal interfacial tensions (not too low and too high).

Procedure:

The pendant drop IFT measurements will be performed together with contact angle measurements and the contact angle apparatus is used (Experiment 9), so refer to this experiment for apparatus description.

1. Fill the cell with oil.

2. Form a pendant drop of water with a syringe (diameter 1.1 mm).

3. Focus the drop and take imaging picture by photo.

4. Measure d_e and d_s, and then calculate S.

5. Determine $1/H$ from Tab. 7.1.
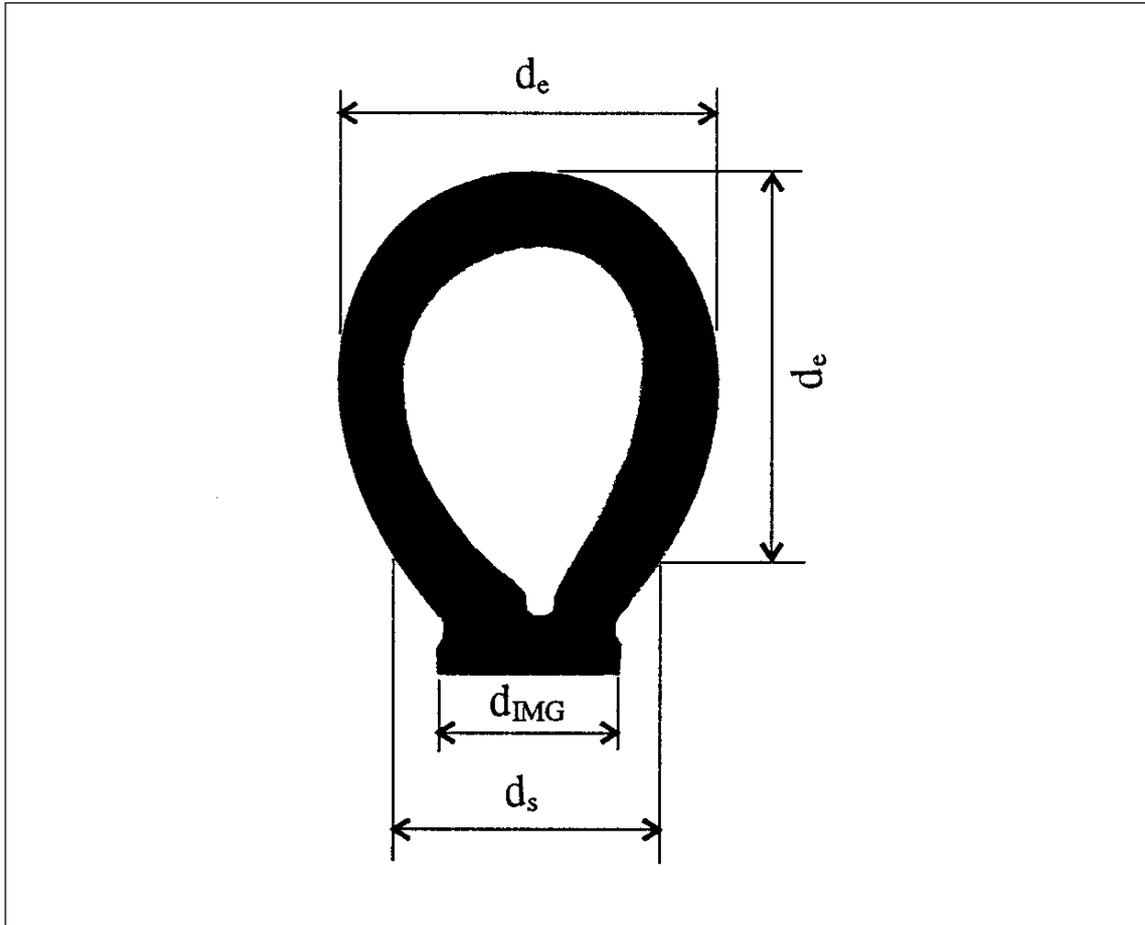
Fig. 7.8: Pendant drop imaging picture.

Calculations and report

Temperature: ^{0}C

Sys- tem	ρ_w (g/cm^3)	ρ_o (g/cm^3)	$\Delta\rho$ (g/cm^3)	Image picture sizes			S (d_s/d_e)	1/H	σ (dyne/ cm)
				d_e (mm)	d_s (mm)	d_{IMG} (mm)			

Equation:

$$\sigma = \frac{\Delta\rho g D_e^2}{H}$$

where $g = 981$ cm/s2

D_e (real size of d_e) = $d_e(1.1/d_{IMG})$, mm.

44

7.3.2 Measurement of IFT with the Ring Tensiometer (Experiment 8)

Description:

This hanging ring method is also called Du Nouy method. The method can determine the interfacial tension of reservoir fluids or petroleum products at typical ambient laboratory temperature and atmospheric pressure.

Definition:

The surface or interfacial tension in the liquid film is the ratio of the surface force to the length (perpendicular to the force) along which the force acts.

$$\sigma = \frac{\text{surface force, F}}{\text{length along which force acts}}$$

Procedure:

1. Calibration of tensiometer.

2. Brine and oil interfacial tension measurements. Two or three readings should be taken, so an average value may be used for calculating apparent interfacial tension.

Calculation and report:

To obtain the true interfacial tension σ, the following relationship will be used:

$$\sigma = \sigma_a.C \tag{7.13}$$

where
σ = the true interfacial tension, dynes/cm
σ_a = the measured apparent value, dynes/cm
C = the correction factor.

The correction factor C is dependent on the size of ring, the diameter of the wire used in the ring, the apparent interfacial tension, and the densities of the two phases. The relationship is expressed by the following equation

$$C = 0.7250 + \sqrt{\frac{0.01452\sigma_a}{l^2(\rho_l - \rho_u)} + 0.04534 - \frac{1.679r}{R}} \tag{7.14}$$

where
C = correction factor
R = radius of the ring, cm
r = radius of the wire of the ring, cm
σ_a = apparent surface or interfacial tension, dynes/cm

ρ_l = density of the lower phase, g/cm^3
ρ_u = density of the upper phase, g/cm^3
l = circumference of the ring, cm

If surface tension was measured in the container which has been open to the air during measuring, air density may be approximated by the equation:

$$\rho_{air} = 4.324 \times 10^{-2}(P/T) \qquad\qquad (7.15)$$

where
ρ_{air} = air density at p and T, g/cm^3
p = pressure, psia (= 14.7 psia)
T = temperature, ^{0}R (= 1.8 (T^{0}C + 273.15))

Temperature: ^{0}C

Measurement	Correction factor, C	Apparent value, σ_a (dynes/cm)	True value, σ (dynes/cm)
σ_{avr} (air/water) =			
σ_{avr} (oil/water) =			

8. CONTACT ANGLE AND WETTABILITY

8.1 Definitions

When a liquid is brought into contact with a solid surface, the liquid either expand over the whole surface or form small drops on the surface. In the first case the liquid will wet the solid completely, whereas in the later case a contact angle θ >0 will develop between the surface and the drop.

When two immiscible fluids contact a solid surface, one of them tends to spread or adhere to it more so than the other. For example, for water-oil-solid system at equilibrium, the following equation (known as Young's equation) can be expressed

$$\sigma_{SO} - \sigma_{SW} = \sigma_{SO} \cos\theta \qquad (8.1)$$

where σ_{so} is the interfacial tension between the oil and solid, σ_{sw} between the water and solid, σ_{wo} between the oil and water. θ is the contact angle measured through the water phase (Fig. 8.1).
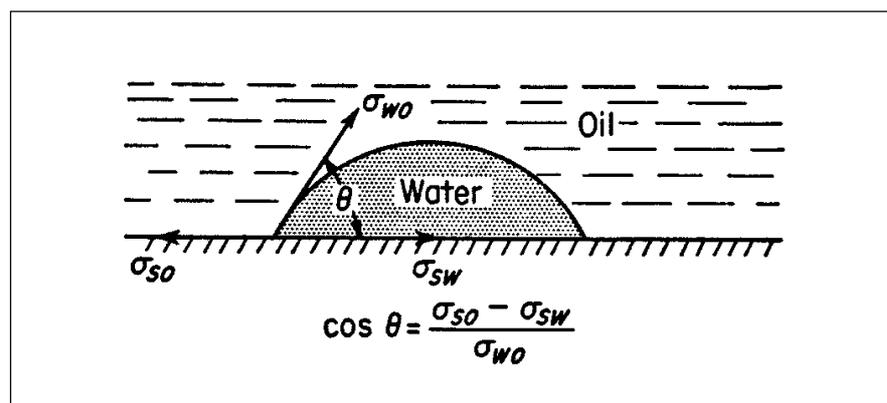
Fig. 8.1: Interfacial tensions for water-oil-solid system at equilibrium.

Adhesion tension, which is a function of the interfacial tension, determines which fluid preferentially wets the solid. In the case of water-oil-solid, the adhesion tension A_T is defined as

$$A_T = \sigma_{so} - \sigma_{sw} = \sigma_{wo} \cos\theta \qquad (8.2)$$

A positive adhesion tension A_T indicates that water preferentially wets the solid surface (water wet). An A_T of zero indicates that both phases have an equal affinity for the surface (neutral system). A negative A_T indicates the oil wets the solid surface (oil wet). The magnitude of the adhesion tension determines the ability of the wetting phase to adhere to the solid and to spread over the surface of the solid.

Wettability of a reservoir rock-fluid system is defined as the ability of one fluid in the presence of another to spread on the surface of the rock. Wettability play an important role in the production of oil and gas as it not only determines initial fluid distributions, but also is a main factor in the flow processes in the reservoir rock. The degree of wetting of solid by liquids is usually measured by the contact angle that a liquid-liquid interface makes with a solid.

Based on the contact angle, the *wetting index WI* is defined according to the tabulation below:

Wetting Index $\cos\theta$	Contact angle θ	Wetting condition
1.0	0^0	completely water wetted
0	90^0	neutral system
-1.0	180^0	completely oil wetted

The limits of the scales are not definite, since a system with contact angle in the range of about 70^0 to 110^0 is considered neutral. Another scaling system is used during Experiment 9.

Another definition related to wetting is *spreading wetting*. In spreading wetting the adhesion forces between the liquid and the solid are greater than the cohesive forces between the liquid molecules, and the liquid will spread on the surface as a thin film. The spreading coefficient *S* is defined by the expression

$$S = -\frac{dG}{dA} = \sigma_{so} - \left(\sigma_{sw} + \sigma_{ow} \right) \tag{8.3}$$

where *dG* is the free energy increase due to spreading and *dA* is change in interfacial area. The liquid spreads spontaneously over the solid surface when *S* is positive or zero. When *S* is negative the liquid remains as a drop having a definite angle of contact with the solid surface. The equilibrium contact angle is such that the total surface free energy of the system is minimum.

To illustrate that, the quantitative relation between interfacial tension, contact angle and spreading coefficient are tabulated below:

Relative values	θ	S
$\sigma_{so} < \sigma_{sw}$	$90^0 < \theta < 180^0$	$S < 0$
$\sigma_{so} = \sigma_{sw}$	$\theta = 90^0$	$S < 0$
$\sigma_{sw} < \sigma_{so} < \sigma_{sw} + \sigma_{ow}$	$0^0 < \theta < 90^0$	$S < 0$
$\sigma_{so} = \sigma_{sw} + \sigma_{ow}$	$\theta = 0^0$	$S = 0$
$\sigma_{so} > \sigma_{sw} + \sigma_{ow}$	θ does not exist	$S > 0$

The wettability of a reservoir rock system will depend on the following factors

- Reservoir rock material and pore geometry
- Geological mechanisms (accumulation and migration)
- Composition and amount of oil and brine
- Physical conditions; pressure and temperature
- Mechanisms occurring during production; i.e. change in saturations, pressure and composition.

Note that it is difficult to make a general model of wettability including all these factors. Although a lot of work has been done on wettability, it is not fully understood how the wettability of a porous rock surface is composed.

8.2 Measurement of Wettability

No satisfactory method exists for in situ measurement of wettability, and therefore it is necessary to estimate the wettability from laboratory measurements.

To obtain representative information on wetting preferences in the reservoir from laboratory experiments, the following conditions should be fulfilled:

- The method should not damage the surface properties of the rock.
- The method should enable differentiation of entire range of wettability from very water-wet to very oil-wet.
- The results should include the effects of microheterogeneities of the rock (except where ideal systems are used).
- The results should not depend on parameters such as rock permeability and fluid viscosity unless these parameters can be isolated.
- The results should be reproducible both with respect to a given core sample and also between different cores having the same rock properties.

One way in which this can be done directly is by using the method of contact angle measurement by photographing a drop. Other indirectly methods are based on measurement on core samples. Three methods have been found worth discussing in more detail. These methods are:

- The Amott method
- The centrifuge method
- The contact angle method.

8.2.1 Measurements on Core Samples

In porous media the contact angle is determined indirectly. The methods are mainly based on measurements during displacement tests. But the problem is that no valid theory is developed for the relationship between displacement pressure and wetting preference.

The most common methods for measuring wettability on core samples are

- Displacement test with two different fluids
- Capillary pressure measurements
- Measurements of nuclear magnetic relaxation rate
- Measurement of dye absorption
- Imbibition measurements
- Imbibition and displacement (Amott method).

The test developed by Amott seems to be most accepted and widely used test in the oil industry.

8.2.1.1 The Amott Method

In principle, a core sample is chosen and saturated with oil. The oil-saturated sample is then placed in an imbibition cell surrounded by water. The water is allowed to imbibe into the core sample displacing oil out of the sample until equilibrium is reached (Fig. 8.2a). The volume of water imbibed is measured.

The core sample is then removed and the remaining oil in the sample is forced down to residual saturation by displacement with water. This may be done either in a centrifuge or displaced with a pump in a sealed core holder. The volume of oil displaced may be measured directly or determined by weight measurements.
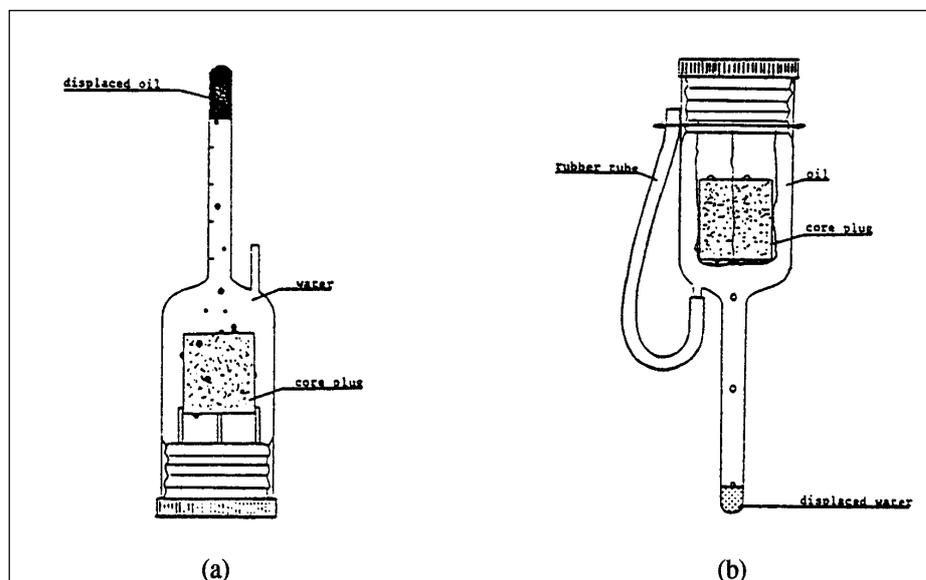
Fig. 8.2: Imbibition cell with oil saturated core plug surrounded by water (a) and water saturated core plug surrounded by oil (b).

The core, now saturated with water at residual oil saturation, is placed in an imbibition cell and surrounded by oil. The oil is allowed to imbibe into the core displacing water out

of the sample (Fig. 8.2b). The volume of water displaced is measured (equal to volume of oil imbibed). The core is removed from the cell after equilibrium is reached, and remaining water in the core is forced out by displacement in a centrifuge. The volume of water displaced is measured.

By recording all volumes produced, it is possible to calculate a wettability-index WI

$$WI = \frac{V_{O1}}{V_{O1} + V_{O2}} - \frac{V_{W1}}{V_{W1} - V_{W2}} = r_W - r_O \qquad (8.4)$$

where V_{O1} = volume of oil produced during water imbibition
V_{O2} = volume of oil produced during water flooding
V_{W1} = volume of water produced during oil "imbibition"
V_{W2} = volume of water produced during oil flooding
r_w = displacement-with-water-ratio
r_o = displacement-with-oil-ratio.

The wettability index will be a number between –1.0 and 1.0 where

$WI = 1.0$ completely water wetting
$WI = 0.0$ neutral
$WI = -1.0$ completely oil wetting.

The test is a fully empirical test but is based on some theoretical reasoning. A drawback is that the tests are difficult to perform at reservoir pressure and temperature.

8.2.1.2 The Centrifuge Method

The centrifuge method for determining wettability is based on a correlation between the degree of wetting and the areas under the capillary pressure curves. The method employs the two areas under the oil-water capillary pressure curves obtained from the centrifuge method (Fig. 8.3).

The examples in Fig. 8.3 show capillary-pressures for a water wet, oil wet and neutral system. The procedure to obtain a set of curves is as follows:

1. A core sample is saturated with brine.
2. The core is then placed in a centrifuge core holder.
3. The core holder is filled with oil and rotated at a certain speeds to obtain curve I (primary drainage) in Fig. 8.3.
4. The core is placed in an inverted core holder filled with brine. The brine is allowed to spontaneously imbibe into the core. Then the core is centrifuged at incremental steps (curve II of Fig. 8.3 - forced imbibition).
5. The core is placed in a core holder filled with oil and curve III (secondary drainage) is obtained in the centrifuge.
6. The areas under the two curves (II and III) are determined.

The method is often called the USBM-method (USBM is abbreviation for United States Bureau of Mines).
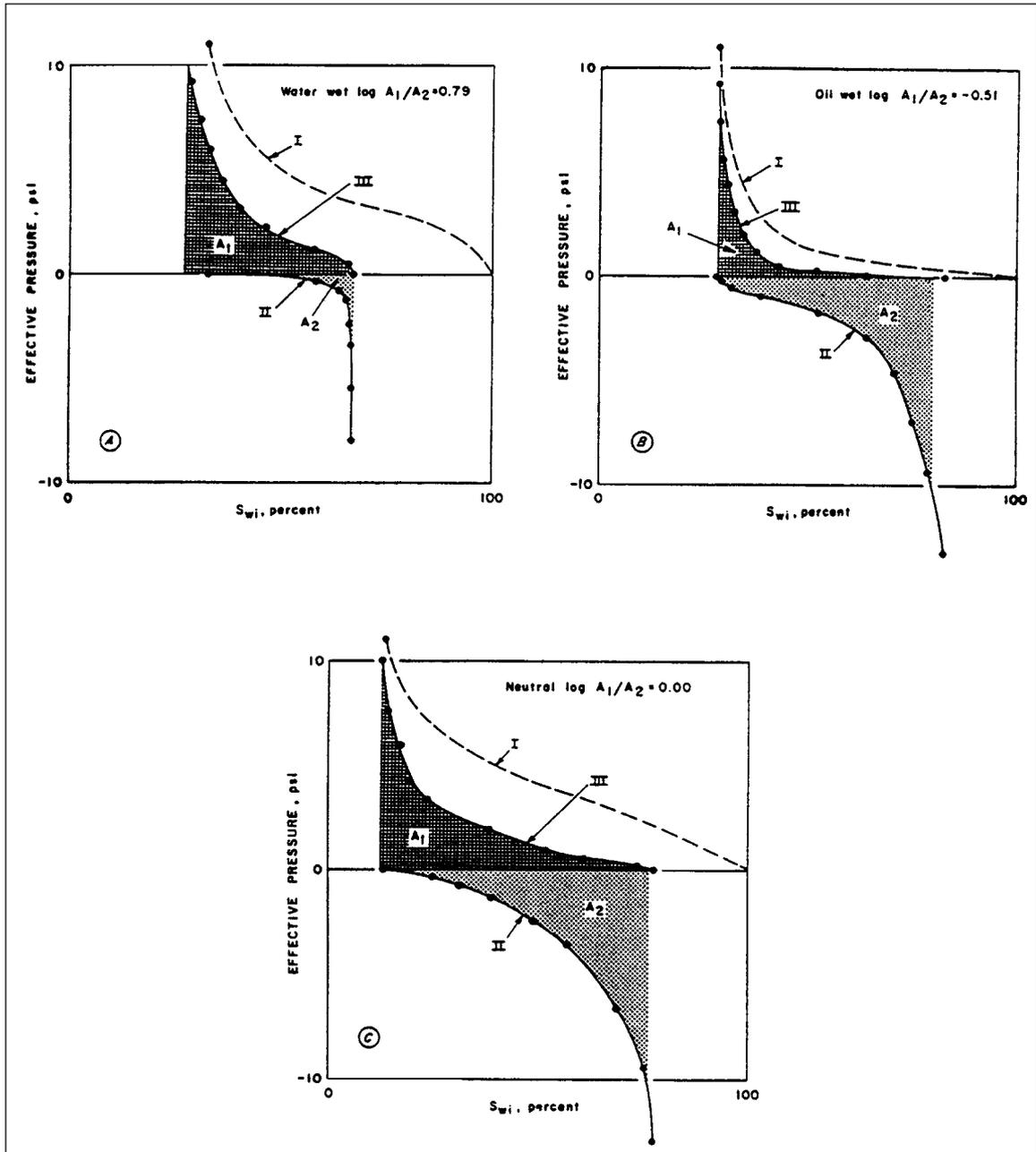
Fig. 8.3: Effect of wettability on the area ratio of capillary-pressure curves:
(A) water wet, (B) oil wet and (C) neutral system.

We select the logarithm of the area ratio to define the wettability scale; $WI_{USBM} = log(A_1/A_2)$. The relative wetting tendencies of the liquids in a porous medium and the distribution of pore sizes determine the shape of the capillary-pressure curves. In general, water-wet systems should have a larger area in the water-displaced-by-oil curves (area A_1 of Fig. 8.3A) than the area under the oil-displaced-by-water curves (area A_2 of Fig. 8.3A). Therefore, the logarithm of the area ratio for the water-wet system is greater than zero. Conversely, the area ratio is less than unity for oil-wet systems (Fig. 8.3B) and the logarithm of the ratio is negative. Fig. 8.3C shows a case where the ratio is close to 1.0.

The method has been tested against the Amott-test, and the two tests gave generally consistent results. The centrifuge test, however, seemed to differentiate better in the near-neutral area.

The centrifuge method is rapid, employs native fluids, and the test was found to be independent of oil viscosity. The method is better physically and mathematically grounded than the Amott-test. As for the Amott method, the method is difficult to perform at elevated pressures (reservoir conditions).

8.2.2   Contact Angle Measurements

There exist a variety of methods for measuring contact angle such as tilting plate method, Wilhelmy gravitational method and capillary rise method. The commonly used method is to measure contact angle directly for a drop of liquid resting on a plane surface of the solid, the so-called imaging method.

8.2.2.1 The Contact Angle/Imaging Method

The measurement of contact angles is based on Young's equation. When placing a drop of liquid on a solid surface, a finite angle of contact will in most cases be observed. However, complete spreading may also occur and then Young's equation ceases to hold.

The measurement of contact angle is simple in concept, but in practice it is a very complex topic and the interpretation of results is not straightforward. The measurement puts up severe demands to the cleaning procedures and the preparation of fluids and solid surface. The contact angle between oil, water and a solid surface will depend on the following:

- crude oil composition
- surface electric properties (pH and salt content of water)
- the solid surface itself
- roughness and heterogeneity of the solid surface
- dynamic effects
- pressure and temperature

In practice, in a porous material it is even more complex because of different pore shapes and complex mineralogy.

The solid surface must be carefully polished, and measurements on mineral surfaces are often performed on the natural plane of cleavage. A drop of liquid is placed on the solid surface and an enlarged image of the drop is obtained by photographing. The dimensions of the drop image are measured and used to determine the contact angle.

Contaminations will effect the contact angle, so the cleaning procedures are critical. Most contact angle measurements are performed at room conditions, and this is often due to the time consuming cleaning procedures necessary for measurement at high pressure and temperature and complex and costly apparatus needed.

Contact angle measurements can also be performed at reservoir conditions, which is one of the main advantages in crude oil-brine-rock system, as it has been shown that especially temperature may change the wettability significantly.

8.3 Experiments

8.3.1 Contact Angle Measurement using Imaging Method (Experiment 9)

Contact angle measurement is a classical method widely used in chemical engineering to derive the wettability in three-phase system (gas/liquid/solid, or liquid/liquid/solid). The method was introduced into petroleum engineering more than 50 years ago. This method is used to determine reservoir formation wettability. The *imaging method* is easily carried out in the laboratory and gives you a clear understanding of wetting mechanism in oil-water-rock system.

Generally, sandstone formation and carbonate formation are represented by small polished quartz and carbonate blocks, respectively. A small drop (2-3 mm^3) of water is laid on the smooth surface of rock which has previously been submerged in an oil-filled transparent cell. Then, the enlarged image of the water drop is obtained by photographing. The dimensions of the drop image are used to calculate the contact angle in the system.

Definition:

Fig. 8.1 shows two liquids, oil and water, in contact with a solid. In petroleum engineering the contact angle, θ, is measured through the denser liquid phase (water), and ranges from 0 to 180^0. In a three phase system, where the three interfacial forces are in thermodynamic equilibrium:

$$\sigma_{so} - \left(\sigma_{sw} + \sigma_{wo}\cos\theta_{wo}\right) = 0 \qquad (8.1)$$

and then,

$$\theta_{wo} = \cos^{-1}\left(\frac{\sigma_{so} - \sigma_{sw}}{\sigma_{wo}}\right) \qquad (8.5)$$

Because the measurements of solid/liquid interfacial tensions (σ_{so}, σ_{sw}) are impractical in the core laboratory, Eq. (8.5) is useless to calculate contact angle θ. Generally, the *image method* is used to obtain the picture of the contact angle or pendant drop. Fig. 8.4 is the set-up of an image system applied in our laboratory.
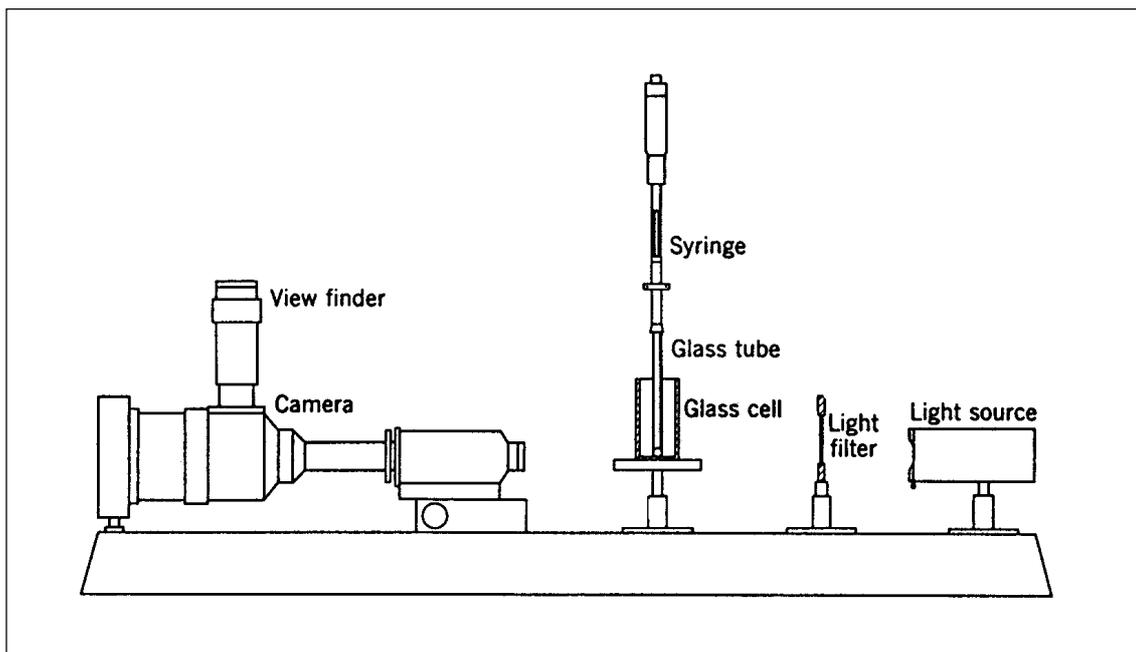
Fig. 8.4: The image system set-up.

Procedure:

1. Fill the cell with oil phase and then put a polished quartz or carbonate cube into the cell

2. Carefully inject several water drops onto the cube surface with a medical syringe.

3. Adjust the imaging system until a drop is in focus (a clear outline of the image appears on the screen).

4. Take image picture and measure the dimension of the drop image.

Calculations and report:

Temperature: ^0C

system	dimension, *mm*		contact angle, degree	system wettability
	H	D		

Equation:

$$\theta = 2\tan^{-1}\left(\frac{2H}{D}\right)$$

$\theta < 62^0$-----water-wet, $\qquad \theta = 62^0$-133^0-----intermediate-wet, $\qquad \theta > 133^0$-----oil-wet
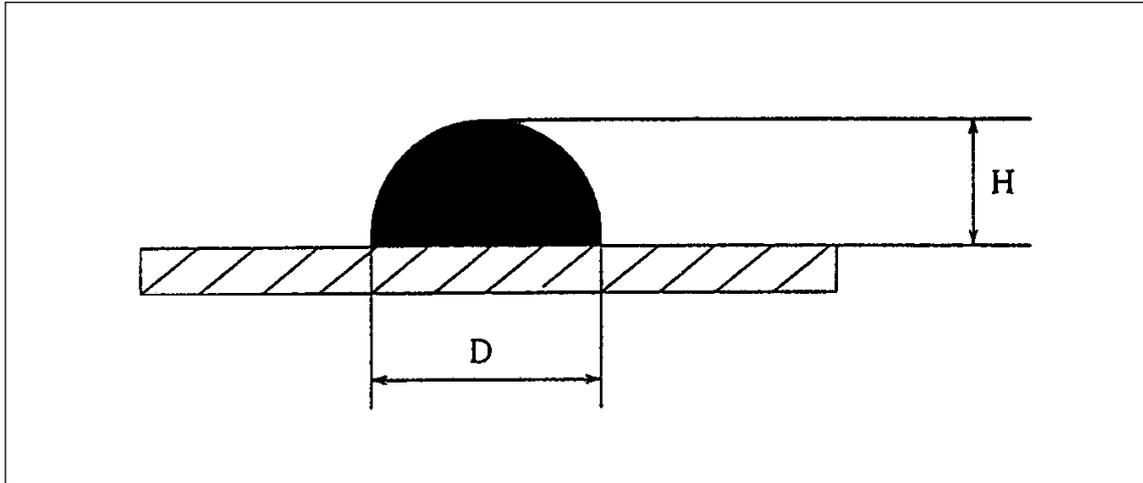
9. CAPILLARY PRESSURE

9.1 Definitions

When two immiscble fluids are in contact in the interstices of a porous medium, a discontinuity in pressure exists across the interface separating them. The difference in pressure P_c is called capillary pressure, which is pressure in the non-wetting phase minus the pressure in the wetting phase

$$P_c = P_{non-wetting} - P_{wetting} \tag{9.1}$$

Thus, the capillary pressure may have either positive or negative values. For an oil-water, gas-water or gas-oil system, capillary pressure is defined as

$$P_c = P_o - P_w \tag{9.2}$$

$$P_c = P_g - P_w \tag{9.3}$$

$$P_c = P_g - P_o \tag{9.4}$$

The hydrostatic pressure of a liquid with density ρ is dependent on the elevation z as follows

$$\frac{dP}{dz} = \rho g \tag{9.5}$$

For an oil-water system, the capillary pressure becomes

$$\frac{dP_c}{dz} = (\rho_w - \rho_w)g \tag{9.6}$$

If fluid columns are continuous in the reservoir, the following relationship holds

$$P_c(z) = P_c(z_0) + g \int_{z_0}^{z} (\rho_w - \rho_o)dz \tag{9.7}$$

where $P_c(z)$ is capillary pressure at height z above z_0 and ρ_w, ρ_o are densities of water and oil, respectively.

The capillary pressure is a result of the curvature of fluid interfaces, according to the well-known Laplace equation

$$P_c = \sigma\left(\frac{1}{r_1} + \frac{1}{r_2}\right) \tag{9.8}$$

where σ is interfacial tension between the two fluids and r_1 and r_2 are principle radii of curvature.

The condition for capillary forces to exist is a certain curvature of the fluid-fluid interface. The relation between fluid saturation and capillary pressure in the reservoir is a function of pore sizes, wettability, interfacial tension and fluid saturation history (drainage and imbibition). Based on laboratory measurements of capillary pressure, it is possible to convert those into reservoir capillary pressure. From these values fluid saturations in the reservoir can be evaluated.

An example of the capillary pressure versus saturation relationship (capillary pressure function) is shown in Fig. 9.1. It is apparent that the relationship between capillary pressure and saturation is not unique, but depends on the saturation history of the system. Definitions of the main terms are as follows (oil-water system):
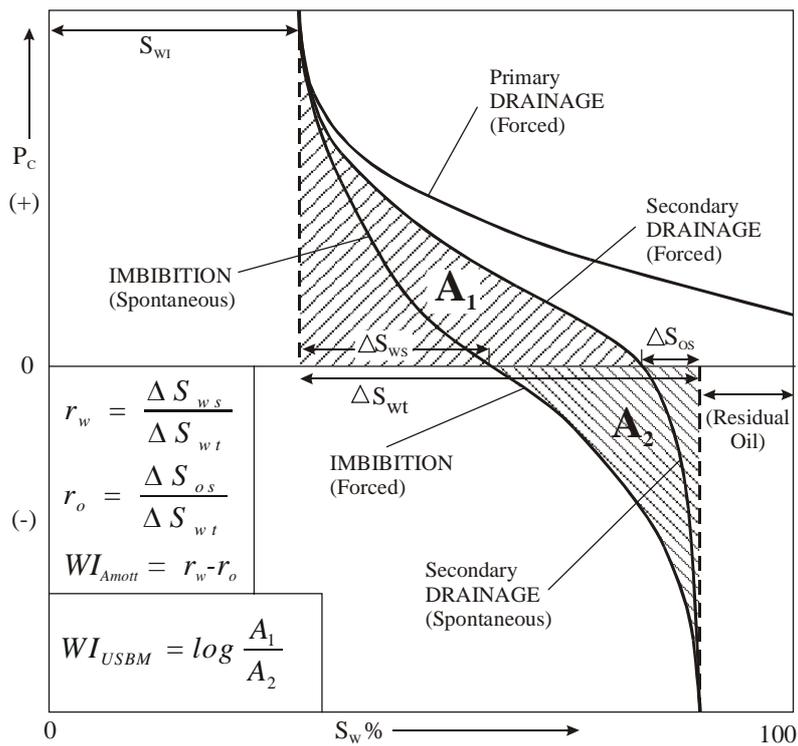
Fig. 9.1: Typical capillary pressure curves and the relationships of wettability measurements by Amott and USBM tests to P_c.

Irreducible water saturation S_{wi}: The reduced volume of the wetting phase retained at the highest capillary pressure where wetting phase saturation appears to be independent of further increases in the externally measured capillary pressure.

Residual oil saturation S_{or}: The reduced volume of the non-wetting phase which is entrapped when externally measured capillary pressure is decreased from a high value to a big negative value.

Primary drainage curve: The relationship characteristic of the displacement of the wetting phase from 100% saturation to the irreducible saturation.

Imbibition curve: The relationship characteristic of the displacement of the non-wetting phase from the irreducible saturation to the residual saturation.

Secondary drainage curve: The relationship characteristic of the displacement of the wetting phase from residual saturation to the irreducible saturation.

Most experimental evidences indicate that the irreducible saturation obtained by primary drainage is the same as that obtained by secondary drainage. When the residual saturation is the same, the imbibition after secondary drainage will follow exactly the imbibition curve obtained after primary drainage. Thus, the secondary drainage curve and the imbibition curve constitute a closed and reproducible hysteresis loop.

The capillary pressure hysteresis as can be seen in Fig. 9.1 is a result of the different mechanisms governing filling/ emptying of pores with a non-wetting or a wetting fluid respectively. Contact angle hysteresis is one factor also contributing to hysteresis.

9.2 Capillary Pressure Measurement Methods

9.2.1 Porous Plate Method (restored state)

Water saturated samples for air-water or oil-water tests and oil saturated cores for air-oil tests are placed on a semi-permeable diaphragm, and a portion of the contained liquid is displaced with the appropriate fluid of air or oil. A schematic diagram of an apparatus for performing such tests is seen in Fig. 9.2. It consists of a cell for imposing pressure, a semi-permeable diaphragm C, manometer for recording pressure M, and a measuring burette for measuring produced volumes.
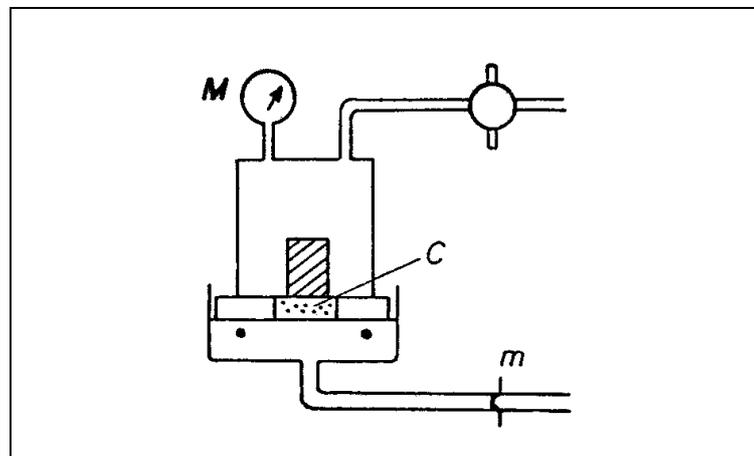
During measurement, the pressure is increased in steps and final equilibrium produced volumes of the wetting phase are recorded for each step.

The porous plate method is slow and one full curve may take up to 40 days or more to obtain. However, equipment needed for this method is simple and inexpensive and the work needed is limited to some volume reading during the process. Several samples may be run in one chamber. Then the samples have to be removed in order to weigh them separately between each pressure increase. Preferably, one and one sample should be run in an assembly of one-sample cells. Then it is not necessary to decrease pressure between each reading.

This method is regarded as the standard method against which all other methods are compared. Routinely only the drainage curve is measured, but with appropriate modifications the imbibition curve may be determined in the same manner. The weakness, as with all the other methods, is the transformation of data to reservoir conditions.

9.2.2 Centrifuge Method

Hassler and Brunner (1945) presented the basic concepts involved in the use of the centrifuge by relating the performance of a small core in a field of high acceleration.

If the cylindrical core of length L is subjected to an acceleration $a_c = -\omega^2 r$ where ω is angular velocity of the centrifuge and r is the distance from the axis of rotation, then from Eq. (9.6) we have

$$\frac{\partial P_c}{\partial r} = \Delta \rho a_c \qquad (9.9)$$

Given the boundary conditions show in Fig. 9.3, the differential equation can be solved by simple integration
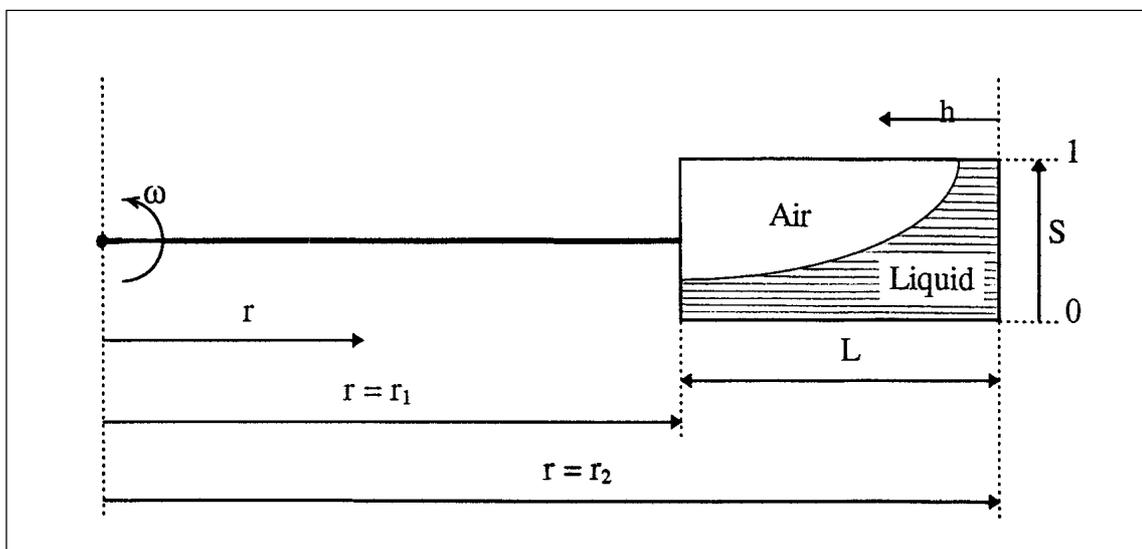
Fig. 9.3: Schematic diagram of a core in a centrifuge and its boundary conditions.

$$P_c = \int_{r_2}^{r} \Delta \rho a_c \, dr \tag{9.10}$$

$$P_c(r) = -\int_{r_2}^{r} \Delta \rho \omega^2 r \, dr \tag{9.11}$$

The capillary pressure at the outer face of the core is zero, $P_c(r_2) = 0$, so

$$P_c(r) = \tfrac{1}{2} \Delta \rho \omega^2 \left(r_2^2 - r^2 \right) \tag{9.12}$$

and for a continuous phase, the capillary pressure at the inner face of the core is

$$P_{cL} = P_c(L) = \tfrac{1}{2} \Delta \rho \omega^2 \left(r_2^2 - r_1^2 \right) \tag{9.13}$$

Now, the main purpose is to relate the capillary pressure and saturation S for a given core which gives the saturation in the core at equilibrium with the capillary pressure, $S = S(P_c)$.

The saturation at a distance h above the outer face of the core can not be measured directly. However, the average saturation, which is the ratio of remaining liquid volume after production to pore volume can be written as

$$\overline{S} = \frac{1}{r_2 - r_1} \int_{r_2}^{r_1} S(r) \, dr \tag{9.14}$$

We will have a relationship of saturation as a function of capillary pressure, $S = S(P_c)$, so Eq. (9.14) can be expressed as follows by changing integration variable

$$P_c(r_2) = 0 \qquad \text{and} \qquad P_c(r_1) = P_{cL}$$

$$\overline{S} = \frac{1}{r_2 - r_1} \int_{P_{cL}}^{0} \frac{S(P_c) \, dP_c}{-\Delta \rho \omega^2 r} \tag{9.15}$$

An expression for r is obtained from Eq. (9.12)

$$r = r_2 \sqrt{1 - \frac{P_c}{\frac{1}{2}\Delta\rho\omega^2 r_2^2}}$$

(9.16)

and we obtain

$$\bar{S} = \frac{1}{(r_2 - r_1)\Delta\rho\omega^2 r_2} \int_0^{P_{cL}} \frac{S(P_c)dP_c}{\sqrt{1 - \frac{P_c}{\frac{1}{2}\Delta\rho\omega^2 r_2^2}}}$$

(9.17)

and with mathematical manipulation it becomes

$$\bar{S}P_{cL} = \cos^2\left(\frac{\alpha}{2}\right) \int_0^{P_{cL}} \frac{S(p_c)dP_c}{\sqrt{1 - \frac{P_c}{P_{cL}}\sin^2\alpha}}$$

(9.18)

where

$$\cos\alpha = \frac{r_1}{r_2}$$

$$\cos^2\left(\frac{\alpha}{2}\right) = \frac{1}{2}(1 + \cos\alpha) = \frac{r_1 + r_2}{2r_2}$$

$$\sin^2\alpha = 1 - \cos^2\alpha = 1 - \frac{r_1^2}{r_2^2}$$

Eq. (9.18) can not be solved so simply for the unknown function *S*. For small values of α (small core sample), the acceleration gradient along the core can be neglected. Assuming

$$r_1/r_2 \approx 1$$

then

$$\cos^2\left(\frac{\alpha}{2}\right) = 1 \quad \text{and} \quad \sin^2\alpha = 0$$

Eq. (9.18) is then reduced to

$$\bar{S}P_{cL} = \int_0^{P_{cL}} S(P_c)dP_c$$

(9.19)

or in differentiation form

63

$$S_L = \frac{d}{dP_{cL}}\left(\overline{S}P_{cL}\right) \qquad\qquad (9.20)$$

In this method the cores is saturated with water (or oil) and rotated at increasing speed. The speed is increased in steps, and average fluid saturations at each speed is calculated from observation of liquid produced. The liquid volume is read with a stroboscope while centrifuge is in motion, and the speed of centrifuge is increased stepwise. When the run is over the cores are removed and weighed.

The value of P_{cL} for each centrifuge speed are then computed from Eq. (9.13), and the average saturation for each core is obtained from the dry and saturated weights and the corresponding pipette reading. From these data a smooth curve is prepared for each core.

Fig. 9.4a shows a typical $\overline{S}P_{cL}$ as a function of P_{cL} and points indicated on the curve are first, second and third speed.
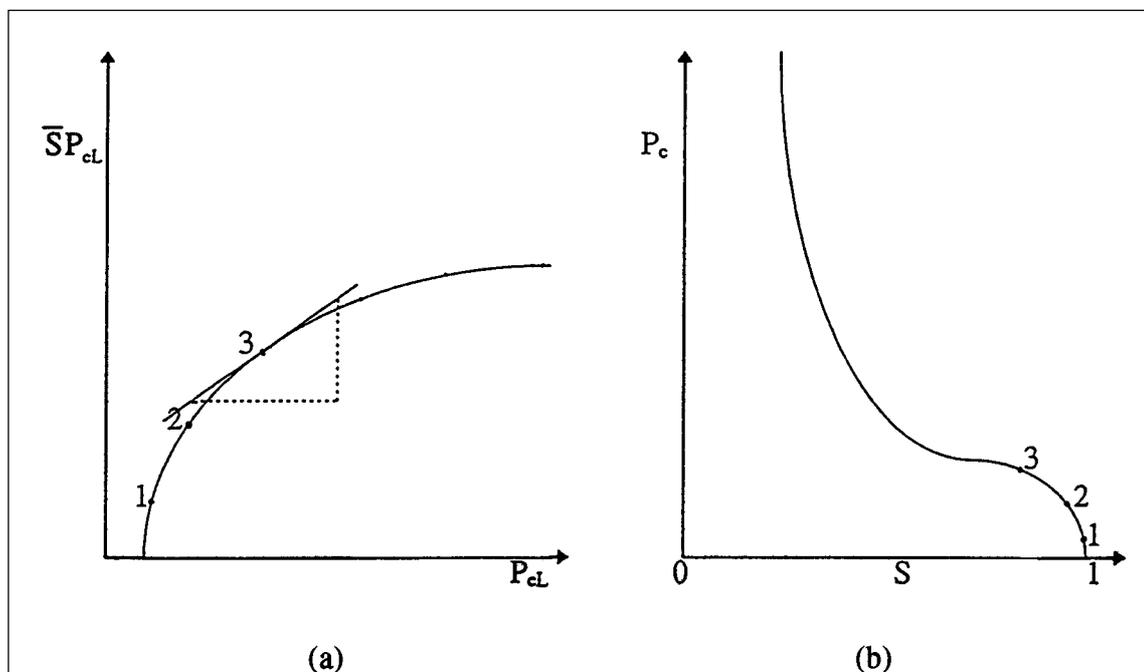
Fig. 9.4: Graphical differentiation of $\overline{S}P_{cL}$ - P_{cL} curve (a) to determine S-P_c curve (b).

The value of saturation that goes with each value of P_{cL}, which now represents the capillary pressure, is obtained from this curve by graphical differentiation according to Eq. (9.20). A typical plot of P_c as a function of S is shown in Fig. 9.4b.

A complete capillary pressure curve by this method may be obtained in a few hours, and several samples are run simultaneously. The method is claimed to be accurate, to reach equilibrium rapidly, give good reproducibility, and is able to produce high pressure differences between phases.

64

9.2.3   Mercury Injection (Purcell Method)

The test specimen is evacuated and mercury is injected in increments into the core at increasing pressure levels. When the entry pressure is reached, one can easily determine the bulk volume of the core. A mercury injection apparatus is schematically shown in Fig. 9.5. The equipment consists basically of a mercury injection pump, a sample holder cell with a window for observing constant mercury level, manometers, vacuum pump, and a pressurized gas reservoir.
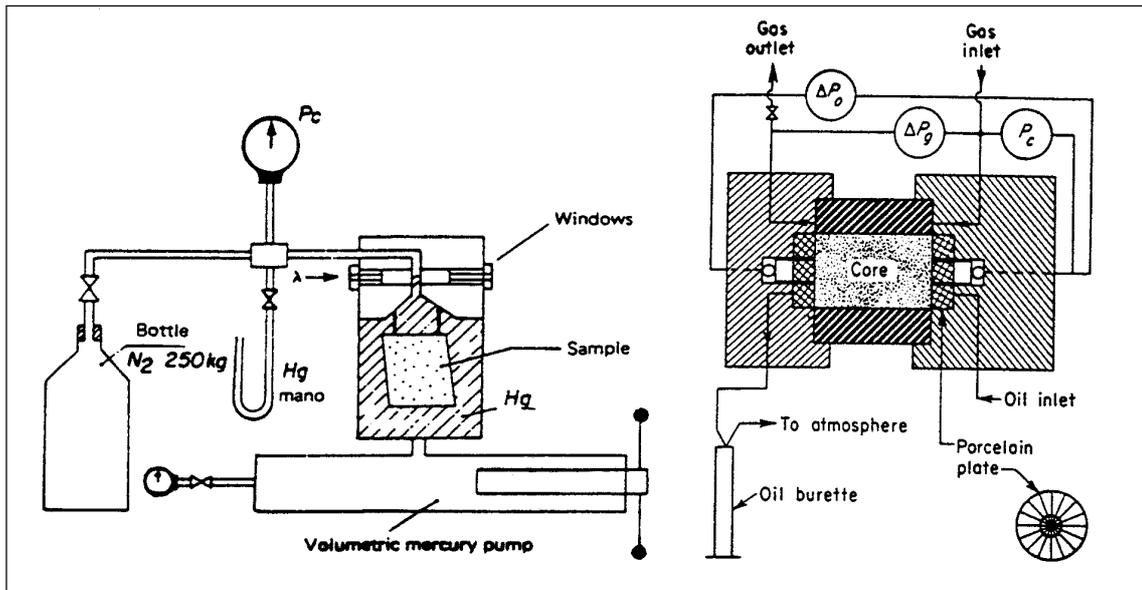
Fig. 9.5: Apparatus for mercury injection method.

Fig. 9.6: Dynamic capillary pressure apparatus.

In this method the mercury injected is calculated as a percentage of pore volume and related to pressure. A practical pressure limit on most equipment is about 15-25 MPa, but equipment for 150 MPa also exists.

Two important advantages are gained with the mercury injection method: (1) the time for determining a complete curve is reduce to less than one hour, and (2) the range of pressure is increased compared with the other methods. However, this method is a destructive method and it is difficult to transform the results to reservoir conditions because of the highly unrealistic fluid system and the uncertainty of wetting of mercury-solid.

Using mercury-air as the fluid-pair, one will not obtain the irreducible saturation as when displacing water with air.

9.2.4 Dynamic Method

The main feature in this method is the way it controls the capillary pressure at both ends of the sample. This is accomplished by placing the tested core between two membranes, or porous plates, which are permeable only to the wetting fluid (Fig. 9.6). This permits maintenance of a uniform saturation throughout the length of the core even at low flow rates.

The membranes permit separate pressure measurements in each of the two phases. The capillary pressure is then equal to the pressure difference between the non-wetting phase and the wetting one at the inflow face. When equilibrium is reached, the sample is removed and its saturation is determined by weighing.

9.2.5 Comparison of Methods

In Table 9.1 advantages and disadvantages of the method are listed. The mercury injection method is primarily used for obtaining pore size distribution data, since it is destructive method. Mercury-air capillary pressure curves have been found to be similar to water-air capillary pressure curves when the mercury-air pressure is divided by a constant. The constant can range from 5.8 to 7.5, depending on the nature of the rock.

The porous plate method is the simplest method conceptually and it must be regarded as the standard method. Small and large samples can be used, and the choice of fluids is not restricted. A serious drawback is the limitation in pressure, since most equipment is limited to about 5 atm.

Table 9.1: Comparison of the methods.

Method	Fluid type	P_c curve type	Max. ΔP in lab.	Test time
Porous plate	Oil-water Gas-water Gas-oil	Imbibition Drainage	2-5 atm.	Weeks
Mercury injection	Hg-air	Drainage	100 atm.	Minutes
Centrifuge	Gas-water Oil-water Gas-oil	(Imbibition) Drainage	10 atm.	Days
Dynamic	Gas-water Gas-oil Oil-water	(Imbibition) Drainage	1-10 atm.	Days

The centrifuge can reach capillary pressures higher than the porous plate method, and a large number of samples can be run in a relatively short time.

9.3 Converting Laboratory Data

To use capillary pressure data in reservoir evaluation it is necessary to convert to reservoir conditions. Laboratory data are obtained with a gas-water or an oil-water system, which does not normally have the same physical properties as the reservoir water, oil and gas system.

As shown previously, by means of the capillary tube, the capillary pressure is expressed as

$$P_c = \frac{2\sigma \cos\theta}{r} \tag{9.21}$$

Considering two specific cases wherein the laboratory and reservoir values are determined with gas-water and water-oil respectively. The capillary pressures become

$$(P_c)_L = \frac{2\sigma_{wg}\cos\theta_{wg}}{r} \quad \text{and} \quad (P_c)_R = \frac{2\sigma_{wo}\cos\theta_{wo}}{r} \tag{9.22}$$

where σ_{wg} = interfacial tension between water and gas used in laboratory test
θ_{wg} = contact angle between water and gas
σ_{wo} = interfacial tension between reservoir water and oil at reservoir conditions
θ_{wo} = contact angle between reservoir, water and oil
r = radius of capillary.

Comparing the equations for laboratory and reservoir capillary pressure and assuming the radius of capillary constant with pressure and temperature, it is found that the reservoir capillary pressure is

$$(P_c)_R = \frac{\sigma_{wo}\cos\theta_{wo}}{\sigma_{wg}\cos\theta_{wg}}(P_c)_L = \frac{(\sigma\cos\theta)_R}{(\sigma\cos\theta)_L}(P_c)_L \tag{9.23}$$

Note that it is difficult to determine the exact value of the contact angle for fluids in a porous matrix, and therefore the contact angles are often neglected. The equation becomes

$$(P_c)_R = \frac{\sigma_R}{\sigma_L}(P_c)_L \tag{9.24}$$

9.4   Experiments

9.4.1   Capillary Pressure Measurement using Porous Plate Method (Exp. 10)

Description:

The porous plate method is the most accurate measurement of capillary pressure in homogeneous and heterogeneous cores. Several plugs can be measured at a time. The limitation is that the capillary discontinuity may distort the results.

Fig. 9.7 shows the capillary pressure apparatus used in our laboratory.

Procedure:

1. Put the saturated core onto the porous plate in the cell.
2. Adjust the pressure regulator and give the cell the pressure difference according to a measuring plan.
3. After 3 days, stop the pressure supply and take off the cores from the cell.
4. Weigh the core and calculate the water saturation corresponding to the capillary pressure.
5. Repeat 1-4 each 3 days until no appreciable water is produced.
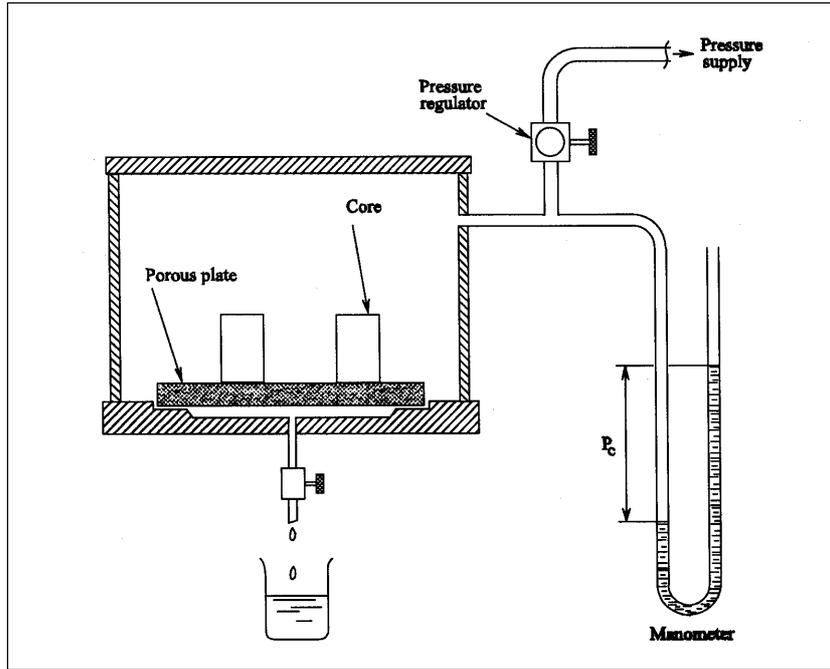
Fig.9.7: The capillary pressure apparatus.

Calculations and report:

1. Calculate and fill the data form.
2. Plot capillary pressure curve (S_w-P_c) and pore size histogram (distribution).

Core No.   D: cm,   L: cm, W_{dry}:   g, W_{sat}:   g, $\phi =$

Date	No. $_{(i)}$	$P_{c(i)}$, H_{water} (*cm*)	$W_{wet(i)}$ (*g*)	$S_{w(i)}$ (*fraction*)	$r_{(i)}$ (μm)	$\dfrac{\Delta W_{(i)}}{W_{water}}$
	0					
	1					
	2					
	3					
	4					
	5					

where

$P_{c(i)}$ = capillary pressure of ith measurement, *cm* of water, reading of U-manometer

W_{wet} = core weight of ith measurement, g

$S_{w(i)} = (W_{wet(i)}-W_{dry})/W_{water}$, i^{th} water saturation of $P_{c(i)}$

$\qquad W_{water} = W_{sat}-W_{dry}$, g

$r_{(i)} = 2\sigma_{g-w}/Pc(i)$, radius corresponding to $P_{c(i)}$

$\qquad \sigma_{g-w} = 70.0$ dynes/cm, interfacial tension of gas-water

$\qquad P_{c(i)} = 981.H_{water}$, dynes/cm^2

$\Delta W_{(i)}/W_{water} = (W_{wet(i-1)}-W_{wet(i)})/W_{water}$, fraction of the capillaries of $r_{(i)}$ in total pore volume.

9.4.2 Capillary Pressure Measurement using Centrifuge Method (Experiment 11)

Description:

The objective of the experiment is to measure capillary pressure in a core sample and plot the capillary pressure versus water saturation curve.

Procedure:

1. Measure the pore volume and bulk volume of a cleaned and dried core sample. Weigh the dry core, W_{dry}.

2. Saturate the core sample with the brine/water with density ρ_w. Weigh the saturated core, W_{sat}.

3. Place the core sample in a centrifuge core holder and start the centrifuge with rotation rate of 500 RPM.

4. Monitor the displaced fluid volume in the measuring tube while the centrifuge is in motion, by adjusting the strobe light frequency to the rotational speed of the centrifuge.

5. Record the collected fluid volume V_{coll} in the graduated tube when the volume of collected fluid shows no further changes.

6. Repeat the procedure described in the steps 4 and 5 at higher rotational speed.

Calculations and report:

1. Calculate pore volume of the core sample: $V_P = \dfrac{W_{sat} - W_{dry}}{\rho_w}$.

2. Convert RPM to rad/s: $\omega = \dfrac{2\pi(RPM)}{60}$.

3. Calculate capillary pressure at each step: $P_{cL} = \frac{1}{2}\rho_w\omega^2\left(r_2^2 - r_1^2\right)$,
   where
   $r_2 = 0.145$ m
   $r_1 = r_2\text{-}L$
   L = length of the core sample

4. Calculate average water saturation $\overline{S}_w$ in the core sample based on the volume of the water collected at corresponding capillary pressure: $\overline{S}_w = 1 - \dfrac{V_{coll}}{V_P}$.

5. Plot $\overline{S}P_{cL}$ versus P_{cL}.

6. Draw tangents to the plot of the curve at each point and calculate the slope of each tangent. These slopes are the water saturation values S_w at the corresponding capillary pressure.

7. Plot the capillary pressures as a function of the water saturations.

Core No.:   D: cm,   L: cm.

RPM	ω (rad/s)	P_{cL} (bar)	V_{coll} (cm^3)	$\overline{S}_w$	$\overline{SP}_{cL}$ (bar)	S_w from plot
500						
750						
1000						
1500						
2000						
2500						

10. PERMEABILITY

10.1 *Definition*

Permeability is a property of the porous medium and it is a measure of capacity of the medium to transmit fluids. Permeability is a tensor that in general is a function of pressure. Usually, the pressure dependence is neglected in reservoir calculations, but the variation with position can be pronounced. Very often the permeability varies by several magnitudes, and such heterogeneity will of course influence any oil recovery.

10.1.1 Darcy's Law

Darcy (1856) performed a series of experiments on the relationship effecting the downward flow of water through sands. The generalised equation called Darcy's law may be written in the form

$$\bar{u} = -\frac{\bar{\bar{k}}}{\mu}\left(\nabla P + \rho \bar{g}\right) \tag{10.1}$$

where $\bar{u}$ is superficial velocity, $\bar{\bar{k}}$ is permeability tensor, μ is fluid viscosity, ∇P is pressure gradient, ρ is fluid density and $\bar{g}$ is gravitational vector. Writing flow velocity v as the ratio of volumetric rate to cross-sectional area perpendicular to flow q/A in distance L, Darcy's law can be expressed

$$\frac{q}{A} = v = \frac{k}{\mu}\frac{\Delta P}{L} \tag{10.2}$$

The dimensions of permeability can be established by substituting the units of the other in the equation. The unit darcy results from the choice of *cgs* system units

$$darcy[D] = \frac{q[cm^3/s]\mu[cp]L[cm]}{\Delta P[atm]A[cm^2]}$$

The permeability in SI system has dimension of m^2.

10.1.2 Kozeny-Carman Model

Formation permeability may be determined or estimated on the basis of core analysis, well tests, production data, well log interpretations, or correlations based on rock permeabilities. One of these often used pore models is Kozeny-Carman Model.

The volumetric flow rate q in a horizontal capillary of radius R and length L_t is given by Hagen-Poiseuille's equation

$$q = \frac{\pi R^4 \Delta P}{8\mu L_t} \tag{10.3}$$

and the average velocity in the tube is

$$\bar{v} = \frac{q}{\pi R^2} = \frac{R^2 \Delta P}{8\mu L_t} \tag{10.4}$$

We have to transform this equation to the scale of a representative element volume (REV). The REV is defined as a volume below which local fluctuations in permeability is large. If we make the travel time in the capillary tube equal to that in a REV, then

$$\left(\frac{L_t}{\bar{v}}\right)_t = \left(\frac{L}{v}\right)_{REV} \tag{10.5}$$

The relation between interstitial and superficial velocity is $v = u/\phi$. Darcy's law can be used to eliminate v and we obtain the permeability component k

$$k = \frac{R^2 \phi}{8\tau} \tag{10.6}$$

where $\tau = (L_t/L)^2$ is the tortuosity. This is an important media property and is usually estimated from electrical resistivity measurements. The tortuosity is in the range of 2 to 5 for most reservoir rocks.

The capillary radius R in Eq. (10.6) is difficult to define for a porous medium, but may be approximated by the hydraulic radius R_h that expresses the ratio between volume open to flow and the wetted surface area. For a porous and permeable medium we have:

$$R_h = \frac{\pi R^2 L}{2\pi R L} = \frac{R}{2} \xrightarrow{\ 10.6\ } k = \frac{R_h^2 \cdot \phi}{2 \cdot \tau} \tag{10.7}$$

$$R_h = \frac{\phi}{a(1-\phi)} \tag{10.8}$$

where a is internal surface area per volume, an important intrinsic property of permeable media. By substituting these expressions for R_h in Eq. (10.6) and solving the equation for an assemblage of uniform spheres where $a = 6/D$ we get the Kozeny-Carman equation

$$k = \frac{1}{72\tau} \frac{\phi^3 D^2}{(1-\phi)^2} \tag{10.9}$$

where D is sphere or particle diameter, and we see that permeability is a strong function of particle size and packing through ϕ. The Kozeny-Carman equation is often used to make order-of-magnitude estimates of pore size from knowledge of permeability. However, the capillary tube model is of limited value since it does not provide alternate pathways for fluid flow within each REV. The consequence is that we can not predict relative permeabilities or trapped phase saturations, parameters of major importance in oil recovery processes.

10.1.3 Klinkenberg Effect

Klinkenberg has reported variations in permeability determined by using gases as the flowing fluid compared to those obtained when using non-reactive liquids. These variations were considered to be due to slippage, a phenomenon well known with respect to gas flow in capillary tubes. The phenomenon of gas slippage occurs when the diameter of the capillary openings approach the mean free path of the gas. The mean free path of a gas is a function of molecular size and the kinetic energy of the gas. Therefore, permeability of gas depends on factors which influence the mean free path, such as temperature, pressure and the molecular size of the gas.

Fig. 10.1 is a plot of the permeability of a porous medium as determined at various mean pressures using three different gases. Note that for each gas a straight line is obtained for the observed permeability as a function of the reciprocal of the mean pressure of the test. All the lines when extrapolated to infinite mean pressure ($1/P_m = 0$) intercept the permeability axis at a common point. This point is designated k_L, or the equivalent liquid permeability.
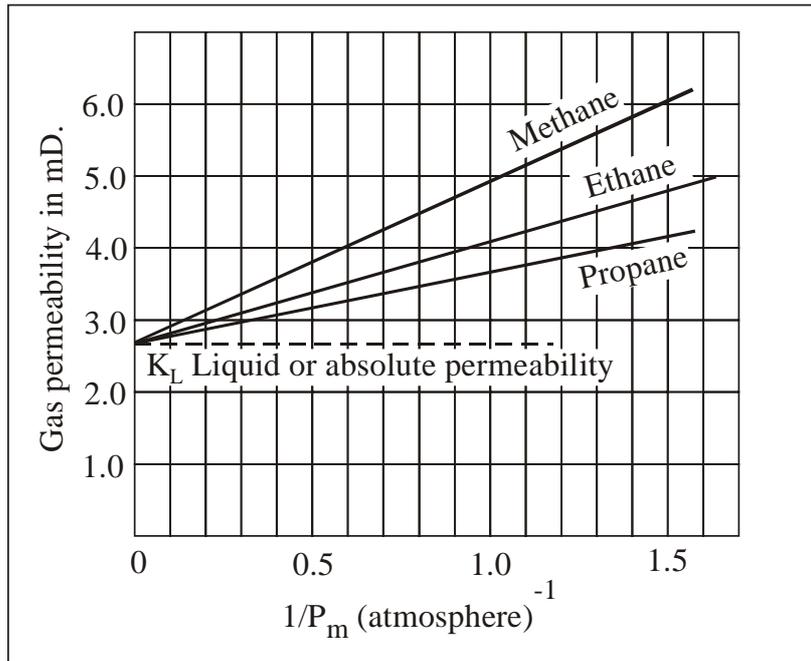
Fig. 10.1: Variation in gas permeability with mean pressure and type of gas.

Klinkenberg has related apparent permeability k_a measured for gas for an average pressure P_m to the true permeability k_L by

$$k_a = k_L\left(1 + \frac{b}{P_m}\right) \tag{10.10}$$

where b is constant depending upon the average free movement λ of the molecule at P_m

$$b = \frac{4C'\lambda P_m}{r} \tag{10.11}$$

where r is channel radius and $C' \approx 1$.

10.1.4 Ideal Gas Flow

Darcy's equation ... ous media. This laminar flow is n... se that there is a metal tube filled ... re P_1 and P_2 are constants.
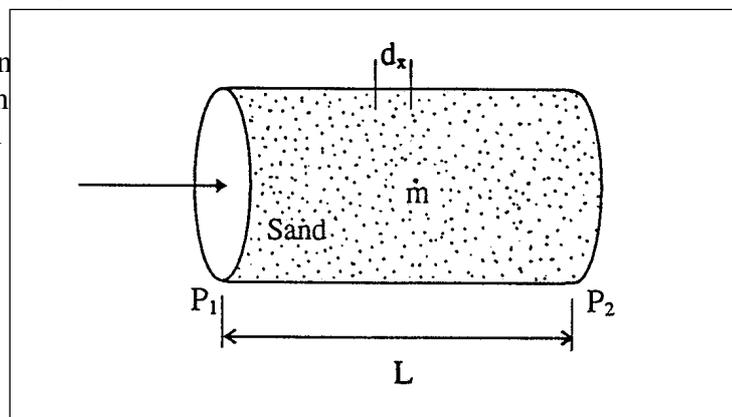
Fig 10.2: Linear flow of an ideal gas in sand-filled tube.

The mass flow $\dot{m}$ is the same in all slices and each slice is related to the volume flow rate Q by

$$\dot{m} = Q.\rho \tag{10.12}$$

where ρ is gas density in the slice when pressure is P. Using Boyle's law, relationship $\rho = bP$ can be applied where b is a constant. And then

$$Q = \frac{1}{bP}\dot{m} \tag{10.13}$$

By substituting Q in Darcy's equation, a differential relation between P and distance x may be obtained

$$bPdP = \frac{\mu}{A}\frac{\dot{m}}{k}dx \tag{10.14}$$

After integration for distance L

$$\frac{b}{2}\left(P_1^2 - P_2^2\right) = \frac{\mu}{A}\frac{\dot{m}}{k}L \tag{10.15}$$

and taking into account that $\dot{m} = QbP$, we get

$$Q_{atm} = \frac{Ak}{\mu L}\frac{\left(P_1^2 - P_2^2\right)}{2P_{atm}} \tag{10.16}$$

The gas flow is measured at atmospheric conditions, thus $P_{atm} = 1$ atm.

10.1.5 High Velocity Flow

For high flow rates, Darcy's law is not valid. The range of flow rate which laminar flow exists is dependent on the Reynolds number which is a dimensionless quantity. The Reynolds number for porous media is defined as

$$R_e^* = \frac{dv\rho}{\mu} \qquad (10.17)$$

where v is average velocity (q/A), ρ is fluid density, μ is fluid viscosity and d is the average sand grain diameter. For example, in sand, transition from laminar to turbulent flow occurs in the range of Reynolds number from 1 to 10.

Many models were suggested to replace or modify Darcy's law for high-velocity flow. The most accepted model for non-Darcy flow was proposed by Forchheimer in 1901

$$-\nabla P = av + bv^2 \qquad (10.18)$$

where a and b are constants and $v = q/A$. Later work resulted in an equation in terms of fluid and rock properties

$$-\nabla P = \frac{\mu}{k}v + \beta\rho v^2 \qquad (10.19)$$

where β is high velocity coefficient and μ, ρ are viscosity and density of the gas respectively. The high velocity coefficient is a property of the formation rock that accounts for the deviation from Darcy's law which is more pronounced in gas flow than in oil flow. Many correlations for β exist in the literature. Usually, β is taken as a property of the reservoir rock which may be estimate from

$$\beta = \frac{const.}{k^\alpha} \qquad (10.20)$$

where α is constant which can be determined experimentally from a known permeable formation.

10.2 Measurement of Permeability

Permeability is measured by passing a fluid of known viscosity through a core sample of measured dimensions and then measuring flow rate and pressure drop. Various techniques are used for permeability measurements of cores, depending on sample dimensions and shape, degree of consolidation, type of fluid used, ranges of confining and fluid pressure applied, and range of permeability of the core. Two types of instruments are usually used in the laboratory:

    (a) Variable head permeameter, IFP type.

(b) Constant head permeameter, Core Laboratories type.

Permeability tests are performed on samples which have been cleaned and dried and a gas (usually air) is used for flowing fluid in the test. This is because:

1. steady state is obtained rapidly,
2. dry air will not alter the minerals in the rock, and
3. 100% fluid saturation is easily obtained.

Measured values using constant head equipment range from a low of 0.1 mD to 20 D. Data accuracy declines at high and low permeability values and is within ± 0.5% of true value otherwise.

10.2.1 Constant Head Permeameter

This equipment is designed for plug or whole core permeability measurements. This experiment may be used for single or multiphase, compressible fluid or liquid measurements and can also be used under reservoir pressure and temperature.

Fig 10.3 shows a diagram of a constant head permeameter. Air is usually used as gas flow. Upstream and downstream pressures are measured by manometers on both sides of the core and air flow is measured by means of a calibrated outlet. Air permeability can then be calculated using Eq. (10.16).

Hassler core holder may be used with this instrument. The Hassler system is an improvement of the rubber plug system whose tightness is limited at certain pressures. The core is placed in a flexible rubber tube (Fig. 10.4). The Hassler cell has these advantages:

- Excellent tightness.
- Can be used for samples of different sizes.
- Much higher pressure or ΔP can be used.
- Can be used for measuring relative permeability.

Darcy's equation may be used for determining permeability of liquids. The volumetric flow ... low thro ...

1. Air supply
2. Reduction valves
3. Core holder
4. Core sample
5. Manometers
6. Sleeve pressure
7. Wet-test meter (gas-volume measurement)
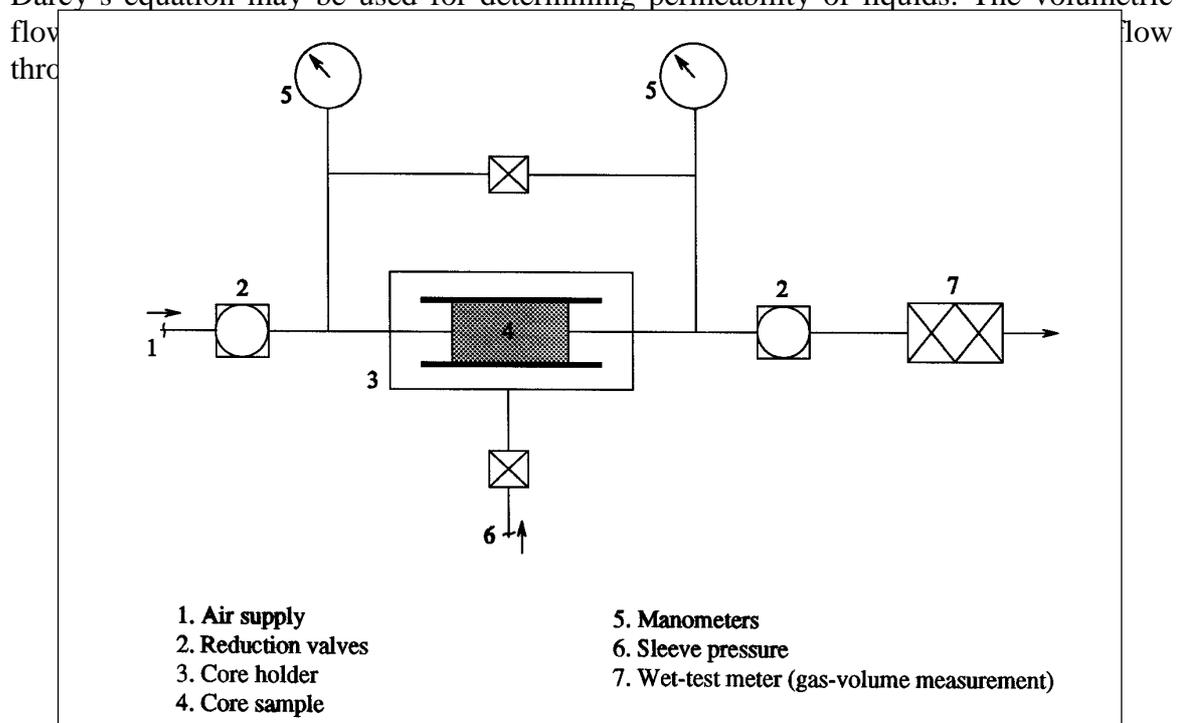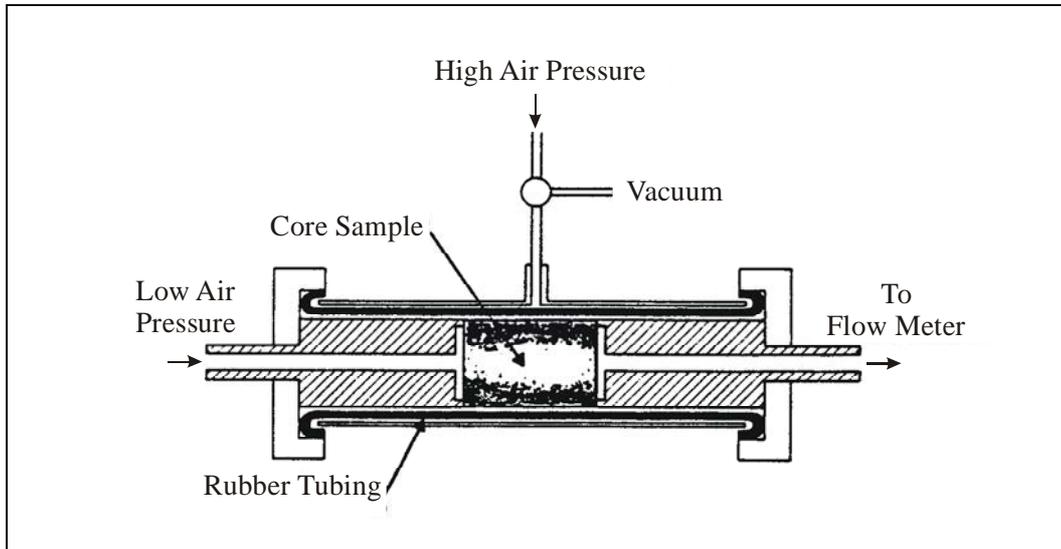
Fig.10.4: Hassler type core holder.

10.3   Experiments

10.3.1 Measurement of Air Permeability (Experiment 12)

Description:

The constant head permeameter with the Hassler cell is used to measure the air permeability.

Procedure:

The measured air permeability is influenced by the mean pressure P_m of the core. The mean pressure is regulated by the upstream and downstream values on the sides of Hassler cell. The rate is measured at atmospheric conditions with a mass flow meter in percent of maximum rate which is 200 l/hour. Air viscosity as a function of temperature is shown in Fig. 10.5.

Four measurements of air permeability will be taken at different pressures. It is important to keep the ΔP constant, because the air flow at the core sample must be laminar. It is best to have relative little pressure difference, ΔP. To avoid turbulent flow, use a maximal ΔP = 0.2 bar.

Results and Calculation:

1.   Calculate air permeability from Eq. (10.16).

2. Plot k versus $1/P_m$ and calculate k_L.

3. Calculate Klinkenberg constant b.

Inlet pressure P_1	Outlet pressure P_2	$1/P_m$	Rate in %	Q_{1atm}
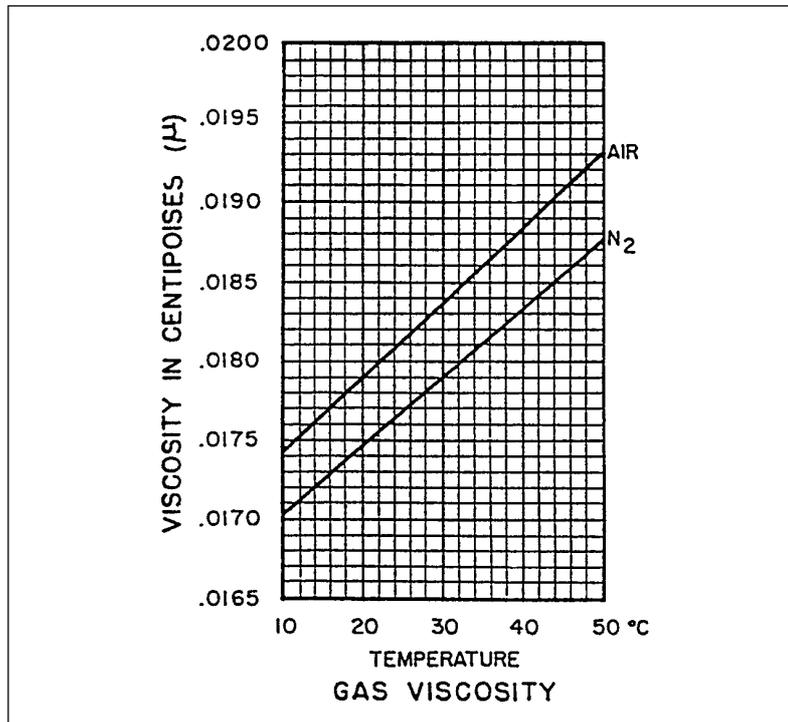
Fig. 10.5: Gas viscosity as a function of temperature.

Thin section

You will see two different thin section in microscope. What sample has lowest or highest permeability? Use the number of sample as reference. Give reasons for your answer.

Number of sample with lowest permeability	Number of sample with highest permeability

10.3.2 Absolute Permeability Measurement of Water (Experiment 13)

Description:

The objective of this experiment is to measure the absolute permeability of water using a method based on the Darcy theory.

Procedure:

1. Weight a dry Berea plug W_{dry}, measure its diameter D and length L, with caliper. Saturate the core with 36 g/l NaCl brine and weigh the plug, W_{sat}.

2. Mount the core in core holder.

3. Measure three flow rates under three driving pressures: 0.6, 0.8, 1.0, or 1.2 bar. Each measurement collects water production V_w, in $\Delta T = 60$ seconds.

4. Plot a line through the three ΔP-V_w data in a grid paper. Calculate the absolute permeability k_{abs} and absolute injectivity I_{abs}.

Calculations and report:

Core No.:   *D*:   cm,   *L*:   cm, W_{dry}:   g, W_{sat}:   g.

$\Delta T_{(i)}$ = 60"	$\Delta P_{(1)}$ bar	$\Delta P_{(2)}$ bar	$\Delta P_{(3)}$ bar	k_{abs} darcy	I_{abs} cm/s.bar
V_w					

Liquid data:

$\rho_w = 1.020$ g/cm^3, $\mu_w = 1.04$ cp

I_{abs} = Absolute (water) injectivity = $V_w/(\Delta T.A.\ \Delta P)$

where V_w is volume of water produced in time ΔT.

Calculation of k_{abs}:

$$k_{abs} = (\mu_w L V_w)/(A \Delta T \Delta P)$$

$(\mu.L)/(k.A.\Delta T)$ = slope of the ΔP-V_w plot

A = Section area of the core, cm^2.

11. RELATIVE PERMEABILITY

11.1 Definitions

As mentioned before, permeability refers to 100% saturation of a single-phase fluid. In petroleum reservoirs, however, the rocks are usually saturated with two or more fluids, such as water, oil and gas. It is necessary to generalise Darcy's law by introducing the concept of effective permeability to describe the simultaneous flow of more than one fluid.

Effective permeability is the ability of the porous material to conduct a fluid when its saturation is less than 100% of the pore space.

Relative permeability is the ratio of the effective permeability of a given phase, say oil k_o, in presence of other phases (water and/or gas), to the absolute permeability k

$$k_{ro} = \frac{k_o}{k}$$

Relative permeabilities are influenced by the following factors:

- Saturation
- Saturation history
- Wettability
- Temperature
- Viscous, capillary and gravitational forces
- Pore geometry

Oil and water relative permeabilities in an oil-water system are usually plotted as a function of water saturation as typically shown in Fig. 11.1.

The saturation S_{or} is called the residual oil saturation. The directions of the curves point out the saturation histories which are called drainage and imbibition. The *drainage* curve applies to processes where the wetting phase is decreasing in magnitude. The *imbibition* curve applies to processes where the wetting phase is increasing in magnitude.

Note that the relative permeability curves consist of three elements:

1. The end point fluid saturations.

2. The end point permeabilities.

3. The curvature of the relative permeability functions.
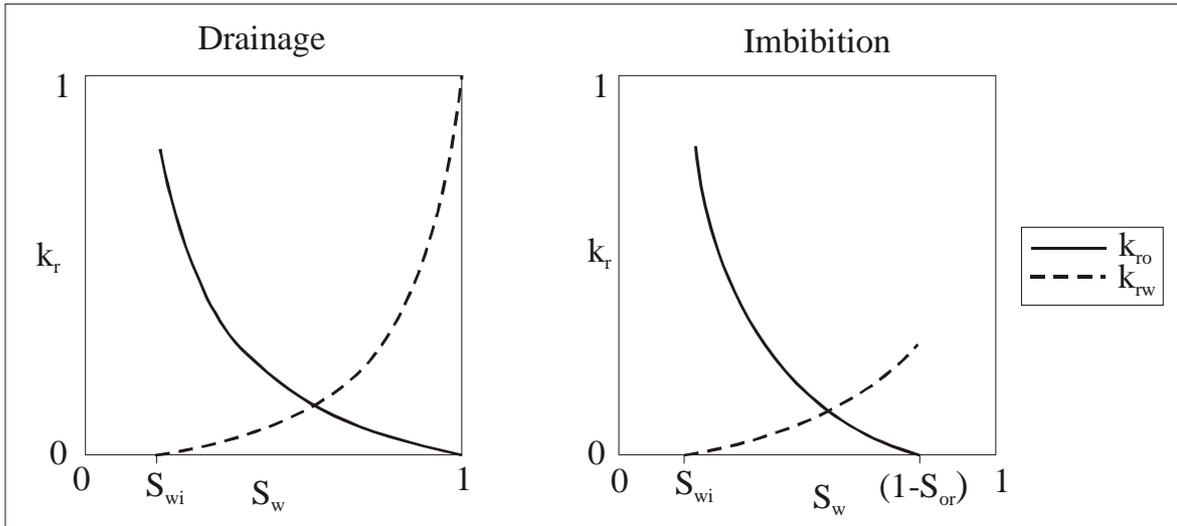
Fig. 11.1: Typical curves for oil-water relative permeability at a water-wetted system.

The end point saturations determine the movable saturation range and is directly related to amount of recoverable oil. The end point of relative permeabilities enter into the expression for the mobility ratio and will determine sweep efficiency of a displacement process. The shape of the curves in between may also have an important bearing on recovery efficiency.

11.2   Flow of Immiscible Fluids in Porous Media

The concept of relative permeability is fundamental to the study of the simultaneous flow of immiscible fluids through porous media. We consider first the case of linear displacement in a thin tube of porous material inclined at an angle α to the horizontal and with a cross section A. From Darcy's law, for the two phases, oil and water, we have

$$q_w = -\frac{k_w A}{\mu_w}\left(\frac{\partial P_w}{\partial x} + \rho_w g \sin\alpha\right)$$
(11.1)

$$q_o = -\frac{k_o A}{\mu_o}\left(\frac{\partial P_o}{\partial x} + \rho_o g \sin\alpha\right)$$
(11.2)

The capillary pressure in the system assuming water as the wetting-phase is written as:

$$P_o - P_w = P_c$$
(11.3)

The fluids are considered to be imcompressible so that the continuity equation applies to each phase

$$\frac{\partial q_w}{\partial x} = -\phi A \frac{\partial S_w}{\partial t}$$
(11.4)

$$\frac{\partial q_o}{\partial x} = -\phi A \frac{\partial S_o}{\partial t} \tag{11.5}$$

$$S_w + S_o = 1.0 \tag{11.6}$$

Adding Eqs. (11.4) and (11.5) to (11.6) yields

$$\frac{\partial}{\partial x}(q_o + q_w) = 0 \tag{11.7}$$

so that the total flow rate $q_t = q_o + q_w$ is constant along the tube.

Now if we combine the Eqs. (11.1), (11.2) and (11.3) to eliminate P_w and P_o we obtain

$$q_o = -\frac{k_o A}{\mu_o}\left(-\frac{\mu_w q_w}{k_w A} + \frac{\partial P_c}{\partial x} - \Delta \rho g \sin \alpha\right) \tag{11.8}$$

We can define the fraction f_w of the flowing stream by

$$f_w = \frac{q_w}{q_t} \quad \text{and} \quad f_o = 1 - f_w \tag{11.9}$$

The substitution of q_w and q_o in Eq. (11.8) yield

$$f_w = \frac{1 + \dfrac{k_o A}{\mu_o q_t}\left(\dfrac{\partial P_c}{\partial x} - \Delta \rho g \sin \alpha\right)}{1 + \dfrac{k_o}{k_w}\dfrac{\mu_w}{\mu_o}} \tag{11.10}$$

This is the fractional flow equation for the displacement of oil by water. For the displacement in a horizontal reservoir, and neglecting effect of capillary pressure gradient, the fractional flow equation is reduced to

$$f_w = \frac{1}{1 + \dfrac{k_{ro}}{k_{rw}}\dfrac{\mu_w}{\mu_o}} \tag{11.11}$$

provided the oil displacement is strictly a function of water saturation, as related through the relative permeabilities. For a typical set of relative permeabilities the fractional flow Eq. (11.11), usually has the shape indicated in Fig. 11.2, with saturation limit S_{wi} and $1-S_{or}$, between which the fractional flow increases from zero to unity.
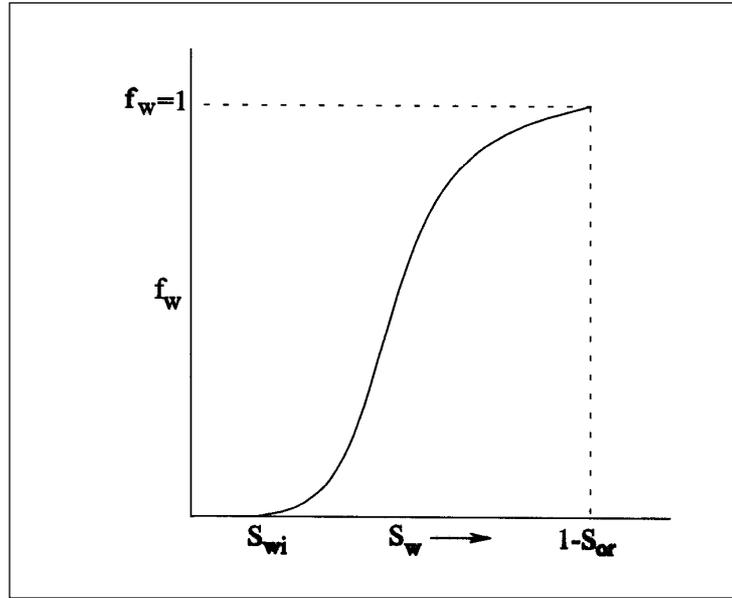
Fig. 11.2: Typical fractional flow curve as a function of water saturation.

11.3 Buckley-Leverett Solution

In 1942 Buckley and Leverett presented the basic equation for describing immiscible displacement in one dimension. For water displacing oil, the equation determines the velocity of a plane of constant water saturation travelling through a linear system. The Buckley-Leverett model discussed in this section is based on the following assumptions:

- Immiscible flow of two fluids in one dimension (no mass transfer between fluids)
- Diffuse, horizontal flow
- Negligible capillary pressure
- Incompressible fluids
- Constant viscosity
- Homogeneous rock (k and ϕ constant)
- Water is injected at $x = 0$ at constant rate q_w.

The conservation of mass of water flowing through the volume element $A.\phi.dx$ shown in Fig. 11.3 may be expressed as:

Mass flow rate – Mass flow rate = Rate of increase of mass in
        In   Out   the volume element

$$q_w \rho_w \big|_x \quad - \quad q_w \rho_w \big|_{x+\Delta x} \quad = \quad A\phi.dx \frac{\partial}{\partial t}\left(\rho_w S_w\right) \tag{11.12}$$

or

$$q_w \rho_w \big|_x - \left(q_w \rho_w \big|_x + \frac{\partial}{\partial x}(q_w \rho_w)dx \right) = A\phi.dx \frac{\partial}{\partial t}(\rho_w S_w) \tag{11.13}$$
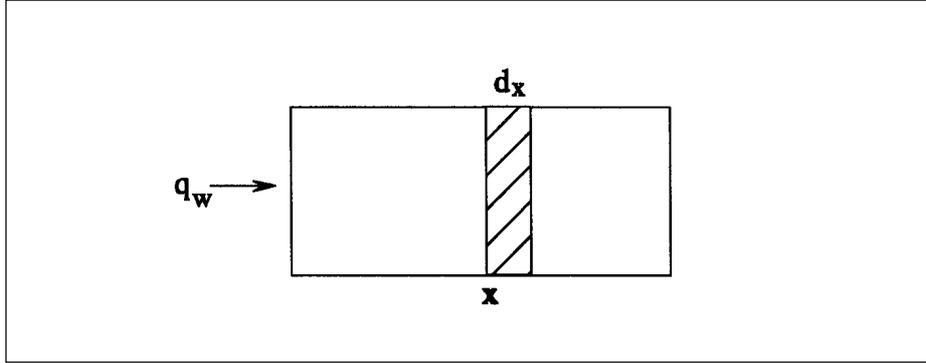
Fig. 11.3: Mass flow rate of water through a linear volume element $A.\phi.dx$.

which can be reduced to

$$\frac{\partial}{\partial x}(q_w \rho_w) = -A\phi \frac{\partial}{\partial t}(\rho_w S_w) \tag{11.14}$$

and for the incompressible displacement which $\rho_w \approx$ constant:

$$\frac{\partial q_w}{\partial x}\bigg|_t = -A\phi \frac{\partial S_w}{\partial t}\bigg|_x \tag{11.15}$$

The water saturation may be written as a full differential:

$$dS_w = \frac{\partial S_w}{\partial x}\bigg|_t .dx + \frac{\partial S_w}{\partial t}\bigg|_x .dt$$

and since it is the intention to study the movement of a plane of constant saturation, that is, $dS_w = 0$, then

$$\frac{\partial S_w}{\partial t}\bigg|_x = -\frac{\partial S_w}{\partial x}\bigg|_t .\frac{dx}{dt}\bigg|_{S_w} \tag{11.16}$$

Furthermore,

$$\left.\frac{\partial q_w}{\partial x}\right|_t = \left(\frac{\partial q_w}{\partial S_w} \cdot \frac{\partial S_w}{\partial x}\right)_t \tag{11.17}$$

and substituting Eqs. (11.16), and (11.17) in Eq. (11.15) gives:

$$\left.\frac{\partial q_w}{\partial S_w}\right|_t = A\phi\left.\frac{dx}{dt}\right|_{S_w} \tag{11.18}$$

Again, for incompressible displacement, q_t, is constant and, since $q_w = q_t.f_w$, Eq. (11.18) may be expressed as:

$$v_{S_w} = \left.\frac{dx}{dt}\right|_{S_w} = \frac{q_t}{A\phi}\left.\frac{df_w}{dS_w}\right|_{S_w} \tag{11.19}$$

This is the equation of Buckley-Leverett which implies that, for a constant rate of water injection q_t, the velocity of a plane of constant water saturation, v_{S_w} is directly proportional to the derivative of the fractional flow equation evaluated for that saturation. With our assumptions the fractional flow is strictly a function of water saturation, hence the use of the total differential of f_w in the Buckley-Leverett equation.

Integrating (11.19) for the total time since the start of injection gives:

$$x_{S_w} = \frac{1}{A\phi}\frac{df_w}{dS_w}\int_0^t q_t \cdot dt$$

or

$$x_{S_w} = \frac{W_i}{A\phi}\left.\frac{df_w}{dS_w}\right|_{S_w} \tag{11.20}$$

where x_{S_w} is the position of plane of constant water saturation and W_i is the cumulative water injected; and it is assumed, as an initial condition, that $W_i = 0$ when $t = 0$. Therefore, at a given time after the start of injection (W_i constant) the position of different water saturation planes can be plotted, using Eq. (11.20), merely by determining the slope of the fractional flow curve for the particular value of each saturation.

11.4 Welge's Extension Solution

A more elegant method of achieving the same results as in the previous section was presented by Welge in 1952. This consists of integrating the saturation distribution over the distance from the injection point to the front, thus obtaining the average water saturation behind the front $\overline{S}_w$, as shown in Fig 11.4.

This situation depicted is at a fixed time, before water breakthrough in the producing well, according to an amount of water injection W_i. At this time the maximum water saturation, $S_w = 1\text{-}S_{or}$, has moved a distance x_1, its velocity being proportional to the slope of the fractional flow curve. The flood front saturation S_{wf} is located at position x_2 measured from the injection point. Applying simple material balance:

$$W_i = x_2 \cdot A \cdot \phi \cdot \left(\overline{S}_w - S_{wi} \right)$$

or $\qquad \overline{S}_w - S_{wi} = \dfrac{W_i}{x_2 A \phi}$
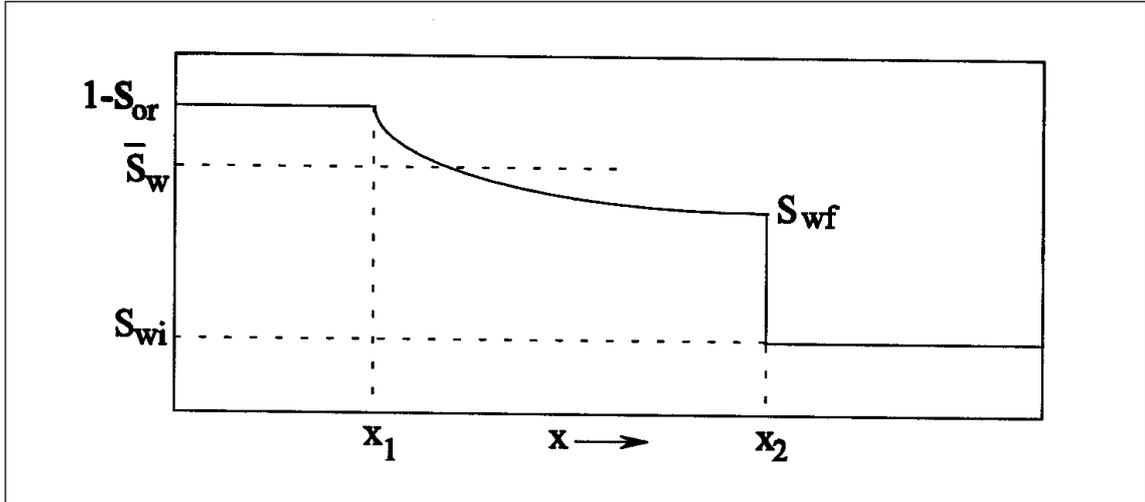
Fig. 11.4: Water saturation distribution as a function of distance

and using Eq. (11.20) which is applicable up to the flood front at x_2, then

$$\overline{S}_w - S_{wi} = \frac{W_i}{x_2 A \phi} = \frac{1}{\left. \dfrac{df_w}{dS_w} \right|_{S_{wf}}} \tag{11.21}$$

The average water saturation behind the front, $\overline{S}_w$ can be determined graphically by drawing a tangent to the curve $f(S_w)$, starting from the initial point (S_{wi}). The significance of this result is illustrated in Fig. 11.5.
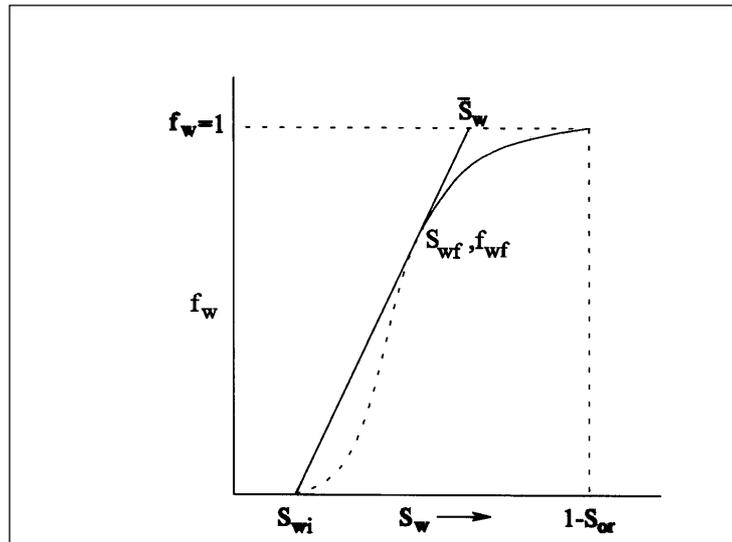
Fig. 11.5: Tangent to the fractional flow curve from $S_w = S_{wi}$.

To satisfy equation (11.21) the tangent to the fractional flow curve, from the point $S_w = S_{wi}$; $f_w = 0$, must have a point of tangency with coordinates $S_w = S_{wf}$; $f_w = f_{wf}$, and the

extrapolated tangent must intercept the line $f_w = 1$. This method of determining S_{wf}, f_{wf} and $\overline{S}_w$, requires that the fractional flow curve must be plotted for the entire water saturation range:

$$S_{wi} < S_w < 1\text{-}S_{or}$$

As noted earlier, the use of these equations ignores the effect of the capillary pressure gradient, $\partial P_c / \partial x$. This neglect, however, is only admissible behind the flood front for:

$$S_{wf} < S_w < 1\text{-}S_{or}$$

and for large flow system or when high rates of displacement are used.

The part of the fractional flow curve for saturations less than S_{wf} is, therefore, virtual and the first real point on the curve has the coordinates S_{wf} and f_{wf}, corresponding to the shock front.

11.5   Relative Permeability Measurement Methods

11.5.1 Steady State Method

In the steady state method, two fluids are injected simultaneously at a fixed ratio until the produced ratio is equal to the injected ratio. Core saturations have to be measured at each equilibrium and new fluid ratio is applied. This is repeated until the relative permeabilities are determined. Most tests are started with the core sample saturated with 100% wetting phase, and the test is then a desaturation test (drainage). This method, however, will most likely not give the endpoint saturations corresponding to the immobile water saturation or residual oil saturations.

The serious experimental problem with the steady state method is that in situ saturations in the core have to be measured or calculated from material balance. There are several methods to measure in situ saturations such as electrical resistance and capacitance methods, physical and chemical methods, nuclear methods, electromagnetic radiation absorption methods, weighing etc.

Another problem is capillary end effects. These may be overcome by using high rate of flow and high pressure differential, or each end of the sample is suitably prepared with porous disks and test sections to minimise end effects.

Advantages of this method are that it is conceptually straightforward and gives relative permeability data for the whole saturation range.

11.5.2 Unsteady State Method

The procedure for performing an unsteady state test is relatively simple and fast. In the following a water-oil test is described, but the procedure in principle is the same for gas-oil or water-gas. First the core is saturated with 100% water and then the sample is desaturated by injecting oil until no more production of water is obtained. Water

production is recorded and S_{wi} calculated. Effective oil permeability is then measured at S_{wi}. Oil is displaced by a predetermined constant rate of water, oil permeability and pressure drop across the core will be recorded. Alternatively, oil is displaced by keeping the differential pressure across the core constant with varying rate of fluid flow.

With the recording of cumulative water injection, pressure drop and produced oil volume, it is possible to calculate relative permeabilities by theory developed by Welge which is discussed in section 11.4. Like steady state method, the pressure across the core must be large enough to make capillary end effects and gravity effects negligible.

Advantages of unsteady state method are:

1. Substantially quicker than the steady state method.

2. The process resembles more the mechanisms taking place in the reservoir, and gives better endpoint data.

3. Simpler experimentally, and better adaptable to reservoir condition applications.

4. Smaller amounts of fluids required.

The main disadvantages are:

1. Relative permeability data will not be over the entire saturation range and might in the extreme case be restricted to endpoint data only.

2. Discontinuities in capillary pressure at the core ends may lead to distortion of the pressure data and recovery measured.

3. Substantially more calculations are necessary, but the mathematics may be solved by computers.

Summary

The following recommendations apply:

1) Use the unsteady state method at reservoir conditions to estimate endpoint data (saturations and relative permeability). These data are used to calculate the plateau production, the reserves and the water-cut throughout the life of the reservoir. This experiment at reservoir conditions of course has a big disadvantage, the huge costs.

2) Use the unsteady state method at standard conditions on a big amount of cores, and correlate with the data from 1). Advantage: cheap.

3) Use the steady state method on a few, chosen cores to estimate the curvature and the form of the relative permeability functions.

11.6 Experiments

11.6.1 Gas-Oil Relative Permeability Measurements, Unsteady State Method (Experiment 14)

The objective of this experiment is to determine gas-oil (air-water in the test) relative permeability in a core sample with an unsteady state method. Air is pressed through the core which is saturated with water 100%. Air injected volume and produced water volume are measured, and then relative permeability for air-water will be calculated.

As mentioned before, the Buckley-Leverett equation modified by Welge provides the unsteady state method for measuring of relative permeability. The following conditions must be satisfied for the laboratory measurements:

1. The pressure gradient should be large enough to minimise capillary pressure end effects.

2. The pressure differential across the core should be sufficiently small compared with total operating pressure so that fluid compressibility effects are insignificant.

3. The core should be homogeneous and initially 100% water saturated.

4. The driving force and fluid properties should be held constant during the test.

5. The flow should be horizontal, the core sample should be small enough, and the test time short enough so that the gravitational forces are insignificant.

Equations:

Welge's extension of the Buckley-Leverett concept states that

$$S_{g,av} - S_{g2} = f_{w2} Q_g \tag{11.22}$$

where subscript 2 denotes the outlet end of the core.

$S_{g,av}$ = average gas saturation
Q_g = cumulative gas injected, pore volumes
f_{w2} = fraction of water in the outlet stream.

$$S_{g,av} = \frac{N_p}{V_p} \tag{11.23}$$

where N_p is cumulative water produced and V_p is pore volume.

Since Q_g and $S_{g,av}$ can be measured experimentally, f_{w2} can be determined from the plot of Q_g as a function of $S_{g,av}$:

$$f_{w2} = \frac{dS_{g,av}}{dQ_g} \qquad (11.24)$$

and the gas saturation at the outlet (S_{g2}) may be calculated using Eq. (11.22).

By definition f_{w2} and f_{g2} may be expressed as:

$$f_{w2} = \frac{q_w}{q_w + q_g} \qquad (11.25)$$

$$f_{g2} = 1 - f_{w2} \qquad (11.26)$$

where q_w and q_g are the instantaneous water and gas flow rates, respectively.

By combining Eq. (11.25) with Darcy's law, it can be shown that:

$$f_{w2} = \frac{1}{1 + \dfrac{k_{rg}}{k_{rw}} \dfrac{\mu_w}{\mu_g}} \qquad (11.27)$$

Since viscosities are known, the relative permeability ratio k_{rg}/k_{rw} can be determined from Eq. (11.27).

Relative permeability for gas can be determined from the following equations

$$k_{rg} = \frac{\Delta G_{inj}}{\Delta t} C_2 \qquad (11.28)$$

where $C_2 = \dfrac{\mu_g L C_1}{A k_1 \Delta P}$ and $C_1 = \dfrac{P_a}{P_m}$

ΔG_{inj} = injected gas volume (cm^3) in the time interval $\Delta t(s)$.
$\quad L$ = length of core sample, cm
$\quad A$ = cross-sectional area, cm^2
$\quad k_1$ = absolute permeability (D), liquid permeability or Klinkenberg-corrected air permeability
$\quad C_1$ = Boyle's constant
$\quad P_a$ = atmosphere pressure
$\quad P_m$ = mean pressure.

Procedure:

1. Measure the pore volume, bulk volume, and air permeability of a cleaned and dried core sample. Determine the dry weight of the core. Measure the viscosity of the water at room temperature (this is done for you).

2. Saturate the core with water, weigh it, and place it inside the sleeve of a Hassler core holder (we have saturated the core).
3. Place the end caps on the core holder and apply appropriate overburden pressure, depending on the core permeability and hardness of the sleeve material used in the experiment.
4. Open the upstream and downstream valves of the core holder and measure the cumulative volume of gas injected and cumulative volume of water produced as function of time.
5. Flow a large volume of gas pore volumes through the core to reduce the water saturation adequately.
6. Open the core holder, remove the core sample and weigh the core to obtain the irreducible water saturation S_{wi}.
7. Plot the cumulative gas injected Q_g as a function of the average gas saturation in the core $S_{g,av}$ and determine the slope of the plot.
8. Calculate f_{w2} and f_{g2} at several values of Q_g using Eqs. (11.24) and (11.26).
9. Calculate the relative permeability ratio k_{rg}/k_{rw} using Eq. (11.27) at several time steps.
10. Plot gas fraction f_{g2} as a function of gas saturation S_{g2} (s-curve).
11. Plot on semi-log paper the relative permeability ratio as a function of S_{g2}.
12. Plot k_{rw} and k_{rg} vs. gas saturation $S_{g,av}$ using Eqs. (11.27) and (11.28).

Results and calculations:

Length of core,	L	=
Cross-sectional area,	A	=
Pore volume,	V_p	=
Bulk volume,	V_b	=
Abs. air Perm.,	k_{air}	=
Weight of dry core,	W_{dry}	=
Weight of sat. core,	W_{sat}	=
Water viscosity,	μ_w	=
Gas viscosity,	μ_g	=
Press. diff. Over core,	ΔP	=
Mean press. in core,	P_m	=
Weight of core after test,	W_{isat}	=

Time	Q_g	N_p	$S_{g,av}$	f_w	f_g	S_{g2}	k_{rg}/k_{rw}	k_{rg}	k_{rw}

11.6.2 Oil-Water Relative Permeability Measurements, Unsteady state Method (Experiment 15)

Description:

The measurements of absolute and relative permeabilities for oil and water are one of the most important tasks in core laboratories. Generally, the tested sample plug is saturated initially with a wetting phase using vacuum pump and the absolute permeability for the wetting phase is measured. Then the relative permeability measurements are conducted under two-phase flow, steady or unsteady method. Based on the data collected in the two measurements the absolute and relative permeabilities are calculated.

The unsteady state method is also called Welge's method because the calculation is based on the theory of the improved Buckley and Leverett's mechanism of fluid displacement in porous media. Our experiments will be carried out on Berea sandstone plugs with oil and water under unsteady state method, a constant pressure driving method.

Fig. 11.6 shows the set-up for relative permeability measurements used in our laboratory.

1. Air supply
2. Reduction valves
3. Core holder
4. Core sample
5. Manometers
6. Sleeve pressure
7. Liquid-volume measurement
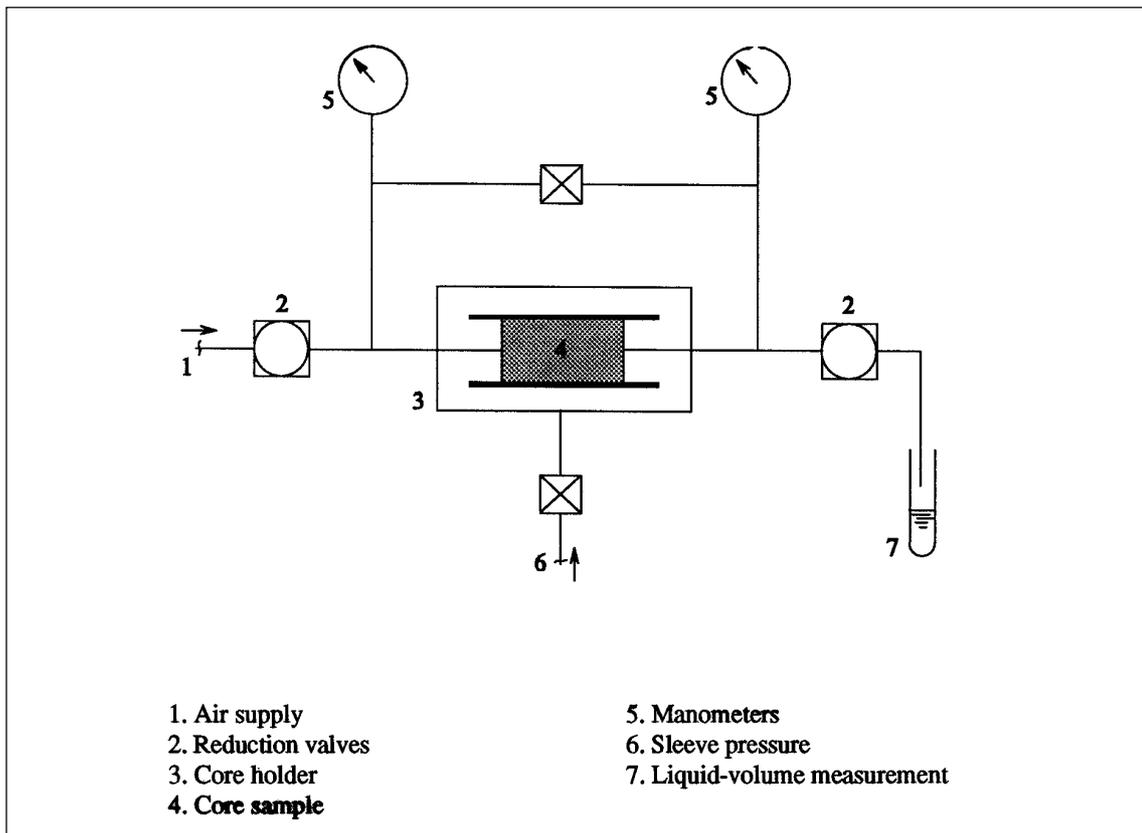
Fig. 11.6: Relative permeability apparatus.

Procedure:

1. Weigh a dry Berea plug, W_{dry}, measure its diameter, D, and length, L, with calliper. Saturate the core with 36 g/l NaCl brine and weigh, W_{sat}.

2. Mount the core in core holder.

3. Displace water by oil under a constant driving pressure, 1 bar.

4. Collect data: $V_{w(o)}$, water production from start of oil-driving to the first oil drop produced. $V_{w(i)}$ and $V_{o(i)}$ are water and oil productions during the time period. $\Delta T_{(i)}$ = 60 seconds.

5. Calculate the oil and relative permeabilities from $i = 2$.

6. Weigh the core and calculate the residual water saturation, $S_{wr(end)}$ and compare it with the $S_{wr(prd)}$, calculated from production data.

Basic Equations:

$$\left(f_w\right)_2 = \frac{dS_{o,avr}}{dW_i} \tag{11.29}$$

$$k_{rw} = \left(f_w\right)_2 \frac{d\left(\frac{1}{w_i}\right)}{d\left(\frac{1}{W_i I_r}\right)} \quad \text{or} \quad k_{rw(i)} = \left(f_w\right)_{2(i)} \frac{\frac{1}{W_{i(i)}} - \frac{1}{W_{i(i-1)}}}{\frac{1}{W_{i(i)}I_{r(i)}} - \frac{1}{W_{i(i-1)}I_{r(i-1)}}} \tag{11.30}$$

$$S_o = S_{o,avr} - W_i\left(f_w\right)_2 \tag{11.31}$$

$$S_w = 1 - S_o \tag{11.32}$$

$$I_r = \text{relative injectivity} = \frac{I_{2-phase}}{I_{abs}} = \frac{\Delta V_t}{\Delta V_w} \tag{11.33}$$

$$k_{ro} = \frac{\left[1-\left(f_w\right)_2\right]\mu_o}{\left(f_w\right)_2 \mu_w} k_{rw} \tag{11.34}$$

$(f_w)_2$	=	water fraction flowing at outlet face
W_i	=	cumulative injection in pore volumes
$S_{o,avr}$	=	average oil saturation in core
S_w	=	water saturation at outlet face
S_o	=	oil saturation at outlet face
$I_{2\text{-}phase}$	=	injectivity of water with two phases present (both water and oil)
ΔV_t	=	total volume of water + oil produced in each time step
ΔV_w	=	volume of water produced in each time step
k_{ro}	=	oil relative permeability at S_o
k_{rw}	=	water relative permeability at S_w
ΔT	=	time step

Calculations and report:

Calculate absolute (water) injectivity $I_{abs} = V_w/(\Delta T.A.\Delta P)$

A = cross-section area of the core.

Liquid data: $\rho_w = 1.020$ g/cm^3, $\mu_w = 1.04$ cp
                 $\rho_o = 0.785$ g/cm^3, $\mu_o = 1.36$ cp

$A =$ cm^2, $V_{pore} =$ cm^3, $I_{abs} =$, $\Delta P =$ bar.

i	$(i=0)$	$(i=1)$	$(i=2)$	$(i=3)$	$(i=4)$	$(i=5)$
$\Delta T_{(i)}$						
$\Delta V_{w(i)}$						
$\Delta V_{o(i)}$						
$\Delta V_{t(i)} = \Delta V_{w(i)} + \Delta V_{o(i)}$						
$u_{(i)} = \Delta V_{t(i)}/(A\Delta T_{(i)})$						
$I_{r(i)} = u_{(i)}/(I_{abs}\Delta P)$						
$W_{i(i)} = (\Sigma\Delta V_{t(i)})/V_{pore}$						
$S_{o,avr(i)} = (\Sigma\Delta V_{w(i)})/V_{pore}$						
$dS_{o,avr(i)} = S_{o,avr(i)} - S_{o,avr(i-1)}$						
$(f_w)_{2(i)} = \Delta V_{w(i)}/\Delta V_{t(i)}$						
$k_{rw(i)}$ {Eq. (11.30)}						
$S_{o(i)}$ {Eq. (11.31)}						
$S_{w(i)}$ {Eq. (11.32)}						
$k_{ro(i)}$ {Eq. (11.34)}						

References

Adamson A.W.: "Physical Chemistry of Surfaces", *John Wiley & Sons*, 1982.

Amyx J.W., Bass Jr. D.M. and Whiting R.L.: "Petroleum Reservoir Engineering", *McGraw-Hill*, 1960.

Archie G.E.: "The Electrical Resistivity Log as an Aid in Determining Some Reservoir Characteristics", *AIME*, 1942, p. 54.

Bear J.C.: "Dynamic of Fluids in Porous Media", *American Elsevier*, 1972.

Berg J.C.: "Wettability", *Marcel Deckker Inc.*, 1993.

Bourgoyne Jr. A.T., Millheim K.K., Chenevert M.E. and Young Jr. F.S.: "Applied Drilling Engineering", *SPE*, 1986.

Buckley, S.E.: "Mechanisms of Fluid Displacement in Sands", *AIME*, 1942, vol. 146, 107.

Collins R.E.: "Flow of Fluid through Porous Materials", *Reinhold Pub. Co.*, 1961.

Cosse R.: "Basics of Reservoir Engineering", *Editions Technip*, Paris, 1993.

Craig F.: "The Reservoir Engineering Aspects of Waterflooding", Monograph Volume 3, *AIME*, 1971.

Dake L.P.: "Fundamentals of Reservoir Engineering", *Elsevier*, 1978.

Golan M. and Whitson C.H.: "Well Performance", *Prentice Hall*, 1991.

Hassler G.L. and Brunner E.: "Measurement of Capillary Pressure in Small Core Samples", *AIME*, 1945 Vol. 160, 114.

Hjelmeland O. and Torsæter O.: "Coring and Core Analysis", *SINTEF Report*, Trondheim, 1984.

Johnson E.F.: "Calculation of Relative Permeability from Displacement Experiments", *AIME*, 1959, vol. 216, 370.

Kleppe J., Berg E.W., Buller A.T., Hjelmeland O. and Torsæter O.: "North Sea Oil and Gas Reservoirs", *Graham & Trolman Lim.*, 1985.

Koederitz L.F., Harvey A.H. and Honarpour M.: "Introduction to Petroleum Reservoir Analysis; Laboratory Workbook", *Gulf Pub. Co.*, 1989.

Mayer-Gürr: "Petroleum Engineering", *Ferninand Enke Verlag*, Stuttgart, 1976.

Miller C.A. and Neogi P.: "Interfacial Phenomena", *Marcel Dekker Inc.*, 1985.

Monicard R.F.: "Properties of Reservoir Rocks; Core Analysis", *Edition Technip*, Paris, 1980.

Morrow, N.R.: "Wettability and Its Effect on Oil Recovery". *JPT*, Dec. 1990, p1476-1484"

Mørk P.C.: "Overfate og Kolloidkjemi", Inst. For Industriell Kjemi, *NTH*, 1994.

Pirson S.J.: "Oil Reservoir Engineering", *McGraw-Hill*, 1958.

Shaw D.J.: "Introduction to Colloid and Surface Chemistry", *Butter Worth & Co.*, 1980.

Skjæveland S.M. and Kleppe J.: "Recent Advances in Improved Oil Recovery Methods for North Sea Sandstone Reservoirs", Norwegian Petroleum Directorate, Stavanger, 1992.

Torsæter O.: Personal Notes.

Torsæter O.: "A comparative Study of Wettability Test Methods Based on Experimental Results from North Sea Reservoir rocks". Paper *SPE* 18281, Houston, Tx., Oct. 1988.

Welge, H.J.: "Simplified Method for Computing Oil Recovery by Gas or Water Drive", *AIME*, 1952, Vol. 195, 91.

Wyllie M.R.J. and Spangler M.B.: "Application of Electrical Resistivity Measurements to Problem of Fluid Flow in Porous Media", Bull. AAPG, Feb. 1952, p. 359.